University of Sussex

Infrared Properties of Scalar Field Theories

Edouard Marchais

Submitted for the degree of Doctor of Philosophy

University of Sussex

01/10/2012

Declaration

I hereby declare that this thesis has not been and will not be submitted in whole or in part to another University for the award of any other degree.

Signature:

Edouard Marchais

UNIVERSITY OF SUSSEX

Edouard Marchais, Doctor of Philosophy

Infrared Properties of Scalar Field Theories

Summary

Phase transitions and critical phenomena are of central importance in quantum field theory and statistical physics. We investigate the low energy properties of $O(N)$ symmetric scalar field theories using functional renormalisation group methods for all N. This modern formulation of Wilson's renormalisation group allows a continuous interpolation between short and long distance physics without resorting to a weak coupling expansion. To leading order in the derivative expansion, we study the phase transition and the approach to convexity in the deep infrared limit. In the limit of infinite N, the fluctuations of the Goldstone modes dominate allowing for a complete analytical discussion of the effective potential. For finite N, the radial fluctuations become important and we resort to systematic series expansions. In both cases a systematic and thorough analysis of the diverse fixed point solutions is carried out. This leads to a comprehensive picture of the scaling potential for a large number of universality classes. We also study the dependence of our results on the regularisation scheme. Finally, we establish that the infrared completion of the effective potential in the broken phase is driven by a fixed point that leads to the flattening of the non-convex part of the potential.

Acknowledgements

In a first place I would like to thank my supervisor Daniel Litim for giving me the opportunity to do this PhD, for his patience during the completion of the research work and for his constant accessibility regarding his other duties. I would like also to thank my fellow research students at the department of Physics and Astronomy. I thank in particular my office mates Kevin, Kostas and Rob for their constant enthusiasm about Physics and other subjects. I thank also Mafalda, Jony, Ippo for their presence and friendship in everyday life. I think as well about the other members of the TPP group, staffs and students, past and present, which provided a stimulating environment as well as a colloquial ambiance. I thank also Andreas Juettner for its collaboration on some of the work presented here. Naturally, I would like to thank as well the people working at the Department of Physics and Astronomy of the University of Sussex, that contribute, everyday, to put this department at the service of the Physics and its students. I would like also to salute here my friends with whom I did my master of theoretical physics in Marseille and that gave me the passion for Physics. I think as well about my friends back in France without whom I would not be the person I am today. Finally, I would like to thank my parents for their constant support and love during the completion of my long studies. Words are vain to describe what I owe them.

Three passions, simple but overwhelmingly strong, have governed my life: the longing for love, the search for knowledge, and unbearable pity for the suffering of mankind.

Bertrand Russell

Contents

List of Tables

List of Figures

Chapter 1

Introduction

Symmetry breaking is a universal physical mechanism that occurs in many, if not all, domains of modern physics in one form or another. At the most fundamental level it happens when the symmetry of a given physical system is not fulfilled by its ground state for certain values of the physical parameters. This situation gives rise to the emergence of a non-trivial vacuum that entails important phenomenological consequences. In particle physics this fact is at the origin of the hypothesis of the scalar Higgs boson whose mass is precisely given by the non-zero amplitude of the ground state. In turn all other particles acquire a mass by simply interacting with this ubiquitous scalar field. This rather simple and elegant mechanism, put forward in [1, 2, 3, 4, 5], possesses as well the advantage of preserving the renormalisability properties of the full theory since all the couplings to the Higgs field are renormalisable. It is worth noticing that the mechanism of spontaneous symmetry breaking itself was introduced earlier [6, 7, 8] in analogy with the BCS theory of superconductivity [9]. Since then a relentless effort has been put into the experimental search for a scalar sector that completes the Standard Model of particle physics. This effort culminates with the joint experimental collaborations ATLAS and CMS related to the Large Hadron Collider at CERN, one of whose principal objectives is the discovery of the Higgs boson. It is only very recently that the elusive nature of the scalar particle has been unveiled with the observation of a significant statistical excess around 126 GeV from both collaborations [10, 11]. This preliminary result is a strong encouragement for the study of scalar models which is the main concern of this work.

Another privileged domain of application of the concept of scalar fields and symmetry breaking are condensed matter systems. It has been known for a long time that statistical systems, like a magnet for instance, exhibit a privileged magnetisation orientation when the temperature T of the system is maintained below a specific critical temperature

denoted T_c. Experimentally it is measured that the global magnetisation ϕ_0 is simply different from zero. Beyond the so-called critical temperature the magnetisation becomes independent of the spatial direction or, in other words, is invariant under three-dimensional rotations. Then the global magnetisation disappears with a local cancellation of the magnetic field thanks to the global rotational symmetry. Taking the reverse of this process we can summarize that the thermal fluctuations are responsible for the transition from a symmetric phase (unoriented magnetisation) to a non-symmetric phase (oriented magnetisation). This process of symmetry breaking can be visualized by the evolution, as a function of these fluctuations, of the free energy per unit volume of the system. This quantity noted V, also referred to as the effective potential, is a function of the microscopic degrees of freedom that correspond to a system of classical spins in the case of a magnet. In turn the spin variables can be represented by a scalar field and we are finally lead to the function $V(\phi)$ whose minimum ϕ_0 corresponds to the global magnetisation or to the vacuum expectation of the Higgs field in a particle physics context. The field expectation value ϕ_0 is the ground state of the theory and it is also an order parameter whose non-vanishing value distinguishes a phase with a spontaneous symmetry breaking.

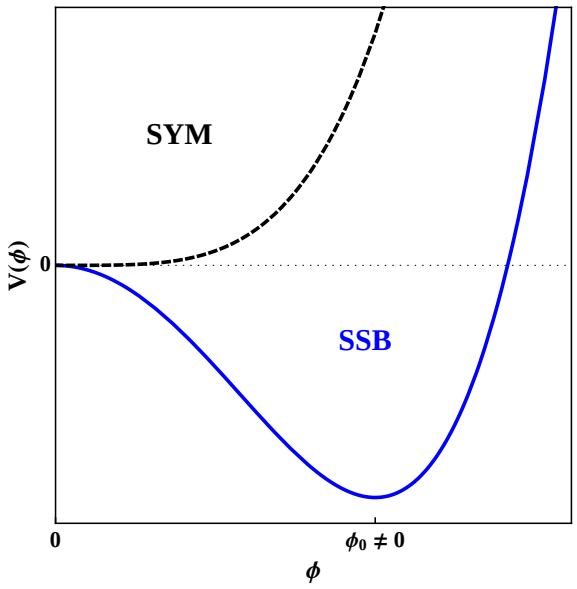

Figure 1.1: Form of the effective potential $V(\phi)$ for the symmetric (SYM) phase with $\phi_0 = 0$ and for the phase with spontaneous symmetry breaking (SSB) with $\phi_0 \neq 0$.

Due to the effect of fluctuations, ϕ_0 is driven continuously towards the origin and the symmetry is finally restored for $\phi_0 = 0$ (see figure 1.1). This evolution is typical of a second-order phase transition identified with the ferro/paramagnetic transition we de-

scribed previously. Continuous transitions are also associated with the divergence of the correlation length in the vicinity of the phase transition interpreted as zero mass excitations in particle theory. There, the divergences of the thermodynamical quantities follow a power law approach and, for instance, the magnetisation reads

$$\phi \propto (T - T_c)^{\beta} \tag{1.1}$$

when the system approaches its critical temperature. In (1.1) the critical exponent β is independent of the details of the microscopic interactions and therefore a particular value is related to a specific universality class. For the three-dimensional Ising universality class, to which belongs the ferro/paramagnetic transition, the critical exponent acquires the value $\beta \sim 0.32$ that is also recovered, for example, in the liquid-vapor transition [12].

From this point of view the method of the renormalisation group (RG) introduced by Kenneth Wilson [13, 14, 15], inspired from Kadanoff's blocking procedure [16], marks a breackthrough in the understanding of continuous transitions or critical phenomena. Not only did it provide a complete and systematic approach to the computation of critical exponents via powerful perturbative techniques [17], but it also renewed the theoretical understanding of field theory divergences. In this new conceptual framework a physical system at criticality ($T = T_c$), whose parameters remain scale independent, is associated with a fixed point of the renormalisation group. Also, beyond its immediate application to statistical physics undergoing continuous phase transition, the renormalisation group method has been commonly used in field theory to improve results from classical perturbative expansions. In this sense it is important to mention that genuine non-perturbative phenomena remain a challenge for such approaches. An important example is the approach to convexity of the effective potential in a phase with spontaneous symmetry breaking. Indeed it has been known a long time that the renormalised potential is a convex potential of the field ϕ [18]. Thus it is expected that fluctuation effects will lead to the flattening of the non-convex part of the potential. However perturbative evaluation of the potential does not reproduce a flat renormalised potential and instead $V(\phi)$ becomes complex at some finite value of the field within the non-convex region [19, 20]. Despite the physical interpretation given to this imaginary part [21] it remains an open challenge to reproduce correctly and analyse the approach to a convex potential in the broken phase. This particular task asks for genuine non-perturbative formulations of Wilson's RG that enable the computation of physical quantities beyond perturbation theory.

Since Wilson's original work, alternative formulations of the renormalisation group concepts have been given that put the emphasis on their non-perturbative content. For

instance in [22] an evolution equation for the Wislonian effective action is formulated with the ambition of simplifying the proof of perturbative renormalisability in scalar theory. However in this work we will use the approach put forward in [23] that allows versatile approximations of the action and therefore has been used in a wide range of domains of applications. Amongst these, and to name but a few, are the calculation of critical exponents in scalar theories [24, 25, 26, 27], the determination of the equation of state [28, 29] or first-order phase transitions [30, 31]. It has also been applied to more complicated theories like thermal field theory [32], gauge theories [33, 34, 35], supersymmetric $O(N)$ models [36, 37] and quantum gravity [38, 39, 40, 41, 42, 43].

In this thesis, we use Wilson's renormalisation group as formulated in [23] to study the low-energy behaviour of scalar, $O(N)$ symmetric theories in low dimensions. The benefit of our formalism is that it allows for controlled and systematic approximations even in the regime of strong coupling and strong correlations. For most of the work, we stick to the leading order in the derivative expansion, which is a quantitatively good approximation, in particular in the infrared limit, due to the known small anomalous dimension of the fields. Furthermore, we take advantage of explicit analytical realisations of the RG flow, which permit a largely analytical study of the salient features. The main new results are a complete exact analytical solution of three-dimensional $O(N)$ symmetric scalar theories in the limit of infinite N, for arbitrary Wilsonian momentum cutoff. In addition, we develop and apply new systematic field expansions including the regimes of large or imaginary fields. These techniques allow for a derivation of 'global' fixed point solutions, for all fields, in generic dimensions. At the same time, our study paves the way towards understanding the approach to convexity in the low energy limit. Here, we establish for the first time that the low-momentum fluctuations of scalar fields in a phase with spontaneous symmetry breaking lead to a well-defined convex effective potential, despite the apparent infrared singularities observed in perturbation theory. The reason for this behaviour is the occurrence of a new attractive infrared fixed point. This result fills a gap in the literature [44, 45, 25]. In the infinite N limit, the leading order of the derivative expansion becomes exact, and hence our results provide an exact solution of the theory. At finite N, corrections due to a small anomalous dimension are expected without changing the key results achieved here.

More specifically, the outline of the thesis is as follows:

We introduce in chapter 2 the main concepts and methods of the functional implementation of the Wilsonian renormalisation group. Then in chapter 3 we start by calculating

exactly the expression for the critical potential in three dimensions at large N. We use this solution to study in depth the fixed point structure of the theory and in particular single out the Wilson-Fisher fixed point solution that indicates a second-order phase transition. Related critical indices are computed systematically and followed by the calculation of an approximated expression of the potential for finite N by means of local expansions. A numerical input is used to fix the remaining parameters of the expansions and finally the potential at criticality is obtained for $O(N)$ universality classes as well as their associated critical exponent ν. These results are used to formulate a unified and comprehensive picture of the critical potential in three dimensions. In chapter 4 we argue that RG scale and momentum integration can be interchanged. We illustrate this principle by computing the exact expression of the renormalised potential at large N, for arbitrary dimension and without specifying the Wilsonian cutoff. In the following we use this solution to study continuous transition in three dimensions, the absence of such phenomenon in two and four dimensions and eventually investigate first-order phase transitions for a sextic coupling with an associated tricritical line. Finally in chapter 5 we focus on the deep infrared scaling of the potential for a non-vanishing minimum and analyse the approach to convexity. There, the flattening of the potential is related to the existence of an infrared stable fixed point that guarantees a convex full potential. The dependence of such process on the Wilsonian regularisation is worked out in detail. We summarize our results in chapter 6.

Chapter 2

Functional renormalisation group

Before discussing the details of the infrared properties of the effective potential we first review concepts from quantum field theory that are constantly used throughout our work. We start with a brief discussion of the path integral and the related functional formalism before switching to the conceptual heart of modern field theory, the Wilsonian renormalisation group. We emphasize the non-perturbative nature of the RG concepts in order to introduce the flow equation for the effective action as formulated in [23]. A concise discussion of this formulation and its main technical aspects (such as approximation and regualrisation) is given, largely inspired from the different reviews existing on the subject [25, 46, 47, 48, 49]. Then, we compute the evolution equation for the effect potential at the leading of the derivative expansion. This equation will be the central piece of investigation for the scaling behaviour of the potential. Finally, we give for completeness the form of the evolution equation for the potential at the next to leading order. We also briefly review the convexity of the effective potential from a conventional point of view as it will be a recurrent theme in our work. Naturally, no claim of originality is made here and this material can be found in many classical references (with an assumed orientation towards common aspects of quantum field theory and statistical physics) such as [50, 51, 52, 53, 54, 55, 56, 57].

2.1 Functional Integral

In quantum field theory (QFT) and statistical physics one of the main objectives is the computation, in the sharpest possible way, of correlation functions. Quantitative informations about specific phenomena such as scattering amplitudes in particle physics or fluctuation length in condensed matter physics can be computed from correlation functions

(or correlators). These functions can be obtained as the integrated product of n field operators at different points in an Euclidean space-time. Also this product is weighted by the exponential of an action $S[\varphi]$ such that

$$\langle \varphi(x_1) \dots \varphi(x_n) \rangle = \mathcal{N} \int_\Lambda \mathcal{D}\varphi \, \varphi(x_1) \dots \varphi(x_n) \, e^{-S[\varphi]} \,, \tag{2.1}$$

where the normalisation constant $\mathcal{N}$ can be fixed with the requirement that $\langle 1 \rangle = 1$. The functional measure

$$\int_\Lambda \mathcal{D}\varphi = \prod_n \int_\Lambda \mathcal{D}\varphi(x_n) \tag{2.2}$$

is defined for a discretized space-time, i.e with an implicit minimum length Λ^{-1} and in a finite volume. It is assumed that this procedure can be extended to a continuous space-time and infinite volume in accordance with the local and global symmetries under consideration.

A natural way of synthesizing all these correlation functions is by using their generating functional given by

$$Z[J] = \int \mathcal{D}\varphi \, e^{-S[\varphi] + \int d^d x J(x)\varphi(x)} \,. \tag{2.3}$$

This corresponds to the partition function of the statistical physics analogue of our system. From a broader perspective, we outline that the use of the euclidean path integral (2.3) is justified from the fact that we are mainly dealing with quantum-statistical systems. In such systems the inverse temperature would correspond to an "imaginary" time in conventional relativistic quantum field theory on a minkowskian space-time.

Here $Z[J]$ is meant as a functional of the source J and we have the property

$$\langle \varphi(x_1) \dots \varphi(x_n) \rangle = \frac{1}{Z[0]} \left. \frac{\delta^n Z[J]}{\delta J(x_1) \dots \delta J(x_n)} \right|_{J=0} . \tag{2.4}$$

This formulation has the implication that if the partition function can be computed completely then all correlators are known and the specific model is considered as solved. Another important object, related to Z, is the generating functional of connected correlations functions

$$W[J] = \ln Z[J] \tag{2.5}$$

referred to as the Schwinger functional. Correlators generated out of $W[J]$ correspond, in the context of standard perturbative expansion, to connected Feynman diagrams without external branches. Then we have, for instance, the 2-point function

$$\langle \varphi(x_1)\varphi(x_2) \rangle - \langle \varphi(x_1) \rangle \langle \varphi(x_2) \rangle = \left. \frac{\delta^2 W[J]}{\delta J(x_1) \delta J(x_2)} \right|_{J=0} \tag{2.6}$$

and the expectation value $\phi(x)$ of a field $\varphi(x)$ at a point x is defined by

$$\phi(x) = \langle \varphi(x) \rangle = \left. \frac{\delta W[J]}{\delta J(x)} \right|_{J=0} . \tag{2.7}$$

We are now in position to introduce the so-called effective action $\Gamma[\phi]$ which provides a more direct access to physical quantities. It is obtained by a Legendre transform of the generating function $W[J]$, to wit

$$\Gamma[\phi] = \sup_J \Big\{ -W[J] + \int d^d x \, J(x)\varphi(x) \Big\}. \tag{2.8}$$

In this expression $\sup_J$ is meant to associate a particular J_s to a fixed ϕ for which $\Gamma[\phi]$ reach its supremum. The effect of this transformation can be understood, at first sight, as the interchange of the variable $J(x)$ with $\phi(x)$. We note that $\Gamma[\phi]$, being a Legendre transform, enjoys the property of convexity which implies by definition

$$\frac{\delta^2 \Gamma}{\delta\phi\delta\phi} \geq 0 \, . \tag{2.9}$$

In the language of operators this indicates that the second functional derivative of the effective action possess positive semi-definite eigenvalues. A concise discussion of the consequence of Γ being a Legendre transform and of the geometric interpretation of (2.9) is given in the last section of this chapter and the link with the convexity is established.

2.2 Renormalisation Group

We develop now the basic concepts of the renormalisation group and their modern formulation in the context of functional methods.

2.2.1 Wilsonian Renormalisation Group

Modern non-perturbative formulations of the renormalisation group are mainly based on the principle of the integration of the highest momenta in order to generate an effective low energy, or long distance, theory [13, 14]. This principle can be simply illustrated by the Kadanoff blocking procedure [16] in position space. In this picture the physical system (i.e a magnet) is represented by a discrete set of spins with a minimal length scale a. Neighboring spins are grouped and an average spin is computed for each small spin block. Therefore the network of spin blocks appears similar to the previous system but with a dilated length scale $a' > a$. Then we choose to redefine the scale a' by dividing it by the dilatation factor such that $a'/\alpha = a$. This contraction allows us to come back to the original length scale with a equivalent description of the system, i.e the partition is

left invariant by the transformation. This simple procedure corresponds to a systematic reduction of the degrees of freedom and is equivalent to the summation (or integration) of the highest momenta leading to a renormalisation flow.

We can extend Kadanoff's concept to the case where the degrees of freedom are represented by a field $\phi(x)$ which is a continuous function of the space-time. In order to compute the partition function (2.3) we translate here the previous discrete procedure into the continuum. For this we separate modes with high momentum $\phi_>$ from those with low momentum $\phi_<$. Then only high momentum modes are integrated to obtain an effective low energy action

$$e^{-S^{eff}_{\Lambda-dq}[\phi_<]} = \int [\mathcal{D}\phi_>]\, e^{-S[\phi_>+\phi_<]} \tag{2.10}$$

where $\Lambda = a^{-1}$ is the ultraviolet cutoff scale. The integration on high momenta is performed on the infinitesimal momentum shell $\Lambda - dq$ and can be iterated as in the previous discrete analog. The action (2.10) does not depend on the high energy modes anymore and leads to the same long distance physics. We note that the mode separation occurs not only in the action but also in the functional measure. The infinitesimal integration leads to the evolution of the Wilsonian effective action S^{eff}_k as a function of a cutoff scale k, that indicates the separation between high and low modes. This evolution can be described by an exact differential equation which was first derived in [58] for a sharp cutoff and a smooth version is given in [15]. Another version of this differential equation has been given in [22] in order to give a simplified proof of perturbative renormalisation. This equation reads in momentum space

$$\partial_k S^{eff}_k = \frac{1}{2}\int \frac{dq^d}{(2\pi)^d}\, \partial_k K_k(q) \left(\frac{\delta^2 S^{eff}_k}{\delta\phi_<(q)\,\delta\phi_<(-q)} - \frac{\delta S^{eff}_k}{\delta\phi_<(q)}\,\frac{\delta S^{eff}_k}{\delta\phi_<(-q)} \right) \tag{2.11}$$

where the function $K_k(q)$ is the cutoff function. The flow equation (2.11) contains all perturbative and non-perturbative effects for a given model, i.e a given bare action S_Λ. However, a few technical aspects have to be mentioned in order to use flow (2.11) for practical purposes. For example if we want compute a thermodynamical quantity out of S_k we still have to determine the partition function (2.3), which implies a functional integration on the lower modes $\phi_<$. Therefore the quantity S_k does not have a direct physical interpretation and we are forced to integrate all modes which makes the formulation and the calculation of genuine effective physical quantities less accessible. Also in the second term in the integrand of (2.11), modes with different momenta are coupled which induces non-local effects in the flow. This does not facilitate the choice of the cutoff function $K_k(q)$ and the results from (2.11) are affected by a great sensitivity on the regularisation

scheme within some necessary approximation [59]. These rather technical remarks show the subtleties related to the utilisation of (2.11) and from this point of view alternative formulations seem desirable. Indeed, it is important to keep in mind that even approximated solutions to an exact flow similar to (2.11) provide precious non-perturbative informations that are difficult, if not impossible, to obtain by other methods. Consequently many studies have been performed on the functional approach to Wilsonian renormalisation [60, 23, 61, 62, 59, 63, 64, 65, 66, 67]. In particular some of these formulations concern formal objects with a more direct physical interpretation than the Wilsonian effective action S_k. For instance a flow equation for the Legendre transform of $\ln Z$ has been given which attenuates some inconvenients of the previous approach. From now on we focus on this type of approach put forward specifically in [23].

2.2.2 Effective average action

In the continuity of the previous presentation on Wilson's renormalisation group ideas it is natural, although highly non-trivial, to try to apply the concept of effective momentum integration at a practical level. As we stated previously, this was originally done by splitting high and low momentum at the level of the functional measure $[\mathcal{D}\phi]$ [15, 22]. However there has been also several propositions for alternative implementation of an effective integration since Wilson's work. In this work we are using the concept of effective average action [68] which has been shown to be particularly suitable for computational purposes among other advantages. In this approach the regularisation of momenta is implemented by adding a regulator term to the action instead of modifying the functional measure. The primary role of the regulator term is to suppress the contributions of lower modes, that are inferior to an effective energy scale k, from the path integration (2.3). Higher modes are left untouched by the regularisation and are integrated as usual. The partition function (2.3) is then modified by the presence of the regulator term and takes the form

$$Z_k[J] = \int \mathcal{D}\chi \, e^{-S[\chi]-\Delta S_k[\chi]+J\cdot\chi} \,. \tag{2.12}$$

In this expression we promoted the scalar field χ to a vector field χ_a that represents a collection of N scalar fields with $a = 1, \ldots, N$. We defined as well the dot product

$$J \cdot \chi \;=\; \int d^d x \, J_a(x) \, \chi^a(x) \;=\; \int \frac{d^d q}{(2\pi)^d} \, J_a(-q) \, \chi^a(q) \tag{2.13}$$

with an implicit summation on field indices. As mentioned earlier the only modification to (2.3) is the addition of an infrared cutoff regulator $\Delta S_k[\chi]$ quadratic in the field and

that reads in momentum space

$$\Delta S_k[\chi] = \int \frac{d^d q}{(2\pi)^d}\, \chi_a(-q)\, R_k(q)\, \chi^a(q)\,. \tag{2.14}$$

The infrared regulator function R_k is required to vanish in the limit $k \to 0$. Then all momenta $0 \leq q^2 \leq \Lambda$ are summed in (2.12). By opposition when $k \to \Lambda$ none of the moment are included in the partition function. In the presence of the regulator term one defines the expectation value of the field by

$$\varphi^a(x) \equiv \langle \chi^a(x) \rangle = \frac{\delta W_k[J]}{\delta J_a(x)} \tag{2.15}$$

where the modified generating functional reads $W_k = \ln Z_k$. Then the relation between J and φ is k-dependent. As previously we can define a modified Legendre transform

$$\Gamma_k[\phi] = \sup_J \Big\{ -W_k[J] + J \cdot \phi \Big\} - \Delta S_k[\phi]\,. \tag{2.16}$$

This expression of a coarse-grained effective action is central to a good understanding of the symmetry breaking mechanism. In particular the only difference is the addition of the regulator term that ensures that the "microscopic" action $S \equiv \Gamma_\Lambda$ is recovered when no momenta are integrated as $k \to \Lambda$. The average action defined through (2.16) differs also fundamentally from the usual effective action Γ as Γ_k does not need to be a convex function of the field, owing to the presence of the infrared regulator term ΔS_k in (2.16). It is only in the limit $k \to 0$ that we recover a convex action [45, 44] as a consequence of the non-modified Legendre transform (2.8). Several noticeable properties can already be stated at this stage [69, 25]. Rotational invariance is respected by the cutoff term and therefore remains a symmetry of Γ_k. This allows to expand Γ_k in terms of invariants with respect to the symmetry group $O(N)$ with couplings depending on k. This property will be essential when we discuss approximations of the action. We note that the functional $\Gamma_k + \Delta S_k$ is the result of a non-modified Legendre transform of W_k and thus it has to be convex. Thus the eigenvalues of the second functional derivative in field space $\Gamma_k^{(2)} + R_k$ are positive semi-definite. For an homogeneous field and at the minimum of R_k (which is not always at $q^2 = 0$) the exact bounds the effective potential are

$$U_k'(\bar\rho) \;\geq\; -\min_{q^2 \geq 0} R_k(q^2)\,, \tag{2.17}$$

$$U_k'(\bar\rho) + 2\bar\rho\, U''(\bar\rho) \;\geq\; -\min_{q^2 \geq 0} R_k(q^2) \tag{2.18}$$

where U_k is the non-derivative part of the coarse-grained action Γ_k. Then it is clear that convexity is reached as $k \to 0$ whichever is the minimum position $\bar\rho_0$. For $\bar\rho_0 > 0$ we remain in a broken phase where the convexity is achieved through a flattening of the "inner" part $\bar\rho < \bar\rho_0$ of the effective potential.

2.2.3 Regulators

The infrared regularisation function $R_k(q^2)$ can be freely chosen but this choice is also constrained by simple restrictions that ensure a well defined evolution of Γ_k when $0 \leq k \leq \Lambda$. Indeed we have to make sure that the effective average action (2.16) interpolates correctly between an initial ultraviolet action and a full quantum action in the infrared. The first condition is that

$$\lim_{q^2/k^2 \to 0} R_k(q^2) > 0 \tag{2.19}$$

which makes sure that the effective propagator $(\Gamma_k^{(2)} + R_k)^{-1}$ remains finite when $q^2 \to 0$ at vanishing field. This permits a control on the contribution of massless modes that usually lead to infrared divergences problems. This fundamental requirement makes $R_k(q^2)$ an infrared regulator. An another condition is the guarantee that $R_k(q^2)$ vanishes when all momenta are integrated, i.e

$$\lim_{k^2/q^2 \to 0} R_k(q^2) \to 0\,. \tag{2.20}$$

This ensures that the cutoff function is properly removed when $k \to 0$ and that we recover a full quantum action $\Gamma \equiv \lim_{k\to 0} \Gamma_k$. The last condition is the requirement that a microscopic , or classical, action is reached when $k \to \Lambda$ and this reads simply

$$\lim_{k \to \Lambda} R_k(q^2) \to \infty\,. \tag{2.21}$$

Then as k approaches Λ the regulator term exponentially suppresses quantum corrections in the path integral (2.12) and leads finally to a microscopic action $S \equiv \lim_{k\to\Lambda} \Gamma_k$. These three conditions together guarantee that the additional mass term ΔS_k acts as a infrared cutoff by which lower modes with $q^2 < k^2$ acquire artificially an effective mass in a continuous fashion, and this without any alteration of the fundamental actions S and Γ. We add that, apart from the conditions (2.19), (2.20) and (2.21), the choice of a specific cutoff function $R_k(q^2)$ is arbitrary and in practice specific schemes are used with a variable impact on the calculation of physical quantities (see [25] for a generic discussion), within some approximations of Γ_k (see later sections). The impact of the regularisation scheme and it optimisation has been examined in detail in [70, 71, 72].

2.2.4 Flow equation

Now that we discussed the correct interpolation limits of the effective action Γ_k we would like to know about its intermediate trajectory between these bounds. We will see that

these possible trajectories are governed by an exact flow equation [23] compatible with continuous symmetry and for an arbitrary effective action Γ_k. We sketch here the derivation of a flow equation for a single scalar field for the sake of simplicity and the generalisation to many fields is straightforward. First we start by differentiating the effective action (2.16) with respect to the logarithmic scale $t = \ln k/\Lambda$ keeping ϕ fixed and k-independent, this gives

$$\begin{aligned} \partial_t \Gamma_k[\phi] &= -\partial_t W_k[J]|_\phi + \partial_t J \cdot \phi - \partial_t \Delta S_k[\phi] \\ &= -\partial_t W_k[J]|_J - \partial_t \Delta S_k[\phi] \end{aligned} \tag{2.22}$$

where $J = J_{sup}$ and is k-dependent. Now we can use the path integral representation (2.16) with $W_k = \ln Z_k$ to express the scale derivative of W_k in terms of the v.e.v of a field χ in the presence of a regulator term. We obtain

$$\begin{aligned} \partial_t W_k[J]|_J &= -\frac{1}{2} \langle \chi \cdot \partial_t R_k \cdot \chi \rangle|_J \\ &= -\frac{1}{2} \int \frac{d^d q}{(2\pi)^d} \, \partial_t R_k \, \langle \chi(q)\chi(-q) \rangle \end{aligned} \tag{2.23}$$

in Fourier space. Then, using the definition of a 2-points function $G(q,-q) = \langle \chi(q)\chi(-q)\rangle - \langle \chi(q)\rangle\langle\chi(-q)\rangle$ and $\partial_t \Delta S_k = (1/2)\langle\chi(q)\rangle \, \partial_t R_k \, \langle\chi(-q)\rangle$ (we recall that $\phi = \langle\chi\rangle$), we express the scale derivative (2.22) simply like

$$\partial_t \Gamma_k[\phi] = \frac{1}{2} \int \frac{d^d q}{(2\pi)^d} \, \partial_t R_k \, G(q,-q) \tag{2.24}$$

where it remains to express the full propagator $G(q,-q)$ in terms of the effective action Γ_k. For this we recall that the quantum equation of motion derived from (2.16) reads

$$\frac{\delta \Gamma_k[\phi]}{\delta \phi(x)} = J(x) - R_k(x) \cdot \phi(x) \, . \tag{2.25}$$

Then the second functional derivative of (2.25) and the use of definition (2.15) lead to the expression of the full propagator in position space

$$\frac{\delta^2 W_k[J]}{\delta\phi(x)\delta\phi(y)} = \left(\frac{\delta^2 \Gamma_k[\phi]}{\delta\phi(x)\delta\phi(y)} + R_k(x,y) \right)^{-1} = G(x,y) \, . \tag{2.26}$$

Taking the Fourier transform of $G(x,y)$ and putting it back into (2.23) we obtain the flow equation for the effective action (first derived under this form in [23])

$$\partial_t \Gamma_k[\phi] = \frac{1}{2} \, \mathrm{Tr} \left\{ \left(\Gamma_k^{(2)}[\phi] + R_k \right)^{-1} \partial_t R_k \right\} \tag{2.27}$$

where the trace operator represents simply the integration over momenta $\mathrm{Tr} = \int dq^d \, (2\pi)^{-d}$ and also the summation over field indices when more that one field is involved. We used

as well the shorthand notation $\Gamma_k^{(2)}[\phi] = \frac{\delta^2\Gamma_k[\phi]}{\delta\phi(x)\delta\phi(y)}$. The flow equation (2.27) is the corner stone of our non-perturbative approach to field theory and its structure and content deserve some comments [25, 47].

First it is a nonlinear functional differential equation for the running effective action Γ_k. Mathematical techniques to solve such an equation are not developed very far and approximation schemes for Γ_k are required to extract quantitative physical results from (2.27). This mandatory step will be explained in more details in the forthcoming section. Nevertheless equation (2.27) possess a one-loop structure as a consequence of the quadratic regulator term [73]. The full propagator can be represented as a closed loop and the scale derivative of the regulator as a vertex on this loop. If we replace $\Gamma_k^{(2)}$ by the second derivative of the classical action $S^{(2)}$ the effective action reads now

$$\Gamma_k = S[\phi] + \frac{1}{2}\,\mathrm{Tr}\ln\Big(S^{(2)} + R_k\Big). \tag{2.28}$$

This form allows for a comparison with the usual perturbative approach where classical couplings and propagators appear now in $S^{(2)}$. If one wants to recover the perturbation theory results from (2.28) it suffices to promote the couplings appearing in the classical action $S^{(2)}$ to k-dependent couplings. This step corresponds to the "RG improvement" of the one-loop expansion of the action. This scale dependence is also enforces from the presence of the infrared regulator in (2.28). With this in mind one can compare, for example, the expression (2.28) to the one-loop correction formula for the effective action (for instance see [74] p.239). Once this improvement is done the action (2.28) can be expanded at the lowest order in the coupling constants to recover standard RG-improved one-loop perturbation theory. It is important to mention that perturbative corrections beyond one loop can not be reproduced via this method [75]. A particularly important property of the flow (2.27) for our purpose is its infrared safety (by construction) thanks the regulator R_k which prevents any divergences as long as $k > 0$. Also the presence of the scale derivative of the regulator entails a localized momentum contribution to the flow around $q^2 \sim k^2$ and so leads to the ultraviolet finiteness of (2.27). This consequence is in absolute agreement with Wilson's renormalisation group ideas where only a shell of momenta is effectively integrated and so the flow is localized in momentum space. However we must indicate that the UV regularisation is also related to a fast decay of $\partial_t R_k$ for $q^2 \gg k^2$ and a very specific choice of regulator may lead to an incomplete higher modes integration that would damage the UV finiteness of (2.27). However as we are interested in infrared behaviour this detail is of a minor importance and we will assume a sufficiently fast UV decay for R_k. Finally we would like the outline that the flow (2.27)

can be visualized as a set of trajectories within the theory space of all possible actions. All these trajectories are regulator dependent and interpolate between the two "points" S and Γ which are evidently regulator independent because of the conditions (2.19), (2.20) and (2.21).

2.3 Approximations

Despite the simple form of (2.27) it is still virtually impossible to solve such an equation for an arbitrary Γ_k. On the other hand, in a physical context, it is quite usual to rely on some approximation not only to make calculations feasible but also to render results intelligible and easily interpretable at a qualitative and quantitative level. Some approximations are already widely known such as the perturbative expansion in power of the coupling constant whose efficiency is at the origin of the development of quantum field theory. But, some others approximation schemes also exist that use, for instance, the dimensionality as an expansion parameter by introducing $\epsilon = d-4$ [17, 76, 77] or $\epsilon = d-2$ [78, 79] which allows for the calculation of critical indices in the vicinity of a continuous phase transition. Evidently, other parameters of the theory can be used to formulate alternative approximations valid for different asymptotic regimes. The celebrated large N approximation [80] (where N is the component number of our vector field) is a good example and it will be used many times in this work. In general the approximation made is supposed to catch the relevant dynamics of the physical system under study and keep the computational effort in a manageable size. However it is important to keep in mind that in the absence of clearly identified small parameter it remains a non-trivial task to control an approximation at a non-perturbative level.

2.3.1 The derivative expansion

In order to extract the physics out of the flow equation (2.27) we resort then to some approximation at the level of the effective action Γ_k. In the context of infrared $O(N)$ symmetric scalar field theories it is expected that long range correlations among collective degrees of freedom are predominant and this entails a domination of the physical phenomena by low momenta. This leads us to employ an expansion of the action in powers of the momentum q^2 which is expected to cope correctly with the critical fluctuations. This derivative expansion has been intensively used [63, 81, 82] and its convergence properties comprehensively discussed [83, 26, 84]. It provides a good description of the effective potential close to criticality but also accurate values for the critical exponents [24, 85, 27].

Within the position space the Ansatz for the effective action takes the form

$$\Gamma_k[\phi] = \int d^dx \left\{ U_k + \frac{1}{2} Z_k \left(\partial_\mu \phi\right)^2 + \frac{1}{4} Y_k \left(\partial_\mu \bar{\rho}\right)^2 + \mathcal{O}(\partial^4) \right\} \tag{2.29}$$

where we recall that $\bar{\rho} = \phi^2/2$. The kinetic terms involve two different renormalisation functions Z_k and Y_k that depend on the fields and the momenta. For $N > 1$ in the broken phase, Z_k is related to the renormalisation of the Goldstone modes whereas the renormalisation of the radial mode includes both Z_k and Y_k. The renormalised potential U_k is the generating function of all the couplings of the theory and is a privileged tool for the study of the ground state of a given theory. Naturally the derivative expansion is consistent with the $O(N)$ symmetry. Another reason for which the approximation (2.29) is expected to reproduce correctly the infrared scaling properties of the effective action is related to the fact that infrared instabilities (in the broken phase) are kept under control and singular behaviour builds itself progressively as $k \to 0$. This technical advantage is more transparent in a qualitative version of the second-derivative of the action appearing in the flow, given at low momenta by [25]

$$\Gamma_k^{(2)} \sim q^2 (q^2 + ck^2)^{-\eta/2} \tag{2.30}$$

where $c > 0$ and η is the anomalous dimension defined from the scaling of the renomalisation wave function (Z_k for instance). There it is clear that the behaviour for small q^2 is completely regular and we note the infrared suppression for $k^2 > 0$. Thus, from (2.30), it is expected that an approximation about $q^2 \sim 0$ will lead to a reasonable evaluation of critical exponents with a small (awaited) error coming from the anomalous dimension.

The approximation (2.29), as other approximation schemes, converts the flow equation (2.27) into a infinite system of coupled nonlinear partial differential equations for U_k, Z_k, etc ... Obviously, for computational purposes, the expansion (2.29) has to be truncated to some order, turning the system into a manageable size. It is important to note that at this level the truncation has the drawback that now any physical quantities computed from the flow equation become regulator dependent. Therefore a sensible choice of a specific infrared cutoff function is fundamental in order to obtain reliable quantitative results. This will be discussed in the next section. Another important aspect of the scheme (2.29) is that it corresponds to a systematic expansion which, a priori, does not have a small physical parameter. However it should be kept in mind that the expansion (2.29) is an expansion in power of the momenta. Therefore it is expected to have a reasonable convergence in a typical phase transition phenomenon dominated by small momenta fluctuations.

Of course this characteristic makes it particularly suitable to explore non-perturbative

phases of field theories but also authorises some supplementary approximations improving the feasibility of analytical calculations. As we mentioned previously the parameter N can be used as an additional variable of expansion. In passing we note that, independently of the functional renormalisation group set-up, an expansion in powers of $1/N$ can be used as a systematic approach to field theory [86]. In this context it is well know that the anomalous dimension is suppressed in the strict limit $1/N \to 0$ (see also [50]). Then, in the large N limit, the leading order of the derivative expansion (2.29), that corresponds to the Local Potential Approximation (LPA) [87], is given by the simplified Ansatz

$$\Gamma_k[\phi] = \int d^d x \left\{ U_k + \frac{1}{2} (\partial_\mu \phi)^2 \right\} \tag{2.31}$$

which becomes exact and leads to the exact determination, for example, of critical indices [88]. As we will see the approximation (2.31) leads to a single evolution equation (at large N or not) for the effective potential that encapsulates all the physics. It is therefore of tremendous importance to solve, even approximatively, such an equation. This will be one of the principal objectives of this work and we will see that a large number of non-perturbative results (sometimes exact), which are otherwise inaccessible by more conventional approaches, can be obtained analytically from (2.31).

2.3.2 The vertex expansion

For the sake of completeness we mention here briefly another approximation scheme that consists into the expansion of the effective action in terms of 1PI Green functions $\Gamma_k^{(n)}$ or vertex functions. This can be seen as an alternative to the derivative expansion described above, focusing on the scaling behaviour of n-points functions. This expansion, that conserves the global information about momenta, takes the form

$$\Gamma_k[\phi] = \sum_n^\infty \frac{1}{n!} \int \left(\prod_k^n d^d x_k \left(\phi(x_k) - \phi_0 \right) \right) \Gamma^{(n)}(x_1, \ldots, x_n) \tag{2.32}$$

where ϕ_0 represents a constant field configuration around which the expansion is performed. If this configuration is identified with the expectation value of ϕ then the expansion starts at $n = 2$ [68, 60, 61, 89, 90, 91, 92, 64]. The evolution equation for the effective vertex functions $\Gamma_k^{(n)}$ can be deduced from the functional differentiation of the flow (2.27) and these can be view as a differential form of the well-known Schwinger-Dyson equations [93, 94]. For an expansion in powers of the field such as (2.32), it is recognized that the choice of a configuration ϕ_0 that minimizes the effective action improves the convergence of the expansion and quantitative results thereof. This can be simply interpreted as the

consequence of the fact that the effective action is the generating function of most of the thermodynamical quantities about the minimum of the effective potential.

2.4 Regularisation

Our discussion of some approximation schemes, that are mandatory to explore non-perturbative aspects of field theory, leads us naturally to focus on the role of the regularisation scheme whose practical impact on quantitative results from functional RG can not be ignored. Indeed the choice of a specific regulator function R_k is intimately related to the convergence of any approximation of Γ_k. Although the exact flow is not concerned by this spurious dependence, the regulator function couples back to all operators appearing in the approximated action. This interdependence between approximation and regularisation was first emphasized in [95] in the framework of the perturbative approach to QCD. In the context of renormalisation group methods this aspect was adressed in [96, 70, 71] with the aim of formulating an optimised version of the RG flow equation providing improved precision. As a first example of regularisation we indicate here the exponential regulator

$$R_k(q^2) = \frac{Z_k\, q^2}{e^{q^2/k^2} - 1} \tag{2.33}$$

that has been used in the earliest functional renormalisation group calculations [24, 97] for scalar theories. It offers a smooth transition between hight and low momenta and an exponential suppression of lowest modes. It also provides a reasonable precision comparatively to other regulator choices and its impact on the convergence of the derivative expansion was studied in [83]. Unfortunately the flow of the potential, using such regulator, can not be represented by a closed analytical form. Another choice is the extreme case of an abrupt separation of modes through a sharp regulator

$$R_k(q^2) = Z_k\, k^2 \left(\frac{1}{\Theta(k^2 - q^2)} - 1 \right) \tag{2.34}$$

where $\Theta(x)$ represents the Heaviside step function. Although it allows for analytic computation of the subsequent flow equations, it is also plagued by poor convergence properties and non-analyticity problems. In this case the momentum contribution comes from an extremely narrow range around k^2. Finally, as a last example, we mention the so-called optimized regulator cutoff introduced in [71]. It has been established mainly following an optimisation criteria detailed in [70] and based on the maximisation of the gap shown by the inverse effective propagator due to its infrared regularisation. It is given by the expression

$$R_k(q^2) = Z_k\, (k^2 - q^2)\, \Theta(k^2 - q^2). \tag{2.35}$$

Beyond the fact that it provides an improved convergence towards physical results like critical exponents for scalar models [72] it entails a mass-like dependence of the inverse effective propagator with no distinction between modes when $q^2 < k^2$. This property is of the utmost importance when we deal with very low momenta behaviour close to a convex full effective action. We outline that the regulator (2.35) will be used exclusively in chapter 3 for a thorough study of the scale invariant solutions of the flow of the effective potential at the level of the LPA.

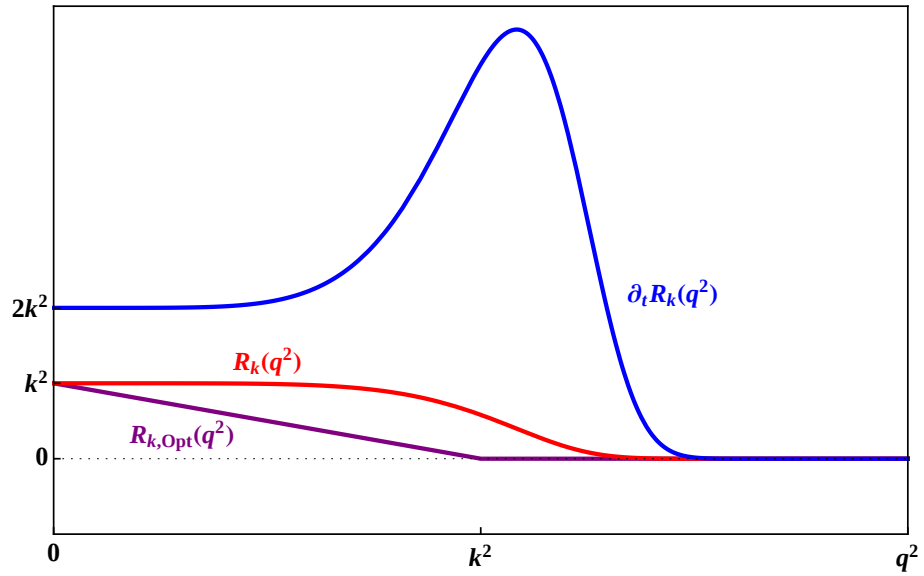

Figure 2.1: Typical form of a cutoff function $R_k(q^2)$ and its scale derivative $\partial_t R_k(q^2)$ for a function similar to (2.33). We also added, for comparison, the profile of the optimised regulator (2.35).

2.5 Effective potential

The effective potential in QFT is an object of central importance as its minimum determines the ground state of the theory and it is also the generating function of all the couplings [98]. The location of this minimum at a non-zero field value signals a spontaneous symmetry breaking of some global symmetry of the original Lagrangian [99]. In the context of phase transitions, this feature is essential as a particular global symmetry is associated to a specific phase of the statistical system for a given temperature (or an equivalent parameter).

2.5.1 The local potential approximation

Having stated the physical motivation for the calculation of an effective scale-dependent potential we derive in this section an evolution equation for it. As an approximation for the effective action we use the Ansatz (2.31) where we consider a collection of N scalar fields with a global $O(N)$ symmetry. Thanks to this global symmetry the action depends only on the modulus of the scalar vector within field space. Therefore we can choose the vector to be represented by $\vec{\phi} = (\phi, 0, \ldots, 0)$ without any lost of generality. On top of this, we defined the square of the field modulus to be

$$\bar{\rho} = \frac{1}{2}\,\phi^2\,. \tag{2.36}$$

Then considering the Ansatz (2.31) for a uniform field configuration ϕ and differentiating with respect to the logarithmic scale we get

$$\partial_t \Gamma_k[\phi] \;=\; \Omega\;\partial_t U_k(\phi) \tag{2.37}$$

where $\Omega \equiv \int d^d x$ is the volume. Following the flow equation (2.27), the remaining step is to evaluate the second functional derivative of the effective action. This process is done in Fourier space and leads to

$$\frac{\delta^2 \Gamma_k}{\delta\phi_a(q)\delta\phi_b(-q)} = \Big[\, q^2 + U'(\bar{\rho})\,\Big]\,\delta_{ab} + \phi_a\phi_b\,U''(\bar{\rho})\,. \tag{2.38}$$

The last expression can be interpreted as a $N \times N$ matrix which is diagonal in field space. Then we can invert it so that the flow of the effective potential in momentum space reads

$$\partial_t U_k(\bar{\rho}) = \frac{1}{2}\int \frac{d^d q}{(2\pi)^d}\,\partial_t R_k \left\{ \frac{N-1}{M_0(\bar{\rho}, q^2)} + \frac{1}{M_1(\bar{\rho}, q^2)} \right\}. \tag{2.39}$$

with

$$M_0(\bar{\rho}, q^2) \;=\; q^2 + R_k(q^2) + U'(\bar{\rho})\,, \tag{2.40}$$

$$M_1(\bar{\rho}, q^2) \;=\; q^2 + R_k(q^2) + U'(\bar{\rho}) + 2\bar{\rho}\,U''(\bar{\rho})\,. \tag{2.41}$$

If we are in the symmetric phase of our model then the potential minimum seats at vanishing field $\bar{\rho}_0 = 0$. As we neglected the effect of the renormalisation of the kinetic term in this phase the squared particle masses are given by the curvature of the potential at the origin $M^2 = U'(0)$. The broken phase is realized when the minimum is located at non-vanishing field i.e $\bar{\rho}_0 \neq 0$. Then one identifies the mass amplitudes for the radial $M^2 = U'(\bar{\rho}_0) + 2\bar{\rho}_0\,U''(\bar{\rho}_0)$ and for the $(N-1)$ Goldstone modes $M^2 = U'(\bar{\rho}_0)$. In order

to study with more precision the flow (2.39) and its connection with critical phenomena it is convenient to introduce the dimensionless variables

$$\begin{cases} y &= \dfrac{q^2}{k^2} \\ u_k &= \dfrac{U_k}{k^d} \\ \rho &= \dfrac{\bar{\rho}}{k^{d-2}} \end{cases} \tag{2.42}$$

and the dimensionless version of the regulator is simply $r(y) = R(q^2)/q^2$. Also the flow (2.39) depends only on q^2 so that the angular integration can be performed using the formula

$$\int_{-\infty}^{+\infty} \frac{d^d q}{(2\pi)^d}\, f(q^2) \;=\; v_d \int_0^{+\infty} dx\, x^{d/2-1} f(x) \tag{2.43}$$

with $v_d^{-1} = 2^d \pi^{d/2} \Gamma(d/2)$. Using the system (2.42) and the formula (2.43) the flow (2.39) can be written in a compact and scale independent way

$$\partial_t u = (d-2)\rho u' - du + v_d(N-1)\,\ell(u') + v_d\,\ell(u' + 2\rho u'') \tag{2.44}$$

where we dropped the scale index on u from now on. The first two linear terms on the right and side of (2.44) corresponds to the classical scaling of respectively the field ($[\bar{\rho}] = d-2$) and the effective potential ($[U] = d$). We introduce as well the dimensionless inverse propagator

$$P^2 \;=\; y\Big[1 + r(y)\Big] \;\equiv\; \frac{1}{k^2}\Big[q^2 + R_k(q^2)\Big] \tag{2.45}$$

which is involved into the expression of the nonlinear part of (2.44). The dimensionful counter part of (2.45) is simply given by $(q^2 + R_k)$ which approaches zero for small momenta q^2 and small k. The nonlinear part of the flow encodes the non-perturbative quantification of the effective potential and is expressed in terms of the so-called threshold function

$$\ell(\omega) = \frac{1}{2}\int_0^{\infty} dy\, y^{d/2-1}\, \frac{\partial_t r(y)}{P^2 + \omega} \tag{2.46}$$

for an arbitrary amplitude ω. At our level of approximation (LPA) the scale derivative of the dimensionless regulator simply reads $\partial_t r(y) = -2y r'(y)$. The function (2.46) dictates the precise way in which momenta are integrated out. The generic behaviour of the threshold function is analysed in some detail in [25]. In our case we will be particularly interested in the situation where $P^2 + \omega$ approaches zero. This is possible in the broken phase, when ω is negative and approaches the negative value of the propagator at its minimum. In this regime the threshold function (2.46) diverges and this phenomenon is closely related to the fact that the potential must be convex in the limit $k \to 0$. In dimensionful units, the precise pole structure of the threshold function is given by evaluating

$q^2 + R_k(q^2)$ at its minimum with respect to q^2 (see chapter 5). There the convexity bound is reached for $k^2(c+\omega) \to 0$ as k approaches zero and where the value of $q^2 + R_k(q^2)$ at its minimum is ck^2. From this we recover the exact bounds (2.17) and (2.18).

For practical purposes it is also useful to analyse eventual symmetries of the differential equation (2.44). For instance it is interesting to observe the effect of an homogeneous scaling in the field and potential

$$\begin{cases} \rho \to \alpha\, \rho \\ \\ u \to \alpha\, u \end{cases} \tag{2.47}$$

where α is a real scaling parameter. Then the flow is invariant under (2.47) if we admit a simple redefinition of the constant v_d. This symmetry can be exploited to absorb any common constant appearing in front of the threshold function $\ell(u')$ and $\ell(u' + 2\rho u'')$ (v_d for instance) in a redefinition of u and ρ. However (2.44) remains a nonlinear partial differential equation of the second order and no fully analytical closed-form solution has been yet found for it. Therefore one has to rely on approximated analytical solution techniques to study the flow of the effective potential. As a final comment it is important to note that solutions to the equation $\partial_t u' = 0$ are scale invariant solutions of the flow among which some of them may correspond to physical fixed point solutions. In practice the equation $\partial_t u' = 0$ is an ordinary differential equation for u' whose solution depends on boundary conditions. Only a specific choice of boundary conditions leads to real well-defined fixed point solutions and one can rely, for example, on a numerical integration to spot genuine fixed points (see e.g [100, 64]).

2.5.2 Beyond the local potential approximation

In the continuation of the previous calculation we would like to briefly present the next step, in the logic of the approximation (2.31), which is to include the effect of the renormalisation of the kinetic term i.e considering a non-vanishing anomalous dimension η. In this case the Ansatz (2.31) is slightly modified to become

$$\Gamma_k[\phi] = \int d^d x \left\{ U_k(\bar{\rho}) + \frac{1}{2} Z_k \left(\partial_\mu \phi^a \, \partial^\mu \phi_a \right) \right\} \tag{2.48}$$

where the wave function renormalisation $Z_k(\rho, -\partial_\mu^2)$ is a function of field and momentum. At the lowest order of approximation we consider Z_k for constant field and momentum with $Z_k(\rho, q^2) \sim Z_k(\rho_0, q_0^2)$ in such a way that only the equation

$$\eta = -\partial_t \ln Z_k \tag{2.49}$$

is needed in addition to the flow of the effective potential. This equation is computed in [60, 24] and is summarized into the expression (in dimensionless units)

$$\eta = -\frac{8v_d}{d}\,\rho\,(u'')^2\;m^d_{2,2}(u', u' + 2\rho u'') \tag{2.50}$$

with the integral $m^d_{2,2}$ defined by

$$m^d_{2,2}(\omega_1, \omega_2) = \int_0^\infty dy\, y^{d/2}\,\partial_t\left\{\frac{(\partial_y P)^2}{(P+\omega_1)^2(P+\omega_2)^2}\right\} \tag{2.51}$$

where the operator $\partial_t \equiv -2y\partial_y$ acts only on regulator dependent term. With the inclusion of the anomalous dimension effect the dimensionless field is simply rewritten as $\rho = Z_k\, k^{2-d}\,\bar{\rho}$ and the scale derivative of the regulator $R_k(q^2) = Z_k q^2\, r(y)$ (with $y = q^2/k^2$) is now

$$\partial_t R_k(q^2) = Z_k\, k^2\left[-2y^2\, r'(y) - \eta\, y\, r(y)\right]. \tag{2.52}$$

In the same spirit the flow equation (2.44) is slightly amended due to a modification of the classical scaling dimension of the field

$$\partial_t u = (d - 2 + \eta)\rho u' - du + v_d(N-1)\,\ell(u') + v_d\,\ell(u' + 2\rho u'') \tag{2.53}$$

where the scaling of the regulator (inside the threshold function $\ell(\omega)$) is simply given by $\partial_t r(y) = -2yr'(y) - \eta r(y)$. At the level of the approximation (2.48), to solve the theory comes down to solve the coupled equations (2.53) and (2.50) which is, as an analytical task, particularly challenging. Also as the anomalous dimension is known to be negligible in the vicinity of critical infrared potential (see [24] for example) we focus principally our attention to the solution of the flow (2.44) that is expected to capture the essential physics of the infrared scaling potential.

2.6 Convexity

To close this introductory chapter, and in order to make this work more self consistent, we would like to put more emphasis on the property of convexity of the effective potential that we outlined earlier as a consequence of the Legendre transform of the Schwinger functional. This aspect will be studied in detail in chapter 5 but we believe it is useful to recall first some of the work that has been done on the subject, as well as provide a simple picture of this genuinely non-perturbative property.

The fact that the effective potential had to be a convex function of the field was first noticed in the classic references [18, 101]. A simple proof, based on the path integral formulation, is given in [102] and the problem of obtaining a non-convex quantum corrected

potential was outlined in [103]. Then, many efforts have been made in order to obtain a well-defined convex potential that takes into account the multiple minima within a perturbative evaluation of the path integral and also using a lattice approach [104, 105, 106, 107, 108]. However it should be noticed that, even if a convex potential is effectively obtained, it is always in the presence of a trivial minimum, i.e in the symmetric phase at finite volume, where the spontaneous symmetric breaking is lost. When the volume is taken to be infinite the bottom of the potential becomes flat and one is left with a degenerate a vacuum that is represented by a continuum of states instead of an expected unique minimum. Following [109], a constrained effective potential is introduced in [110] where the expectation value of the field is kept non-zero, maintaining the system in a broken phase. There a convex potential is reached in the infinite volume limit with a meaningful flattening of the inner part of the potential. Also we should mention the important alternative interpretation of the perturbative complex and non-convex potential in [21] where the imaginary part of the inner potential is related to the decay rate of unstable vacuum located between the classical minima. Finally we note the use of variational methods [111] and renormalisation group improved loop expansion [112] where the latter reference provides a careful analysis of the non-trivial saddle-point contribution to the path integral leading to the flattening of the potential. Also the Wilsonian renormalisation group approach, based on the effective average approach, has been already used in [44, 45] where the full inclusion of quantum corrections leads to a convex potential through a one-loop flow equation of the potential.

The convexity of the effective potential is a simple geometrical property that can be stated through the formal inequality

$$V(\lambda\phi_1 + (1-\lambda)\phi_2) \leq \lambda V(\phi_1) + (1-\lambda)V(\phi_2) \tag{2.54}$$

provided that λ is real and $0 \leq \lambda \leq 1$. The fields $\phi_{1,2}$ can take any values and they can also represent vector fields. The relation (2.54) concretely means that a linear interpolation between the two points ϕ_1 and ϕ_2 is always larger or equal to $V(\phi)$ itself. In other words, any segment between two points belonging to the curve representing V do not intersect with the curve of V (see figure 2.2). The inequality (2.54) is a direct consequence of the semi-positivity of the second functional derivative of the action stated in (2.9) which, in turn, resulted from the Legendre transform of the Schwinger functional. Indeed the second functional derivative of $W[J]$ is given by the 2-point function that fulfills the inequality

$$\frac{\delta^2 W}{\delta J \delta J} = \langle\phi\phi\rangle - \langle\phi\rangle\langle\phi\rangle \geq 0 \tag{2.55}$$

which is nothing else but one of the Griffiths inequalities that states that a pair correlation is positive or nul [113]. Then we clearly see that, through the exchange of variables ϕ and J, the Legendre transform ensures a convex effective action hence a convex potential.

In the context of the application of (functional) renormalisation group techniques to the computation of the effective potential, it is also important to precise the meaning of a convex potential in the presence of a infrared cutoff scale k^2. In such case, as we detailed earlier, only fluctuations with momenta $q^2 \geq k^2$ are actually included in the evaluation of $U_k(\bar{\rho})$. Consequently, only in the limit $k \to 0$ we recover the full convex effective potential $V = U_{k\to 0}$. Also, as long as $k > 0$ the potential U_k does not have to be convex and the approach to a flat potential due to the effects of long-distance fluctuations is controled by the infrared scale k as we stay in the broken phase. A typical flattening of the non-convex part of the potential potential is given by the relation [45] (see also chapter 5 and reference therein)

$$U_k'(\bar{\rho}) \;=\; -\,\alpha\, k^2 \tag{2.56}$$

where the prime corresponds to a differentiation with respect to $\bar{\rho} = \phi^2/2$ and α is a constant that depends on the specific infrared regularisation. From (2.56) we directly see that when $k \to 0$ the curvature U_k' of the potential vanishes leading to a flat hence convex function of the field. In terms of the dimensionless units (2.42), the relation (2.56) is even more simple thanks to the relation $u_k'(\rho) = U'(\bar{\rho})/k^2$ which implies that when all fluctuations are integrated (i.e $k \to 0$) the derivative of the dimensionless potential simply approaches

$$u_k'(\rho) \;=\; -\,\alpha. \tag{2.57}$$

as $k \to 0$. Indeed the convexity bound (2.57) is related to the singularity structure of the threshold function (2.46) which depends on the choice the dimensionless cutoff function $r(y)$. The position of the pole is irrelevant for the convexity approach and consequently the constant α can be normalised to one. Only the nature of the nature of the singularity is relevant here and, at this level, we refer the reader to the chapter 5 for a complete discussion of the convexity approach within the functional renormalisation group.

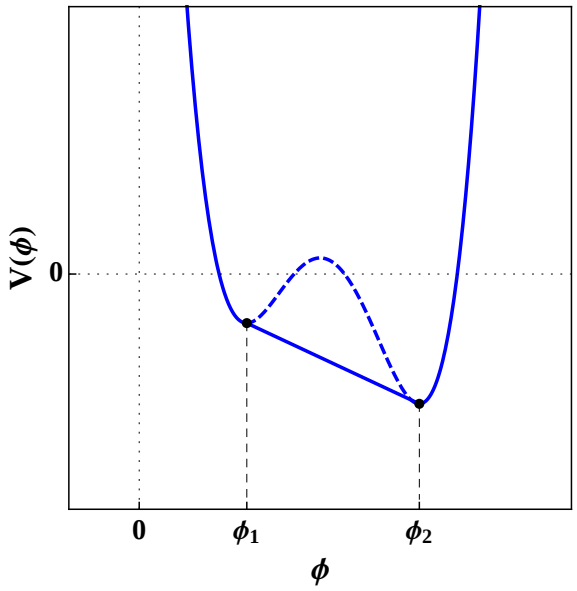

Figure 2.2: Example of an effective potential $V(\phi)$ with two different minima at ϕ_1 and ϕ_2. The non-convex part corresponds to the dashed line whereas the full line represents a strictly convex potential with $V''(\phi) > 0$.

Chapter 3

Fixed points

In this chapter we study in detail the scaling effective potential for a 3-dimensional $O(N)$ scalar theory. We compute the exact expression of the critical potential when only transverse modes are included ($N \to \infty$) and give an extensive analysis of the fixed point structure of the theory. When N is finite, the presence of a longitudinal mode allows for an analytical solution at the leading order of the derivative expansion only through local expansions. In this case a numerical input is used to fix parameters expansion allowing for the calculation of critical indices related to the Wilson-Fisher solution. In both cases, finite and infinite N, local expansions around finite values of the field and asymptotic expansions are provided. This allows for a complete and comprehensive picture of the scaling potential.

3.1 Critical flow

We start by discussing briefly the critical flow equation at the level of the local potential approximation. It is also argued that critical exponents, characterising second-order phase transition, can be computed from scaling flow equations, therefore the study of critical flow provides a reliable approach to the infrared scaling potential.

3.1.1 Critical local potential

In the previous chapter we detailed how Wilson's ideas on the renormalisation group can be formulated through functional methods, allowing for a flexible choice of approximation schemes for the effective action. In particular, an expansion of the action in terms of derivatives of the field was used to derive an evolution equation for the effective potential. It is an important fact that even at the lowest order of this approximation, i.e the local

potential approximation (LPA), reliable quantitative results can be extracted from flows similar to (2.44) in the critical regime, as long as quantum corrections to the propagator are neglected [87]. Over the years many results have been accumulated within the LPA with different implementations of Wilsonian renormalisation (for instance see [46, 114] and references therein). For our analysis we use the flow equation for the effective potential proposed in [23] in its optimised version [72]. This equation provides a unified treatment of $O(N)$ invariant scalar theories with a good estimation of critical indices for a reasonable calculational effort. Choosing $r(y) = (1/y - 1)\Theta(1 - y)$ [70], the equation (2.44) in three dimensions reads simply

$$\partial_t u = \rho u' - 3u + \frac{N-1}{1+u'} + \frac{1}{1+u'+2\rho u''} \tag{3.1}$$

where the prime indicates a derivative with respect to the dimensionless field squared $\rho = \phi^2/2$. Notice that a numerical factor $\alpha = 4\pi^2$ has been absorbed into the potential and the field using the rescaling (2.47). Scale invariant solutions to (3.1) are potential for which $\partial_t u' = 0$ and they include the Gaussian and the Wilson-Fisher fixed point solutions [71]. Following this remark the scaling effective potential fulfils the equation

$$0 = \rho u'' - 2u' - (N-1)\,\frac{u''}{(1+u')^2} - \frac{3u'' + 2\rho u'''}{(1+u'+2\rho u'')^2}. \tag{3.2}$$

The scaling equation (3.2) is the cornerstone of our analysis of the effective potential at criticality. It is a nonlinear differential equation that is a challenge to be solved in a closed form as long as N is kept finite. Nevertheless, even local solutions to (3.2) provide useful non-perturbative informations about the scaling effective potential that are hard to obtain otherwise. Such polynomial expressions for the scaling potential have been extensively used [24, 91, 115] and their convergence studied and demonstrated [72, 89, 90, 64].

3.1.2 Critical exponents

Once a valid solution to (3.2) has been determined, critical exponents that chararaterise the universal behaviour of the theory close to the fixed point are computable in a fairly easy way. A direct calculational method consists in a perturbation $\delta u'$ around a particular fixed point solution $u'_\star$ of (3.2). This can be implemented through the replacement $u' \to u'_\star + \delta u'$ in the full flow (2.44). Then the problem reduces to the eigenvalue equation

$$\partial_t \delta u^{(n)} = \omega_n\, \delta u^{(n)} \tag{3.3}$$

for the eigenperturbation $\delta u^{(n)}$ around the n-derivative of the fixed point solution $u'_\star$. The response to the scaling induced by the operator ∂_t on $\delta u^{(n)}$ is proportional to the

perturbation itself accordingly to the eigenvalue ω_n. The critical index ν is related to the first eigenvalue through

$$\nu = -\frac{1}{\omega_0} \tag{3.4}$$

and $\omega_1 > 0$ represents the first smallest irrelevant eigenvalue. At the physical level ν drives the rate a which the (relevant) mass parameter vanishes when its bare value approaches its critical value. Interestingly, there exists an ordering relation between the first five eigenvalues such that $\omega_0 < 0 < \omega_1 < \omega_2 < \omega_3 < \omega_4$ (see [72]). The same strategy holds for arbitrary dimension and a simple illustration of this technique is given by the calculation of the spectrum ω_n around the Gaussian fixed point solution $u_\star^{(n)} = 0$ for $n \geq 1$ (see also [116]). In that case the eigenvalue problem (3.3) can be written as a linear differential equation for $\delta u^{(m)}$ [72]

$$0 = [\omega_n + d - n(d-2)]\, \delta u^{(m)} + [A(N+2m) - (d-2)\rho]\, \delta u^{(m+1)} + 2\rho A\, \delta u^{(m+2)} \tag{3.5}$$

with $A = 2/d$. Using the simple notation $x = (d-2)\rho/2A$ and $f(x) = \delta u(\rho)$ the last equation corresponds to the generalized Laguerre differential equation [117, 118]

$$0 = x\, f^{(m+2)}(x) + (\alpha + 1 - x)\, f^{(m+1)}(x) + n\, f^{(m)}(x) \tag{3.6}$$

with $\alpha = N/2 + m - 1$. In this case we consider only polynomial solutions to (3.5) which entails the discrete eigenvalue spectrum

$$\omega_n = (d-2)(n+m) - d \tag{3.7}$$

for the corresponding complete set of eigenfunctions form by the generalized Laguerre polynomials. Then the eigenperturbations are simply given by

$$\delta u^{(m)}(\rho) = L_n^{(\alpha)}(x). \tag{3.8}$$

It is now easy to note that the eigenvalues ω_n are independent of the infrared regulator as A enters only into the argument of $L_n^{(\alpha)}$ in (3.8). This can also be justified from the A-independence of the rescaled form (3.6). Coming back to the 3-dimensional case and taking $m = 0$, the Gaussian eigenvalues spectrum simply reads $\theta \equiv \omega_n = n - 3$ with n a non-negative integer, to wit

$$\theta = -3, -2, -1, 0, 1, 2, \ldots \tag{3.9}$$

Although the previous method is neat and natural it relies on a second order linear differential equation, similar to (3.5), which may be excessively demanding to solve analytically

or even numerically for perturbations around a non-trivial solution of (3.2). In this case it is useful to consider an alternative approach which requires only the knowledge of the couplings at criticality. Indeed we know that the flow of the couplings, given by the set of all beta functions $\beta_n \equiv \partial_t \lambda_n$, vanishes for a precise value of the couplings $\lambda_n = \lambda_{n,\star}$. Therefore the linearisation of the flow in the vicinity of the fixed point leads to the construction of a stability matrix whose eigenvalues are precisely given by ω_n. This stability matrix is simply expressed in terms of the beta functions

$$M_{ij} = \left.\frac{\partial \beta_i}{\partial \lambda_j}\right|_{\lambda=\lambda_\star} . \tag{3.10}$$

This general method asks essentially for the knowledge of the couplings at the fixed point $\lambda_{n,\star}$ and these correspond naturally to the Taylor coefficients of the local solution to (3.2). In the following these polynomial solutions will be computed (for N finite and infinite) around vanishing field ($\rho = 0$) and also around the minimum of the potential ρ_0 ($0 = u'(\rho_0)$). The expansion around the minimum is known to possess faster convergence properties comparatively to the expansion about vanishing field [90, 70]. Also, it should be noticed that although a polynomial solution to (3.2) can be computed to a reasonably high order, this expansion will be dependent on one or several parameters. This dependence on the parameters will be lifted exactly only when we consider the limit $N \to \infty$, otherwise we will need numerical methods to single out specific values of the parameters that corresponds to a genuine fixed point solution.

3.1.3 Classical fixed points

Before studying fixed point solutions from the scaling flow (3.2) induced by quantum/thermal fluctuations, we include a brief discussion of the classical fixed points solutions. These can arise when we consider an RG flow where the fluctuation-induced part is switched off. This lead to the linear classical flow

$$\partial_t u' + 2u' - (d-2)\rho u'' = 0 \tag{3.11}$$

in d euclidean dimensions. As it is a linear flow, it possess a Gaussian fixed point $u' = 0$. Along the same line, if we write down the flow (3.11) for the inverse $\upsilon \equiv 1/u'$, we obtain then

$$\partial_t \upsilon + 2\upsilon - (d-2)\rho \upsilon' = 0\,, \tag{3.12}$$

therefore we conclude that the theory also shows a infinite Gaussian fixed point solution about $\upsilon \equiv 1/u' = 0$ [119, 120]. The flows (3.11) and (3.12) can also be solved analytically

thanks to their simple linear structure. We find

$$u' = \rho^{2/(d-2)} H\left(\rho\, e^{t(d-2)}\right) \tag{3.13}$$

where the function $H(x)$ is fixed by boundary conditions which amounts to give the form of the bare potential at $t = 0$. Scale independent solution does not dependent on the RG "time" parameter t. This type of fixed point solution is trivially reproduced for $H(x)$ constant from (3.13) and gives the line of fixed points

$$u' = c\,\rho^{2/(d-2)}\,, \tag{3.14}$$

parametrized by the coupling c. As the mass dimension of the squared field is $[\rho] = d-2$ and $[u'] = 2$ we conclude that the coupling c is dimensionless for any dimensions. The eigenvalues corresponding to this fixed point solutions can be easily computed as we have a linear flow from which field monomials can be studied independently via $u' = \lambda_n \rho^n$ without implicit summation. We find that for the monomial basis $\lambda_n(t) = \lambda(0)\, e^{\omega_n t}$, the spectrum of eigenvalues is given by

$$\omega_n = (d-2)n - 2 \tag{3.15}$$

that are the well-known classical eigenvalues at the (infinite) Gaussian fixed point. For $n > 2/(d-2)$, we have $\omega_n > 0$ and the related couplings are infrared repulsive, approaching the infinite Gaussian fixed point. By opposition, when $\omega_n < 0$ (i.e $n < 2/(d-2)$), the coupling is attractive and approaches the Gaussian fixed point. Therefore when $\omega_n = 0$ we ends up with a marginal coupling with a finite fixed point value for u'.

3.2 Transverse modes

We start our study by the case where $N \to \infty$, i.e when only massless or transverse modes are included in (3.1). First a closed form analytical solution is found for the scaling flow equation. Then systematic expansions of this solution are provided for finite as well as asymptotic values of the field. A comprehensive analysis of the singularity structure of the critical potential is given through these expansions, that cover the entire real axis. These results will be compared to the finite N case in subsequent sections.

3.2.1 Full solution

As mentioned previously the flow (3.1) as well as its scale invariant counter part (3.2) are difficult equations to solve in a analytically closed form. However the situation is not so

hopeless considering that it still remain the parameter N corresponding to the number of scalar fields in our theory. The existence of this parameter allows for a supplementary approximation technique, the so-called large N expansion. This approximation scheme was put forward in [121, 122, 123] at leading order and it has been applied below the transition point in [124]. It has been also shown in [125] that the classical vector model in the large N limit corresponds to the spherical model solved in [126]. The large N limit entails that the anomalous dimension of the Goldstone modes vanishes with no corrections for the kinetic term and a simple momentum dependence of the propagator [50, 54]. Thus, within the LPA the large N approximation become exact and this is a specific feature of $O(N)$ symmetric scalar theories. One of the principal advantages of this limit is that it provides a non-trivial model where the critical potential can be computed in a closed form as well as all the physical quantities that derive from it. This model has been studied in many occasions within different formulations of the renormalisation group and for different regulators [58, 24, 127, 128, 88]. Technically, it suffices to divide the equation (3.1) by the parameter N and rescale the variables such that $\rho \to \rho/N$ and $u \to u/N$. After this we can take safely the limit $N \to \infty$ and reduce considerably the complexity of (3.1). Finally, we can differentiate with respect to ρ to obtain

$$\partial_t u' = \rho u'' - 2u' - \frac{u''}{(1+u')^2}. \tag{3.16}$$

Here we see that only the term corresponding to the massless modes within a broken phase survives at large N entailing a drastic simplification of the original equation (3.1). Finally, imposing the scale invariance of the potential $\partial_t u' = 0$ leads to the simple equation

$$0 = \rho u'' - 2u' - \frac{u''}{(1+u')^2}. \tag{3.17}$$

The scaling equation (3.17) can be integrated analytically in closed form by interchanging the dependent and independent variables, i.e by looking for a solution $\rho(u')$. We obtain a pair of solutions which are related by analytical continuation. For $u' \geq 0$ the solution is

$$\frac{\rho - 1}{\sqrt{u'}} - \frac{1}{2}\frac{\sqrt{u'}}{1+u'} - \frac{3}{2}\arctan\left[\sqrt{u'}\right] = c\,, \tag{3.18}$$

whereas for $u' \leq 0$ we obtain

$$\frac{\rho - 1}{\sqrt{-u'}} + \frac{1}{2}\frac{\sqrt{-u'}}{1+u'} - \frac{3}{4}\ln\left[\frac{1-\sqrt{-u'}}{1+\sqrt{-u'}}\right] = c\,. \tag{3.19}$$

The coefficient c is a free parameter of which only a specific value matches a true fixed point solution and for instance the choice $c = 0$ corresponds to the Wilson-Fisher fixed point. In this precise case the solution extends over all fields $\rho \in [-\infty, \infty]$, also exhausting

the range of available values for $u' \in [-1, \infty]$ (see Fig. 3.3). The scaling solution of (3.19) can be represented as well by a single expression using hypergeometric functions, which can be defined by the Gauss series [118, 117]

$$ {}_2F_1(a,b,c,z) = \frac{\Gamma(c)}{\Gamma(a)\Gamma(b)} \sum_{n=0}^{\infty} \frac{\Gamma(a+n)\Gamma(b+n)}{\Gamma(c+n)} \frac{z^n}{n!} \tag{3.20} $$

on the disc $|z| < 1$ and by analytic continuation elsewhere. Also, the representation (3.20) becomes meaningless when $c = 0, -1, -2, \ldots$ [129]. We notice that the branch point in (3.19) at $u' = -1$ corresponds to the branch point of (3.20) at $z = 1$ from which starts a branch cut from 1 to $+\infty$ on the real z-axis. Choosing the appropriate values for the coefficients of (3.20), the branches (3.18) and (3.19) reduce to the expression

$$ \rho = {}_2F_1(2, -1/2, 1/2, -u') + c\sqrt{u'}\,, \tag{3.21} $$

where c is the constant of integration. The expression (3.21), although implicit, provides a unified view on all possible scaling solutions at large N. As mentioned before, for $c = 0$ we recover the well-known Wilson-Fisher fixed point related to the existence of continuous phase transitions. For this case only the scaling solution describes a potential derivative u' that changes its sign for the transition from $\rho > 1$ to $\rho < 1$. Otherwise, for $c \neq 0$ the function u' remains positive (negative) for c real (imaginary). This mechanism is clear if we write the solution (3.21) like

$$ \Big[\rho - {}_2F_1(2, -1/2, 1/2, -u')\Big]^2 = c^2\, u' \tag{3.22} $$

where the left hand side remains positive for all possible values of u' and ρ. Then for $u' > 0$ the constant c is real and the sign is arbitrary and leads to a unique sextic coupling. By opposition if $u' < 0$ then c must be purely imaginary with again an arbitrary sign. The solution for $u' < 0$ defines a multivalued potential which is considered as unphysical although it shows an exceptional case when the complex constant c is taken to be infinite. This specific case is discussed in the last chapter. For the time being we concentrate on the physical solutions for $u' > 0$ represented on figure 3.2. On this figure the red curve corresponds to the Wilson-Fisher solution ($c = 0$) well-defined on the whole ρ-axis. For completeness we give as well the form of the potential at the Wilson-Fisher fixed point in terms of the field ϕ itself on figure 3.1.

For $0 < c < 3\pi/4$, we start with the set of curves interpolating between C and A and belonging to the region II_+. These solutions can be continued to $\rho < 1$ by changing $c \to -c$ and this continuation corresponds to the curves belonging to the region II_-.

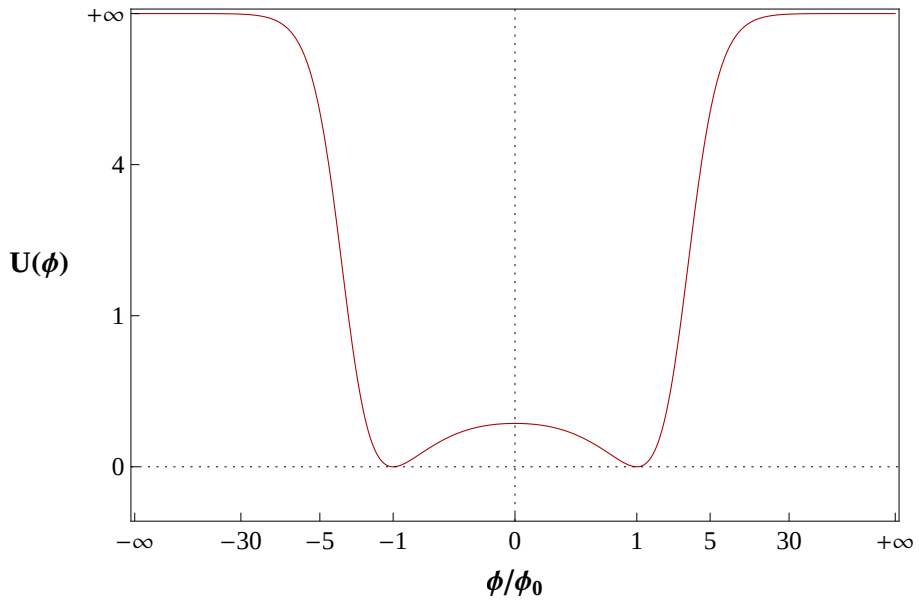

Figure 3.1: Effective potential $U(\phi)$ at the Wilson-Fisher fixed point. We used the rescaled variables $\phi \to \frac{\phi}{3+|\phi|}$ and $U \to \frac{U}{2+U}$.

There the set of curves shows a turning point at some finite value of $\rho = \rho_c > 0$ and the physical solution at strong coupling ($|c| < 3\pi/4$) is not defined on the entire positive real axis. An important change appears when we reach the specific value $c = 3\pi/4$, for $\rho > 1$ this corresponds to the continuous blue curve from C to A (upper boundary of I_+). In this case the process of continuation $c \to -c$ leads to a potential derivative singular at vanishing field (upper boundary of I_-) but well-defined for all positive ρ. This solution at $|c| = 3\pi/4$ offers a qualitatively different behaviour for large value of the field and is related to the BMB phenomenon [130, 131, 132]. The specificities of this solution will be briefly studied in chapter 4. For the time being we continue our analysis for $3\pi/4 < c < +\infty$ for which we cover the region I_+, for $\rho > 1$ with curves going from C to A. Here again the solutions can be continued to the region I_- by a simple sign change of c and u' remains positive. Finally for $|c| \to +\infty$, the curves belonging to $I_\pm$ tends to $u' = 0$ (for all ρ), the Gaussian solution, exhausting all physically plausible solution to (3.2). As we pointed out before the last regions $III_\pm$ correspond to solutions whose physical interpretation is dubious, with the existence of a turning point at some positive value of the field for all $|c| < \infty$.

Having determined a complete solution to the scaling equation (3.2) it is quite natural to look now for perturbations around it and their response to scaling. Indeed, from these perturbations we can compute critical indices related to the approach of the fixed point

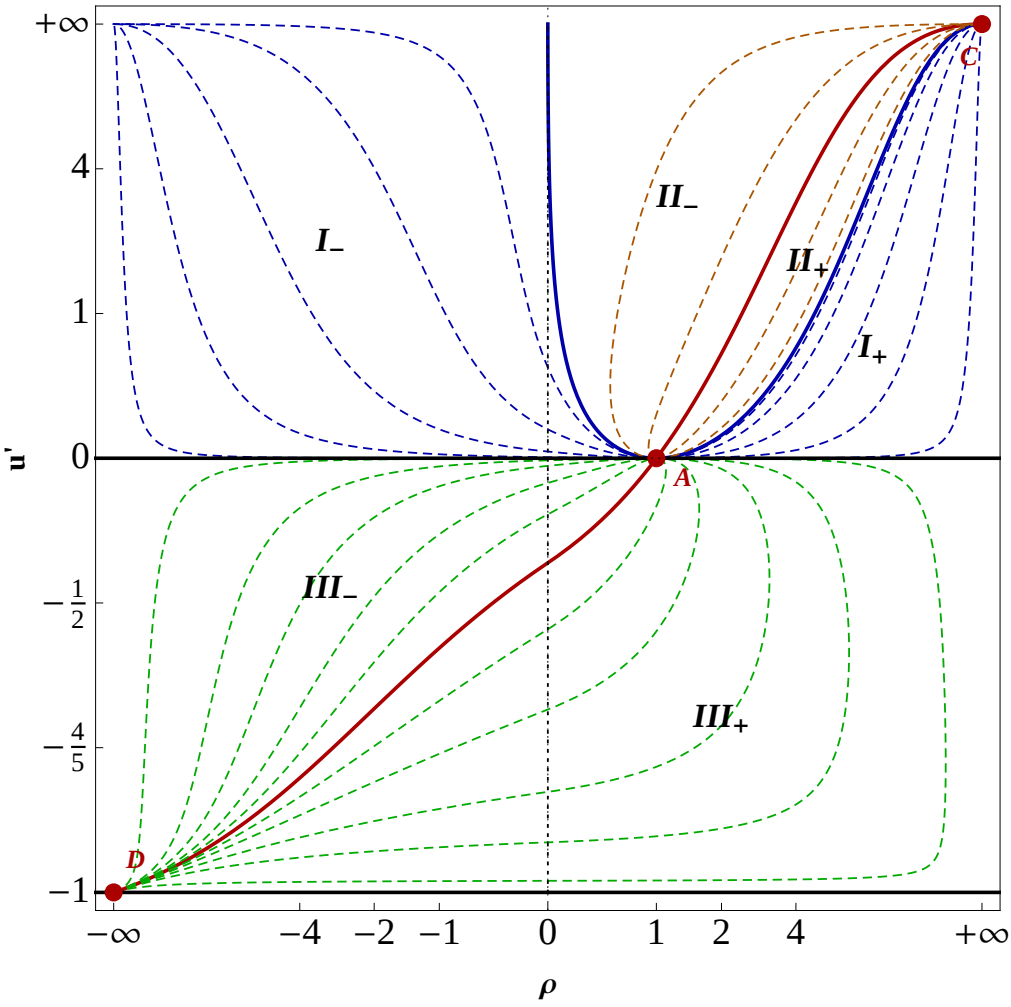

Figure 3.2: Scaling potential at large N in 3 dimensions for different values of the parameter c and an optimised infrared regulator. We rescaled the variables such that $\rho \to \frac{\rho}{3+|\rho|}$ and $u' \to \frac{u'}{2+u'}$.

solution we perturbing about, as mentioned previously. In the case of the large N limit the equation (3.3) for the eigenperturbations $\delta u'$ around a scaling solution of (3.16) is simple and can be solved in a closed form for an arbitrary scaling solution. The linear perturbation $u' \to u' + \delta u'$ (with $\partial_t u' = 0$) leads to

$$\partial_t \delta u' = 2\,\partial_\rho \left(\frac{u'}{u''}\,\delta u' \right) - 3\,\delta u'. \tag{3.23}$$

The fluctuation equation (3.23) is a separable equation that can be transformed into a pair of ordinary differential equations, one for each of the independent variables. For this

purpose we introduce $\delta u'(\rho,t) = v(t)\cdot w(\rho)$ and construct the system

$$v' = \theta\, v \tag{3.24}$$

$$w' = \frac{u''}{u'}\left[\frac{\theta+3}{2} - \partial_\rho\left(\frac{u'}{u''}\right)\right] w \tag{3.25}$$

where θ indicates the eigenvalue and u' (u'') is the first (second) derivative of the scaling potential. Both equations are easily integrable and we finally get the following expression for the eigenperturbation

$$\delta u' = C\, e^{\theta t}\, u''\, (u')^{\frac{1}{2}(\theta+1)} \tag{3.26}$$

where C is just an integration constant. The expression (3.26) allows us, in conjunction with the full solution (3.21), to compute the full spectrum of possible eigenvalues for θ, corresponding to perturbations around a specific fixed point solution. A first example to consider is the WF solution for which the solution (3.21) leads us to the local expression $u' \propto (\rho-1)$ about the minimum of the potential. If we plug this relation into the expression (3.26) we obtain that the field dependent part of the perturbation behaves like

$$\delta u' \propto (\rho-1)^{\frac{1}{2}(\theta+1)} \tag{3.27}$$

about the potential minimum. Now requiring that the perturbation is an analytic function of the field (as the WF solution) constrains us to consider only non negative integer powers in (3.27). We are then left with the spectrum

$$\theta = -1, 1, 3, 5, 7, \ldots \tag{3.28}$$

where there is only one negative eigenvalue, related to the relevant scaling of the mass. The complete spectrum is given by $\theta \equiv \omega_n = 2n-1$ where n is a non-negative integer. Through the relation (3.4) we can then conclude that $\nu = 1$ which is a well-known result from the large N approach [50]. We can as well recover the eigenvalue spectrum for the Gaussian fixed point along the same line of thought. Assuming the analyticity of the perturbation (3.26) about $u' = 0$ and $u'' = 0$ we recover

$$\theta = -3, -2, -1, 0, 1, 2, 3, \ldots \tag{3.29}$$

which is the same spectrum that we computed previously by another method. It can be summarized into $\omega_n = n-3$ with n a non-negative integer. We recall that the trivial solution $u' = 0$ is produced from (3.21) for $c \to +\infty$ (see previous discussion). This approach can also be applied for less known fixed solutions of the scaling flow (3.2). For instance, we consider an expansion for large u' from (3.21) within the range $3\pi/4 < |c| <$

$+\infty$. This corresponds to the curves interpolating between the Gaussian solution ($u' = 0$ and $|c| = +\infty$) and the BMB solution at $|c| = 3\pi/4$ (regions $I_\pm$). There, we have the asymptotic behaviour

$$u' = \frac{\rho^2}{\left(c + \frac{3\pi}{4}\right)^2} - \frac{2}{5}\left(c + \frac{3\pi}{4}\right)^2 \frac{1}{\rho^3} + \mathcal{O}\left(\frac{1}{\rho^5}\right) \tag{3.30}$$

with the local relation $u' \propto \rho^2$ for large positive field. Using this relation with (3.26), the eigenperturbations behave like $\delta u' \propto \rho^{\theta+2}$ for large field. Again, assuming the analyticity, of the perturbation we end up with the spectrum

$$\theta = -2, -1, 0, 1, 2, \ldots \tag{3.31}$$

that leads to the critical exponent $\nu = 1/2$. The two negative eigenvalues -2 and -1 relate to the mass term and the quartic coupling, and the zero eigenvalue relates to the exactly marginal ϕ^6 coupling. The result for ν matches the mean field value computed in [127] using the same functional RG method and also [133] using a variationnal approach, it is related to the tricritical behaviour of the system. This aspect will be discussed with more details in chapter 4. To conclude this section we remark that we took full advantage of the fact that the large N approximation is exact within LPA. This leads to an exact localisation of fixed point solutions (the stability matrix is diagonal) hence eigenperturbations around it conduct to exact eigenvalues.

3.2.2 Minimum

Next we turn to systematic local expansions of the critical potential, starting with the expansion about the potential minimum, denoted as expansion A. The existence of a non-trivial minimum in the fixed point solution follows from the RG flow at $u' = 0$. Therefore we can make the polynomial expansion

$$u(\rho) = \sum_{n=2}^{\infty} \frac{\lambda_n}{n!} (\rho - \rho_0)^n \tag{3.32}$$

up to some finite maximum order in the expansion. Prior to discussing the solutions, it is interesting to consider the β-functions for the relevant and marginal couplings of the Ansatz (3.32). Using the RG flow, we have

$$\begin{aligned} \partial_t \rho_0 &= 1 - \rho_0 \,, \\ \partial_t \lambda &= -\lambda(1 - 2\lambda) \,, \\ \partial_t \tau &= -6\lambda(\lambda^2 - \tau) \,, \end{aligned} \tag{3.33}$$

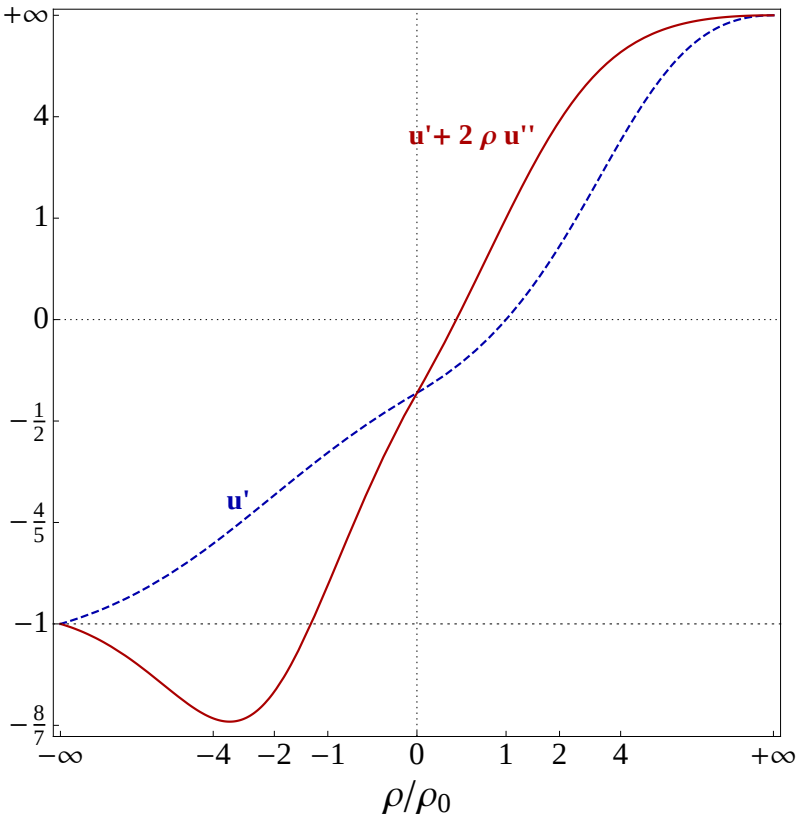

Figure 3.3: The Wilson-Fisher fixed point u'_* (dashed line) and the amplitude $u'_* + 2\rho u''_*$ (full line) for all fields.

where we used $\lambda \equiv \lambda_2$ and $\tau \equiv \lambda_3$. Note that the RG flow of the VEV ρ_0 and for the quartic interaction fully decouple from the system. The flow for the VEV displays an IR repulsive fixed point at

$$\rho_{0,*} = 1 \tag{3.34}$$

and two IR attractive fixed points at $1/|\rho_0| = 0$, corresponding to the symmetric and the symmetry broken phases of the theory. The flow for the quartic coupling displays an IR repulsive fixed point at $\lambda = 0$ and an IR attractive fixed point at

$$\lambda_* = \frac{1}{2}\,. \tag{3.35}$$

The latter is the Wilson-Fisher fixed point together with (3.34), while the former corresponds to tricritical fixed points including the BMB phenomenon [130, 131, 132, 133]. Finally, the RG flow of the sextic coupling is fully controlled by the quartic interactions. At the tricritical fixed point with (3.34) and $\lambda_* = 0$, the sextic coupling becomes exactly marginal, i.e $\partial_t \tau \equiv 0$, leaving τ as a free parameter of the theory. On the other hand, at

the Wilson-Fisher fixed point, the sextic coupling achieves the IR attractive fixed point

$$\tau_* = \frac{1}{4}\,. \tag{3.36}$$

This pattern is at the root for the entire fixed point structure of the theory. At either of the above fixed points, the expansion (3.32) allows for a recursive solution. At the tricritical point, all higher couplings λ_n with $n > 3$ become functions of the exactly marginal coupling τ. At the Wilson-Fisher fixed point, remarkably, the recursive fixed point solution is unique and free of any parameters. This is a consequence of the decoupling of both the VEV and the quartic interactions. For the first few couplings at the Wilson-Fisher fixed point, we find

$$\begin{aligned} &\rho_0 = 1\,, \quad \lambda_2 = \frac{1}{2}\,, \quad \lambda_3 = \frac{1}{4}\,, \quad \lambda_4 = \frac{3}{40}, \\ &\lambda_5 = -\frac{3}{112}\,, \quad \lambda_6 = -\frac{29}{1120}\,, \ldots \end{aligned} \tag{3.37}$$

The absolute values of the coefficients (3.37) grows roughly as

$$|\lambda_n| \approx \frac{n!}{\pi^n \ln(2\pi n)} \tag{3.38}$$

for large n, suggesting that the radius of convergence is close to $R_A \approx \pi$. The sign pattern of the coefficients to very good accuracy is given by $\sim \cos(n\phi_0 - \phi_1)$ where $(\phi_0, \phi_1) = (\frac{17}{31}\pi, 19\pi)$. The pattern is close to $(++--)$. We therefore expect that the convergence-limiting pole in the complex plane is close to the imaginary axis, under the angle $\phi_0 = 98.71°$. The standard criteria for convergence such as root or ratio tests are not applicable. We use a criterion by Mercer and Roberts [134] designed for series dominated by a pair of complex conjugate poles to estimate the radius of convergence R, the angle θ under which the convergence-limiting pole occurs in the complexified ρ-plane, and the nature of the singularity ν (see appendix A). Based on the first 500 coefficients, we find

$$\begin{aligned} R_A &= 3.18(35) \\ \theta_A &= 98.7(4)° \\ \nu_A &= 0.50(7)\,. \end{aligned} \tag{3.39}$$

We conclude that the polynomial expansion about the potential minimum determines the fixed point solution exactly in the entire domain

$$1 - R_A \leq \frac{\rho}{\rho_0} \leq 1 + R_A\,. \tag{3.40}$$

We will exploit this result below to connect the fixed point solution to its large-field solution.

3.2.3 Vanishing field

For sufficiently small fields $|\rho|$, the flow (3.16) admits a Taylor expansion in powers of the fields $\sim \rho^n$. Hence we write an order M Ansatz for u' as

$$u(\rho) = \sum_{n=0}^{M} \frac{\lambda_n}{n!} \rho^n \,. \tag{3.41}$$

The fixed point condition $\partial_t u' = 0$ translates into $M+1$ equations $\partial_t \lambda_n = 0$. The flow for the potential minimum λ_0 is irrelevant because the physics is invariant $\lambda_0 \to \lambda_0 + c$. The algebraic equations for the couplings λ_n are solved recursively in terms of $u'(0) = \lambda_1 \equiv m^2$. The reason for this is twofold. Firstly, none of the local couplings at vanishing field decouples - unlike those at the potential minimum. Secondly, the recursive solution is simplified because the fixed point equation, at vanishing field, is effectively one order lower. Consequently, the recursive solution retains one (rather than two) free parameters. We find

$$\begin{aligned}
\lambda_0 &= \frac{1}{3}(1+m^2)^{-1} \\
\lambda_2 &= -2m^2(1+m^2)^2 \\
\lambda_3 &= 2m^2(1+m^2)^3(1+5m^2) \\
\lambda_4 &= -24m^4(1+m^2)^4(1+3m^2) \\
\lambda_5 &= 48m^6(1+m^2)^5(5+13m^2) \\
\lambda_6 &= -48m^6(1+m^2)^6(-5+34m^2+119m^4)
\end{aligned} \tag{3.42}$$

for the first few coefficients, and similarly to higher order. There is a unique choice for m^2 corresponding to the Wilson-Fisher solution. There is a range of values for m^2 which corresponds to the tricritical fixed points. We also recover the (trivial) Gaussian fixed point

$$m^2 = 0 \,. \tag{3.43}$$

In either of these cases the global solution extends over all fields. Interestingly, the series expansion also displays the non-perturbative fixed point

$$m^2 = -1 \tag{3.44}$$

which entails the vanishing of all higher order couplings. It is responsible for the approach to convexity in a phase with spontaneous symmetry breaking. The convexity fixed point is only visible in the inner part of the effective potential $\rho < \rho_0$ and as such cannot extend over the entire field space. For the same reason the convexity fixed point is not visible in the expansion about the potential minimum. More details are given in chapter 5.

Returning to the Wilson-Fisher fixed point, it remains to determine the corresponding value for the mass. This can be done either by exploiting the analytical solution, or by exploiting the expansion about vanishing field. From the analytical solution, we find the mass term from solving a transcendental equation $f(m^2) = 0$, with

$$f(x) = 1 - \frac{1}{2}\frac{(-x)}{1+x} + \frac{3}{4}\sqrt{-x}\ \ln\left[\frac{1-\sqrt{-x}}{1+\sqrt{-x}}\right] \tag{3.45}$$

and $x < 0$. The unique solution reads

$$m^2 = -0.388\,346\,718\,912\,782\,\cdots\,. \tag{3.46}$$

Alternatively we may exploit that $\rho = 0$ lies within the radius of convergence (3.40) to determine m^2 from (3.37). The rate of convergence is fast. From the first 300 terms of the expansion (3.37), we checked that the first n terms suffice to reproduce $n/2$ significant figures of (3.46).

We estimate the radius of convergence for the expansion about vanishing field, which we denote as expansion B. Using (3.46) together with the first 500 terms of the expansion (3.42), we find that the coefficients grow as in (3.38) for large n, suggesting that the radius of convergence is close to $R_B \approx \pi$. The sign pattern is again close to $(++--)$, with $\phi_0 = \frac{14}{31}\pi \approx 81°$. We therefore expect that the convergence-limiting pole in the complex plane is close to the imaginary axis. Using the Mercer-Roberts technique for the first 500 terms, we find

$$\begin{aligned} R_B &= 3.18(86) \\ \theta_B &= 80.68(2)° \\ \nu_B &= 0.50(8)\,. \end{aligned} \tag{3.47}$$

Comparing with (3.39) we have $R_A = R_B$ to within our numerical accuracy. Furthermore, the nature of the singularity equally appears to be the same. Interestingly, the estimated singularity in the complex plane derived from either of the expansions (3.39) and (3.47) are the same, see Fig. 3.4. We conclude that the polynomial expansion about vanishing field determines the fixed point solution exactly in the entire domain

$$-R_B \le \frac{\rho}{\rho_0} \le R_B\,. \tag{3.48}$$

The overlap between the expansions (3.32) and (3.41) therefore allow a complete determination of the fixed point solution in the junction of (3.40) and (3.48).

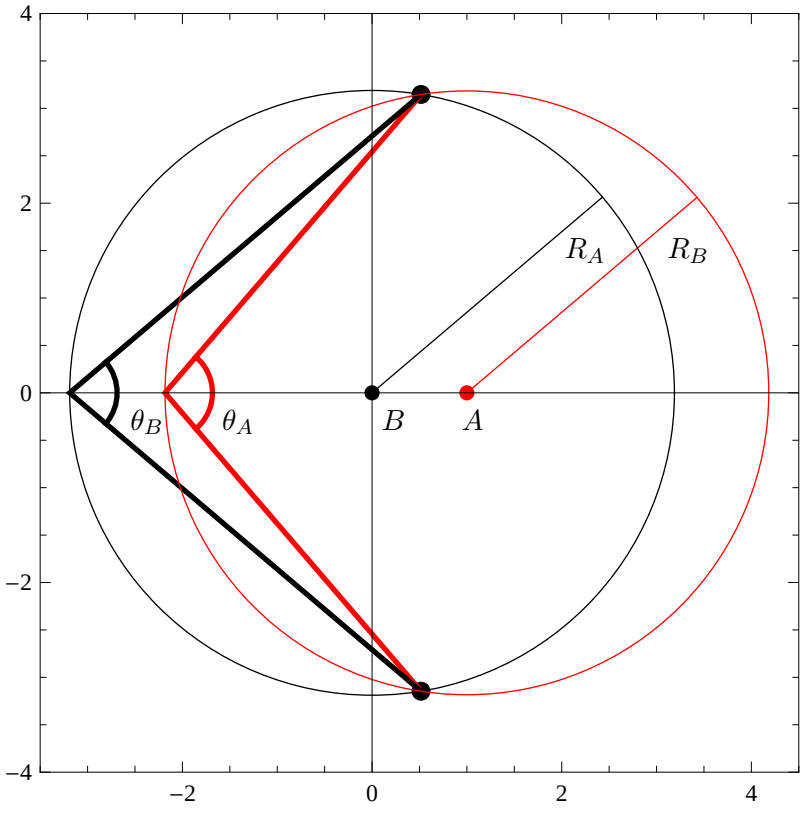

Figure 3.4: Radii of convergence for the expansions A and B of the Wilson-Fisher fixed point solution, and location of the convergence-limiting poles (dots) in the complexified ρ-plane.

3.2.4 Large fields

For asymptotically large fields $\rho/\rho_0 \gg 1$ and $u' > 0$, the quantum corrections to the RG flow become suppressed and the effective potential approaches an infinite Gaussian fixed point [120, 72, 135]

$$u'_*(\rho) = \gamma\,\rho^2 \tag{3.49}$$

where γ is a free parameter. The fixed point (3.49) is Gaussian in the strict sense that quantum effects are switched off, and the remaining scaling behaviour is a consequence of the canonical dimension of the fields. The infinite Gaussian fixed point is also approached from the Wilson-Fisher fixed point solution in the limit where $\rho_0/\rho \to 0$. Therefore we can find the Wilson-Fisher fixed point by expanding about (3.49). The Laurent expansion involves inverse powers of the field to which we will refer as expansion C. We write

$$u'(\rho) = \gamma\,\rho^2\left[1 + \sum_{n=1}^{M} \gamma_n\,\rho^{-n}\right]. \tag{3.50}$$

Inserting (3.50) into (3.16) with $\partial_t u' = 0$ leads to equations $\partial_t \gamma_n$, which are solved recursively for fixed points. Alternatively this can be achieved by introducing

$$v(x) = u'(\rho)/\rho^2\,, \quad x = 1/\rho \tag{3.51}$$

and Taylor-expanding $v(x) = \sum_{n=0} \gamma_n\, x^n$ for $x \ll 1$ (and $\gamma \equiv \gamma_0$). The interpretation of (3.51) is that the infinite Gaussian fixed point is factored out. All couplings are determined uniquely as functions of the free parameter γ, of which we have computed the first 500 coefficients. The first few non-vanishing coefficients read

$$\begin{aligned} \gamma_5 &= -\frac{2}{5\gamma^2},\ \gamma_7 = \frac{4}{7\gamma^3},\ \gamma_9 = -\frac{2}{3\gamma^4}, \\ \gamma_{10} &= -\frac{7}{25\gamma^4},\ \gamma_{11} = \frac{8}{11\gamma^5},\ \gamma_{12} = \frac{36}{35\gamma^5}, \end{aligned} \tag{3.52}$$

and similarly to higher order. Note that the first four coefficients vanish identically. One may wonder how the scaling exponents vary with the free parameter γ. The stability matrix for the flows $\partial_t \gamma_n$ has no entries on the upper diagonal, and the dependence on γ only appears on the lower off-diagonal elements. The eigenvalues then reduce to

$$\theta = 0, -1, -2, -3, -4, -5, \cdots \tag{3.53}$$

independently of the finite value $\gamma \neq 0$. The vanishing eigenvalue signals that γ is an exactly marginal coupling at the infinite Gaussian fixed point (3.49). The remaining eigenvalues measure the canonical dimension of the field monomials $1/\rho^n$, and the negative

sign states that this fixed point is UV attractive in all couplings except for the marginal one. Note that the global Wilson-Fisher fixed point solution connects to this set of fixed points for a specific value of the parameter γ, despite the fact that the scaling properties seem different. In fact, the Wilson- Fisher fixed point corresponds to

$$\gamma = \frac{16}{9\pi^2} = 0.180\,126\,548\,697\,489\,\cdots \tag{3.54}$$

This unique value either follows from the closed analytical solution (3.18), or from matching to the expansion A using (3.37) in a regime where both radii of convergence overlap. Using the same techniques as before, we estimate the radius of convergence from the first 500 coefficients of the expansion (3.52) as

$$\begin{aligned} R_C &= 3.18(85), \\ \theta_C &= 80.68(3)^\circ, \\ \nu_C &= 0.4(79)\,. \end{aligned} \tag{3.55}$$

Comparing (3.55) with (3.39) and (3.47) we have $R_A = R_B = R_C$ to within our numerical accuracy. Furthermore, the angle and the radius under which the singularity appears for the Laurent series in $1/\rho$ and for the Taylor series about ρ are identical, within our numerical accuracy. We conclude that the Laurent series about asymptotic fields determines the fixed point solution exactly in the entire domain

$$R_C \leq \frac{\rho}{\rho_0}\,, \tag{3.56}$$

and the overlap between the expansions (3.32), (3.41) and (3.50) therefore allows a complete determination of the fixed point solution in the junction of (3.40), (3.48) and (3.56).

3.2.5 Imaginary fields

Finally we turn to the regime of purely imaginary fields, corresponding to negative ρ and the regime where $u' < 0$. For small imaginary fields, the Taylor expansion (3.41) is applicable since the radius of convergence (3.47) is finite and extends to negative values. For large negative ρ or large imaginary fields $\pm i\varphi \to \infty$, the presence of the term $\sim u''/(1+u')^2$ in the flow equation implies that $-1 \leq u' < 0$. This is different from the behaviour at large positive ρ where $0 < u'$, see previously. We find that the fixed point solution approaches

$$u'_*(\rho) = -1 \tag{3.57}$$

for asymptotically large negative ρ, thereby exhausting the domain of achievable values for u'. This is the non-perturbative fixed point of convexity, which is approached in a

phase with spontaneous symmetry breaking where $u'(\rho) \leq 0$ (see chapter 5). Since the Wilson-Fisher fixed point solution has $u' < 0$ for field values below the VEV, it must be possible to re-cover it through an expansion about (3.57), which we denote as expansion D. The full asymptotic expansion of the Wilson-Fisher fixed point $u'(\rho)$ about (3.57) for large negative ρ contains inverse powers of the fields, powers of logarithms of the field, and products thereof. The set of non-trivial operators appearing in the fixed point solution is given by the Ansatz

$$u'(\rho) = -1 + \sum_{m=1}^{M} \sum_{n=0}^{m-1} \zeta_{m,n} \, (-\rho)^{-m} \, \ln^n(-\rho) \, . \tag{3.58}$$

The structure of (3.58) can be understood as follows. In the limit where $u' + 1 \to 0^+$, the first term in (3.16) approaches 2, while the second term is subleading. Therefore, the first and the last term in (3.16) have to cancel, which is the case if

$$0 \leq 1 + u' = \frac{1}{2(-\rho)} + \text{subleading} \, . \tag{3.59}$$

The next-to-leading term must contain a logarithm $\sim \ln(-\rho)/(-\rho)^2$ or else the fixed point condition cannot be satisfied. This leads to the pattern (3.58). Inserting (3.58) into (3.19) we find $\frac{1}{2}M(M+1)$ algebraic equations for the expansion coefficients $\zeta_{m,n}$, all of which can be solved recursively in terms of a single free parameter $\zeta \equiv \zeta_{2,0}$. The first few coefficients are

$$\begin{aligned}
\zeta_{1,0} &= \frac{1}{2} \, , \quad \zeta_{2,1} = \frac{3}{8} \, , \quad \zeta_{3,2} = \frac{9}{32} \, , \\
\zeta_{3,1} &= \frac{3}{8}(4\zeta - 1) \, , \quad \zeta_{3,0} = -\frac{1}{32}(9 + 32 - 64\zeta^2) \, , \\
\zeta_{4,3} &= \frac{27}{128} \, , \quad \zeta_{4,2} = \frac{27}{256}(16\zeta - 7) \, , \\
\zeta_{4,1} &= -\frac{3}{256}(25 + 336\zeta - 384\zeta^2) \, , \\
\zeta_{4,0} &= -\frac{1}{512}(99 - 400\zeta - 2688\zeta^2 + 2048\zeta^3) \, .
\end{aligned} \tag{3.60}$$

Using the exact result, we find

$$\zeta = \frac{3}{8}(3 \ln 2 - 2) = 0.029\,790\,578\,129\,938 \cdots \tag{3.61}$$

On the contrary to the expansion about $\rho = +\infty$, the leading behaviour of the potential close to the boundary $u' = -1$ is expected to be highly sensible on the infrared regularisation. Indeed for large imaginary field the regulator dependent term in (3.16) is now dominating the flow at criticality.

To estimate the convergence radius of the expansion D we adopt an iterative version of the Mercer-Roberts technique to account for the logarithms. We write the series $u' = -1 +$

$\sum \tau_m(\rho)(-\rho)^{-m}$ in terms of coefficients $\tau_m(\rho) = \sum_{n=0}^{m-1} \zeta_{m,n} \ln^m(-\rho)$. Since the logarithm varies only slowly compared to powers, we approximate the coefficients $\tau_m = \tau_m(R^{(0)})$ for some trial coordinate $\rho = R^{(0)}$ to determine the radius of convergence $R^{(1)} = f(R^{(0)})$, subject to the initial choice $R^{(0)}$. Subsequently the initial choice is replaced by the first estimate $R^{(1)}$ to provide the input for the second estimate $R^{(2)} = f(R^{(1)})$ and so forth, until the procedure has converged towards a fixed point $R_D = f(R_D)$. Based on the first 100 coefficients $\zeta_{m,n}$ we find a rapid convergence with

$$R_D = -1.511(97)\,, \tag{3.62}$$

implying the expansion fully determines the solution in the domain

$$\frac{\rho}{\rho_0} \leq R_D\,. \tag{3.63}$$

Most importantly, the domain overlaps with both (3.40) and (3.48). We conclude that the unique Wilson-Fisher fixed point solution in the local expansion about the minimum A actually fixes the fixed point fixed point solution globally, for all fields.

3.2.6 Discussion

The main results of this section are summarized in figure 3.5, where we compare the analytical Wilson-Fisher fixed point solution with analytical approximations. Four expansions including their respective radii of convergence are indicated. The local polynomial expansions about vanishing field and the potential minimum are referred to as A and B, and the large real and imaginary field expansions are denoted as C and D, respectively. Each of these have a radius of convergence and a domain of validity

$$\begin{aligned} -R_A < \rho < R_A \\ 1 - R_B < \rho < 1 + R_B \\ R_C < \rho < \infty \\ R_D < -\rho < \infty\,. \end{aligned} \tag{3.64}$$

To estimate the radii for the polynomial expansions A, B and C we have computed the first 500 coefficients analytically. The coefficients have fluctuating signs and standard tests for convergence such as the root test converge very slowly. We use the method by Mercer and Roberts, developed for series expansions governed by near-by singularities in the complex plane. We find that all three radii of convergence R_A, R_B and R_C approach the same value R_c given by

$$R_c \;=\; 3.188\cdots \tag{3.65}$$

within numerical errors. This implies that the small-field expansion about vanishing A field asymptotically touches, without overlap, the large field expansion C. Also, the expansion about the potential minimum has the same radius of convergence as the one about vanishing field. Therefore the expansions B and C overlap in the regime between $\rho = \rho_R$ and $\rho = \rho_R + 1$. For the expansion D we have analysed the first 100 coefficients. Due to the logarithmic terms the convergence of the expansion is slower and the radius of convergence is estimated in comparison with the exact result. The most important overlap region is the one between B and C, which is sufficient to cover the whole positive real axis. At the present order, the accuracy is never below $|\partial_t u'| < 10^{-30}$ for all fields. There is also an overlap between A and C, though here the accuracy drops to the percent level. For negative ρ, we find a fair overlap between the expansions A and D, and B and D. In these cases, the accuracy is only limited by the expansion about D, which we have not pushed to the same order.

For completeness we plotted on figure 3.3 the amplitudes u' and $u' + 2\rho u''$. When $N < \infty$ the latter corresponds to the mass of the radial mode. In accordance with the convexity bound u' remains always larger than -1 and tends to this asymptotic value as $\rho \to -\infty$, thus avoiding the flow to diverge for finite values of the field. On the contrary $u' + 2\rho u''$ drops innocuously below -1 for $\rho \lesssim 1.26\cdots$ as only Goldstone modes are considered there. On a global level we note the inversion of the amplitudes at vanishing field. Despite the fictitious character of the radial mass amplitude when $N \to \infty$ it is instructive to detail the behaviour of our solution around $u'_\star = -1$ where contributions from massive and massless modes are fundamentally differentiated. This will be fully appreciated in the next section where the approach towards $u'_\star$ is detailed in the presence of a radial mode .

3.3 Longitudinal mode

Now we consider the presence of a radial mode with the full equation (3.2) adding the term

$$-\frac{3u'' + 2\rho u'''}{(1 + u' + 2\rho u'')^2} \tag{3.66}$$

in comparison with the previous treatment at large N. For the time being we also stay with a continuous symmetry by keeping $N > 1$ and the Ising model $N = 1$ will be discussed in the next section. The inclusion of the term (3.66) makes the search for an analytical solution virtually impossible. However approximated analytical solutions are still available through polynomial expansions similar the large N case. This will allow us

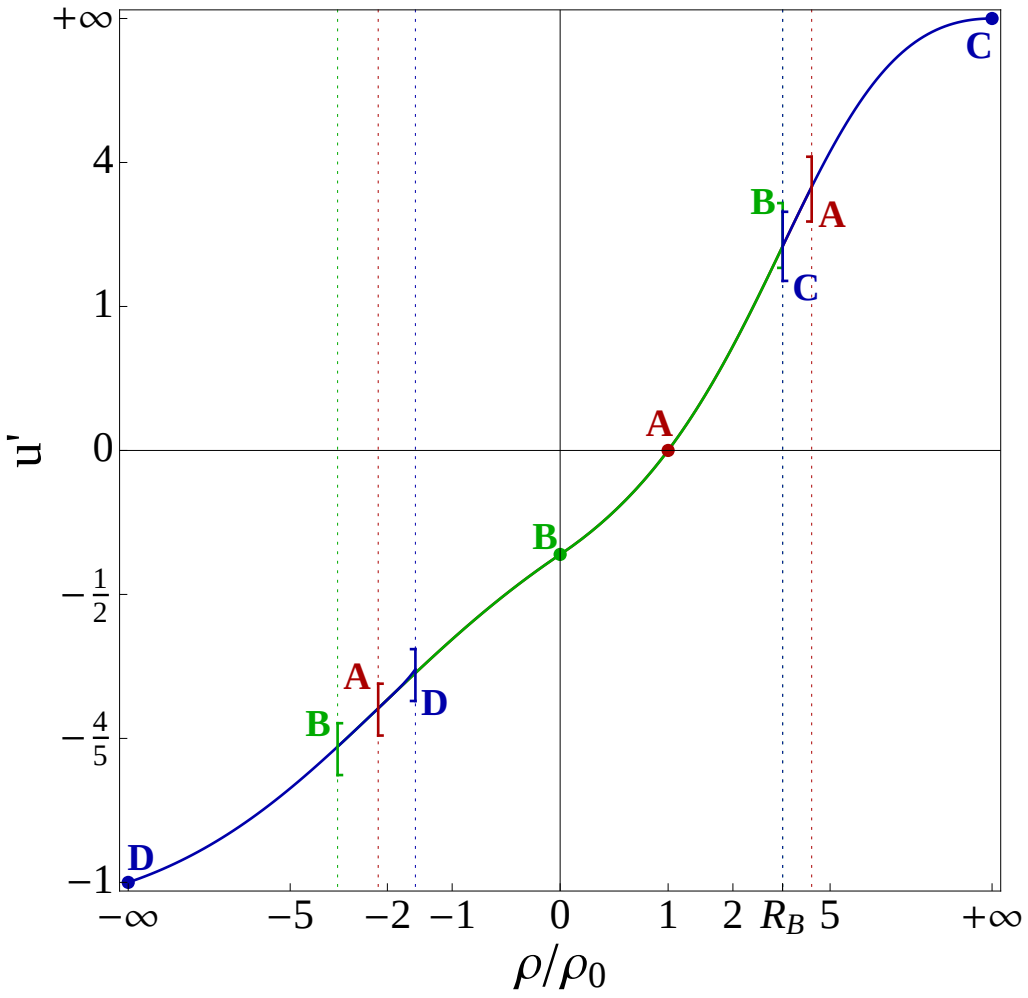

Figure 3.5: The Wilson-Fisher fixed point solution u'_* for all fields. The four local expansions A, B, C and D and their respective radii of convergence are indicated. The expansion A yields a unique local Wilson-Fisher solution. Its overlap with B, C and D then extends the local to a global solution for all fields.

to analyse the competition between massive and massless modes especially when we are close to the convexity bounds for negative u'.

3.3.1 Minimum

We begin with an expansion about the potential minimum ρ. This expansion is of the form

$$u(\rho) = \sum_{n=2}^{M} \frac{\lambda_n}{n!} (\rho - \rho_0)^n \tag{3.67}$$

and leads to coupled ordinary differential equations for the couplings and the VEV. The flow for the VEV and the two first couplings $u''(\rho_0) = \lambda_2 \equiv \lambda$ and $u'''(\rho_0) = \lambda_3 \equiv \tau$ are

$$\partial_t \rho_0 = N - 1 - \rho_0 + \frac{1}{\lambda} \frac{3\lambda + 2\tau\rho_0}{(1 + 2\lambda\rho_0)^2}\,, \tag{3.68}$$

$$\partial_t \lambda = \rho_0\,\tau - \lambda(N-1)(2\lambda^2 - \tau) - \frac{2\lambda_4\rho_0 + 5\tau}{(1+2\lambda\rho_0)^2} + \frac{2(3\lambda + 2\tau\rho_0)^2}{(1+2\lambda\rho_0)^3}\,, \tag{3.69}$$

$$\begin{aligned}\partial_t \tau &= \lambda_4\rho_0 - (N-1)(6\lambda^3 - 6\lambda\tau + \lambda_4) - \frac{2\lambda_5\rho_0 + 7\lambda_4}{(1+2\lambda\rho_0)^{\,2}} \\ &\quad + \frac{6\,(2\lambda_4\rho_0 + 5\tau)\,(3\lambda + 2\tau\rho_0)}{(1+2\lambda\rho_0)^{\,3}} - \frac{6\,(3\lambda + 2\tau\rho_0)^{\,3}}{(1+2\lambda\rho_0)^{\,4}}\end{aligned} \tag{3.70}$$

and similarly for the flow of higher couplings. We note that, in contrast to the large N case, the flow for the VEV no longer decouples. The dependence on the quartic and sextic interactions implies that the recursively obtained fixed point solution will depend on two free parameters. By using the same iterative procedure as before we arrive at expressions for all expansion coefficients in terms of only two free parameters, $u''(\rho_0) = \lambda_2 \equiv \lambda$ and the minimum ρ_0:

$$\lambda_n = \frac{\lambda}{(2\rho_0)^{n-2}}\; P_n(\lambda, \rho_0, N) \tag{3.71}$$

where $P_n(\lambda, \rho_0, N)$ are N-dependent polynomials in ρ_0 and λ, *eg.*

$$P_3 = -(N+2) + \Big(1 - 4\lambda(N-1)\Big)\,\rho_0 + 4\lambda\Big(1 - \lambda(N-1)\Big)\,\rho_0^2 + 4\lambda^2\,\rho_0^3\,, \tag{3.72}$$

$$\begin{aligned}P_4 &= (N+2)(N+4) + \Big(12(N^2+N-2)\lambda - 2(N+4)\Big)\,\rho_0 \\ &\quad + \Big(12(N^2+N-2)\lambda - 2N - 8\Big)\,\rho_0^2 \\ &\quad + \Big(48(N-1)N\lambda^2 - 8(3N+2)\lambda + 1\Big)\,\rho_0^3 \\ &\quad + 4\lambda\Big(4(5N^2 - 9N + 4)\lambda^2 + (14 - 24N)\lambda + 3\Big)\,\rho_0^4 \\ &\quad + 16\lambda^2\left(3(N-1)^2\lambda^2 - 10(N-1)\lambda + 3\right)\rho_0^5 + 48\lambda^4\,\rho_0^6\end{aligned} \tag{3.73}$$

Higher coefficients have a similar form but their expressions are too lengthy to be reproduced here.

3.3.2 Vanishing field

For small fields, the flow is solved by Taylor-expanding the potential as

$$u(\rho) = \sum_{n=0}^{m} \frac{\lambda_n}{n!}\,\rho^n\,, \tag{3.74}$$

in field monomials ρ^n. Inserting (3.74) into (3.1) leads to unique algebraic expressions for λ_n with $n \neq 1$ as functions of $\lambda_1 \equiv m^2$. The explicit solution is of the form

$$\begin{aligned} \lambda_0 &= \frac{N}{3(1+m^2)}\,, \\ \lambda_n &= \frac{(1+m^2)^n}{(N+2)^{n-1}}\, P_n(m^2, N) \quad (n>1)\,, \end{aligned} \tag{3.75}$$

where P_n is a polynomial in m^2 of degree $n-1$ [1]. We note that λ_0 (3.75) is fixed by the normalisation of the potential, $u(0) = \lambda_0$ and can be set to zero. For other choices, λ_0 is modified correspondingly. Changes in λ_0 leave the fixed point solution and universal scaling exponents unaffected. The non-trivial fixed point coordinates λ_n for $n > 1$ are explicitly determined via the polynomials P_n, given by

$$\begin{aligned} P_2 &= -2m^2\,, \\ P_3 &= \frac{2(N+2)}{(N+4)}\, m^2 + \left(\frac{28}{N+4} + 10\right) m^4\,, \\ P_4 &= -\frac{24(N+2)(N+14)}{(N+4)(N+6)}\, m^4 + 24\left(\frac{56}{N+6} - \frac{70}{N+4} - 3\right) m^6\,, \\ P_5 &= \frac{96(N+2)^2(3N+22)}{(N+4)^2(N+6)(N+8)}\, m^4 \\ &\quad + \frac{48(N+2)\left(5N^3+126N^2+2016N+6928\right)}{(N+4)^2(N+6)(N+8)}\, m^6 \\ &\quad + \frac{48\left(13N^4+370N^3+4248N^2+35848N+99696\right)}{(N+4)^2(N+6)(N+8)}\, m^8 \end{aligned} \tag{3.76}$$

and similarly to higher order. A few comments are in order. Firstly, the coefficients in (3.75), (3.76) are finite and well-defined for all N except for even negative integers. A special role is taken by $N = -2$ where finiteness of the fixed point solution requires finiteness for $m^2/(N+2)$ in the limit $N \to -2$. Furthermore, some of the coefficients (3.76) become singular for even negative integer N leading to constraints on m^2. Secondly, the expansion displays the Gaussian fixed point $m^2 = 0$ which entails $\lambda_n = 0$. Thirdly, the expansion also displays the convexity fixed point $m^2 = -1$ with $\lambda_n = 0$ to all orders in the expansion. Finally, the Wilson-Fisher fixed point corresponds to a specific value for $-1 < m^2 < 0$.

An important remark can be already made from the expansion (3.75) as the mass

[1] The fixed point solution (3.75) are linked to the explicit solution given for $N = 1$ in (3.5) of [72] by $\lambda_n \to (6\pi^2)^{n-1}\lambda_n$.

amplitudes term read

$$u' = m^2 - \frac{m^2}{2}\frac{(1+m^2)^2}{(N+2)}\rho + \dots \tag{3.77}$$

$$u' + 2\rho u'' = m^2 - \frac{3m^2}{2}\frac{(1+m^2)^2}{(N+2)}\rho + \dots \tag{3.78}$$

Then we have an inversion of the mass hierarchy with $u' > u' + 2\rho u''$ as ρ is getting negative and as long as $m^2 < 0$. This is relevant in the sense that for imaginary field the radial contribution dominates already the solution of (3.2) for $\rho < 0$. It is also important to note that this inversion of hierarchy takes place as we are getting closer to the pole induced by a convex infrared potential.

3.3.3 Large fields

At large fields $\rho/\rho_0 \gg 1$, the potential approaches an infinite Gaussian fixed point

$$u'_*(\rho) = \gamma\,\rho^2\,. \tag{3.79}$$

All fluctuations are suppressed for $1/\rho \to 0$, in full analogy to the results found for large N. We therefore can follow the strategy given there and expand the Wilson-Fisher fixed point about the infinite Gaussian

$$u' = \gamma\,\rho^2\left[1 + \sum_{n=1}^{M}\gamma_n\,\rho^{-n}\right]. \tag{3.80}$$

The coefficients γ_n of the remaining field monomials are unique algebraic functions of the leading-order coefficient γ and N. Explicitly, we find

$$\begin{aligned}\gamma_5 &= -\frac{2}{5\gamma^2}\left(N-\frac{4}{5}\right), \quad \gamma_7 = \frac{4}{7\gamma^3}\left(N-\frac{24}{25}\right)\\ \gamma_9 &= -\frac{2}{3\gamma^4}\left(N-\frac{124}{125}\right), \quad \gamma_{10} = -\frac{7}{25\gamma^5}\left(N-\frac{6}{5}\right)\left(N-\frac{4}{5}\right)\end{aligned} \tag{3.81}$$

for the first few coefficients. Comparing with (3.52) we note that the radial mode only introduces mild modifications in the structure of the solution. In the large-N limit, the coefficients (3.81) fall back on (3.52), modulo a trivial overall re-scaling with N. Identifying the WF solution corresponds to determining the remaining free parameter γ.

3.3.4 Imaginary fields

The contribution from the radial mode (3.66) modifies the structure of the expansion significantly compared to the case with only the Goldstone mode. This can be understood as follows. Suppose we have

$$1 + u' = \frac{a}{\sqrt{-\rho}} + \frac{b}{\rho} + \text{subleading}\,, \tag{3.82}$$

in the limit of large negative ρ. This becomes the leading order solution in the large-N case provided $a = 0$. The expansion (3.82) satisfies the fixed point equation (3.2) in two ways, with either $a = 0$ or $a \neq 0$. In the first case, inserting (3.82) into (3.2), we find

$$a = 0\,, \quad b = \frac{2-N}{2}\,. \tag{3.83}$$

Here, $\partial_t u' = 0$ is fulfilled because the term $-2u'$ in (3.2) is cancelled jointly by the Goldstone and by the radial mode. The subsequent iteration continues as in the large-N case. For $a \neq 0$, however, there is a new branch of expansions available, starting off with

$$a > 0\,, \quad b = \frac{1}{2} > 0\,. \tag{3.84}$$

In this case, the term $-2u'$ in (3.2) is cancelled only by the radial mode, and the Goldstone contribution has become subleading.

Next, we consider $1 + u' + 2\rho u''$, the argument in the denominator of the radial contribution (3.66). Finiteness of the full flow requires that the pole at $1 + u' + 2\rho u'' = 0$ cannot be crossed, and hence both $1 + u' > 0$ and $1 + u' + 2\rho u'' > 0$ must hold for all finite ρ. Evaluating it in the limit $\rho \to -\infty$, using (3.82), we find

$$1 + u' + 2\rho u'' = \frac{b}{(-\rho)} + \text{subleading}\,. \tag{3.85}$$

We note that the behaviour is independent of a. This comes about because the operator $1 + 2\rho\partial_\rho$ has a 'zero mode' $\propto |\rho|^{-1/2}$. We conclude that the parameter b must obey $b > 0$, which applies for the expansion (3.85). Consequently, the expansion (3.82) cannot be achieved at $N = \infty$. This excludes the expansion (3.83) and imposes the expansion (3.84), which implies

$$u'(\rho) = -1 + \sum_{m=1}^{M} \sum_{n=0}^{m-1} \zeta_{m,n} \left(\sqrt{-\rho}\right)^{-m} \ln^n\!\left(\sqrt{-\rho}\right), \tag{3.86}$$

of which we have determined the first few hundred expansion coefficients. In terms of two free expansion parameters ζ and $\bar{\zeta}$, the first non-vanishing coefficients are

$$\begin{aligned}
\zeta_{1,0} &\equiv \zeta\,, \\
\zeta_{2,0} &= -\frac{1}{2}\,, \\
\zeta_{3,0} &= -\frac{5}{8}\zeta - \frac{N-1}{8\zeta}\,, \\
\zeta_{4,1} &= \frac{1}{4}\,, \\
\zeta_{4,0} &\equiv \bar{\zeta}\,, \\
\zeta_{5,1} &= \frac{15}{16}\zeta + \frac{3(N-1)}{16\zeta}\,, \\
&\vdots
\end{aligned} \tag{3.87}$$

Beyond this order, the coefficients $\zeta_{m,n}$ become functions of both ζ and $\bar{\zeta}$, eg. $\zeta_{5,0} = -\frac{5}{128}\,\zeta\,(9 - 96\,\bar{\zeta} - 50\,\zeta^2)$ for $N = 1$.

3.3.5 The Ising model

The Ising universality class is one of the most studied model of phase transitions and many results, both theoretical and experimental, have been accumulated over the year since its proposition by Ising [136]. It describes many statistical physical systems close to criticality with a specific power-law behaviour of thermodynamical quantities and where the order parameter is a single scalar field (see [12] for a review). Among examples are the liquid-vapor transition but also transition in binary mixtures and of course the emblematic ferro/paramagnetic transition. In the context of the functional renormalisation within LPA, the flow equation for the 3-dimensional effective potential is simply given by

$$\partial_t u = \rho u' - 3u' + \frac{1}{1 + u' + 2\rho u''}. \tag{3.88}$$

The simplicity of this equation (comparable to the large N case) makes it an ideal model to illustrate, in a non-trivial way, computational techniques to extract quantities, like critical exponents directly comparable to experiments. For instance, setting $N \to 1$ into the expansions (3.74) and (3.67), we can use those to compute the critical exponent ν with the method involving the stability matrix that we introduced at the beginning of this chapter. Naturally the asymptotic expansion (3.50) is also valid for $N = 1$ but of a lesser computational relevance. But specifically, we intend here to reformulate the flow equation in view of the expansion about $\rho = -\infty$ to take into account the unique radial mode.

We already noticed the specificity of the expansion about $\rho = -\infty$ when both massless and massive mode contribute to the expansion. In the continuation of the discussion it is interesting to compute the case $N = 1$ separately. Here the Goldstone modes are absent throughout, and we are left with only the radial mode. For this reason, we can formulate the RG flow in terms of the field-dependent radial mass

$$w(\rho) = u'(\rho) + 2\rho u''(\rho)\,, \tag{3.89}$$

leading to

$$\partial_t w = -2w + \rho w' - \frac{w' + 2\rho w''}{(1+w)^2} + \frac{4\rho (w')^2}{(1+w)^3}\,. \tag{3.90}$$

From the structure of the flow, we conclude that the regime $0 < 1 + w \ll 1$ allows for an asymptotic expansion of the form

$$w(\rho) = -1 + \sum_{n=2}^{M} \sum_{m=0}^{n-1} \zeta_{n,m} (\sqrt{-\rho})^{-n} \ln^m(\sqrt{-\rho}) \tag{3.91}$$

where only the contribution $\propto \sqrt{-\rho}$ is ignored by comparison with (3.86). Note that here, we can expand (3.90) in the 'operator basis' (3.91) to find the couplings $\zeta_{m,n}$ recursively [2]. The first few non-vanishing coefficients are

$$\begin{aligned}
\zeta_{2,0} &= \frac{1}{2}, \\
\zeta_{4,1} &= -\frac{3}{4}, \\
\zeta_{5,1} &= -3\zeta, \\
\zeta_{5,0} &= \frac{1}{8}(7\zeta - 32\zeta^3 + 32\zeta\chi)\,, \\
\zeta_{6,2} &= \frac{9}{8}\,, \\
\zeta_{6,1} &= -\frac{1}{4}(1 + 12\zeta^2 - 12\chi)\,, \\
\zeta_{6,0} &= \frac{1}{96}(-17 + 336\zeta^2 - 768\zeta^4 + 32\chi \\
&\qquad +384\zeta^2\chi + 192\chi^2)\,, \\
&\vdots
\end{aligned} \tag{3.92}$$

by expanding (3.90) and we have two parameters $\zeta_{3,0} = \zeta$ and $\zeta_{4,0} = \chi$. Such expansion can be easily recovered from (3.86) with the subtitutions

$$\zeta \to \frac{4}{5}\zeta \quad \text{and} \quad \bar{\zeta} \to \frac{1}{3}\Big(\frac{1}{4} - \chi\Big). \tag{3.93}$$

This reformulation of the expansion in terms of the amplitude ω about $\rho = -\infty$ is insightful for at least two reasons. First we clearly identify $\sqrt{-\rho}$, by comparison with (3.86), as a zero mode of the radial mass amplitude and this is the signature of the absence of massless modes. To a higher level it can be linked to a global discrete symmetry of the potential (Z_2). Secondly it facilitates as well the comparison with the large N case where we have only contributions from integer powers of the field.

3.3.6 Boundary conditions

By opposition to the large N case, the free parameters in the expansions (3.67), (3.80) and (3.86) remain to be determined thanks to the absence of a full solution of the flow (3.2) at finite N. Thus we resort to a numerical approach to compute the values of these parameters and the critical indices with high accuracy. For this purpose we consider a polynomial truncation around the minimum like (3.67) up to the order M. We set the boundary conditions by choosing the two highest couplings to vanish such that

$$\lambda_{M+1} = \lambda_{M+2} = 0 \tag{3.94}$$

[2] We have computed the coefficients up to $M = 50$. Higher orders can be achieved as well.

N	M	ν	ω	ω_2	ω_3
-1	33	0.5415364745	0.6757184	3.4431	6.4099
0	33	0.5920826926	0.65787947	3.3084	6.1631
1	33	0.6495617738	0.65574593	3.18001	5.91223
2	33	0.70821090748	0.671221194	3.071402	5.67904
3	33	0.7611231371	0.6998373178	2.9914230	5.4826528
4	33	0.804347696	0.733752926	2.9399940	5.330637
5	31	0.8377407110	0.76673529	2.9108908	5.219539
6	31	0.8630761595	0.795814494	2.896726	5.140977
7	31	0.8823889567	0.820316404620	2.8916166	5.086305
8	33	0.897337664625	0.8406122805	2.89163472	5.04848125
9	33	0.909128139450	0.85738397045	2.89438031	5.0223239
10	33	0.918605123154	0.87131097659	2.898458278	5.00419855
20	33	0.960678346035	0.936742371978	2.93751369319	4.96566025423
30	33	0.974173017876	0.958441374389	2.95672986621	4.97022378261
40	33	0.980781323265	0.969097610936	2.96709100884	4.97540746495
50	33	0.984698956658	0.975413687073	2.97348964704	4.97932916821
60	33	0.987290505905	0.979589069170	2.97781818967	4.98225142783
70	33	0.989131594889	0.982553360520	2.98093683915	4.98447973715
80	33	0.990506893951	0.984766383156	2.98328905465	4.98622431780
90	33	0.991573286057	0.986481464992	2.98512577783	4.98762303949
100	33	0.992424323549	0.987849597646	2.98659941340	4.98876757415
1000	31	0.999249240822	0.998798467576	2.99865080272	4.99880711432
10000	31	0.999924992406	0.999879984650	2.99986500784	4.99988007059
∞		1	1	3	5

Table 3.1: Numerical results for the scaling exponents for all universality classes considered. For some indices the achieved accuracy reaches about 30 digits. For display purposes, we have cut the number of quoted digits at a maximum of 12.

following the strategy adopted in [114]. Inserting the Ansatz (3.67) in the flow (3.1) we obtain a coupled system of ordinary differential equations $\partial_t \lambda_n = \beta_n(\{\lambda_i\})$ for the couplings λ_n that is solved numerically. Then, with a carefully monitored accuracy, we obtain the couplings of (3.67) [137]. From this polynomial expansion the universal critical

exponent ν and its subleading scaling exponents ω_n can be calculated (see table 3.1) via the stability matrix at criticality (3.10). This technique has been already used with success for the Ising model exponents in [114]. The parameters of the asymptotic expansions (3.80) and (3.86) can be determined via a careful numerical integration of (3.2) that used implicitly the overlapping of the local approximations (3.67), (3.80) and (3.86). For this we consider first two points ρ_1 and ρ_2 that lie into the validity range of the small and large positive field expansions respectively. Then the scaling flow (3.2) is integrated from ρ_2 towards ρ_1, connecting the two expansions. The value of parameter γ of (3.80) is adjusted iteratively such that the value of the potential at ρ_1 agreed with the one from the expansion at the minimum (3.67), within a desired accuracy. A similar but adapted version of this strategy is applied to the computation of the coefficients ζ and $\bar{\zeta}$ of the expansion (3.86) about large negative ρ [137].

From the obtained data the full scaling potential can be plotted (see figure 3.6) and the critical indices can be computed for many universality classes (see table 3.1). The figure 3.6 represents the amplitudes u' and $u' + 2\rho u''$ for $N = 10^n$ with $n = 0, 1, 2, 3, 4$ (the intensity of the line increases with n). We note that the potential and the field as been rescaled like $u \to N\, u$ and $\rho \to N\, \rho$. The dashed line corresponds to the case $N \to \infty$. We observe that the amplitude u' at large N is approached smoothly by the finite N curves for $\rho > 0$. On the contrary, the transition to large N is less progressive for $\rho < 0$ where the approach of the convexity bound $u' = -1$ is qualitatively different as long as $N \neq \infty$. This difference in the asymptotic behaviour for large negative ρ can be explained by the specific operator contributions from (3.58) and (3.86) that were detailed previously. This characteristic seems to indicate the limits $\rho \to -\infty$ and $N \to \infty$ are not commutative. The figure 3.6 (down) for the mass amplitude $u' + 2\rho u''$ shows as well a smooth approach of the large N results for $\rho > 0$ but a radically different behaviour in the vicinity of $\rho = -\infty$. This can be easily explained by the presence of a limiting singularity at $u' = -1$ for $N = \infty$. This bound is related to the convexity of the infrared potential and it can be crossed by the mass amplitude of the longitudinal mode $u' + 2\rho u''$ as it is not a singularity of the flow $\partial_t u'$ at finite N.

Finally the table 3.1 illustrates the efficiency of the LPA which provide a reliable method of computation of critical exponents as long as the renormalisation of the field can be neglected. All quoted digits are significant according to the criterion detailed in [137]. Here the order of the polynomial truncation (3.67) is $M = 33$ and there is hope that much higher order can be achieved in the future taking into account that only two

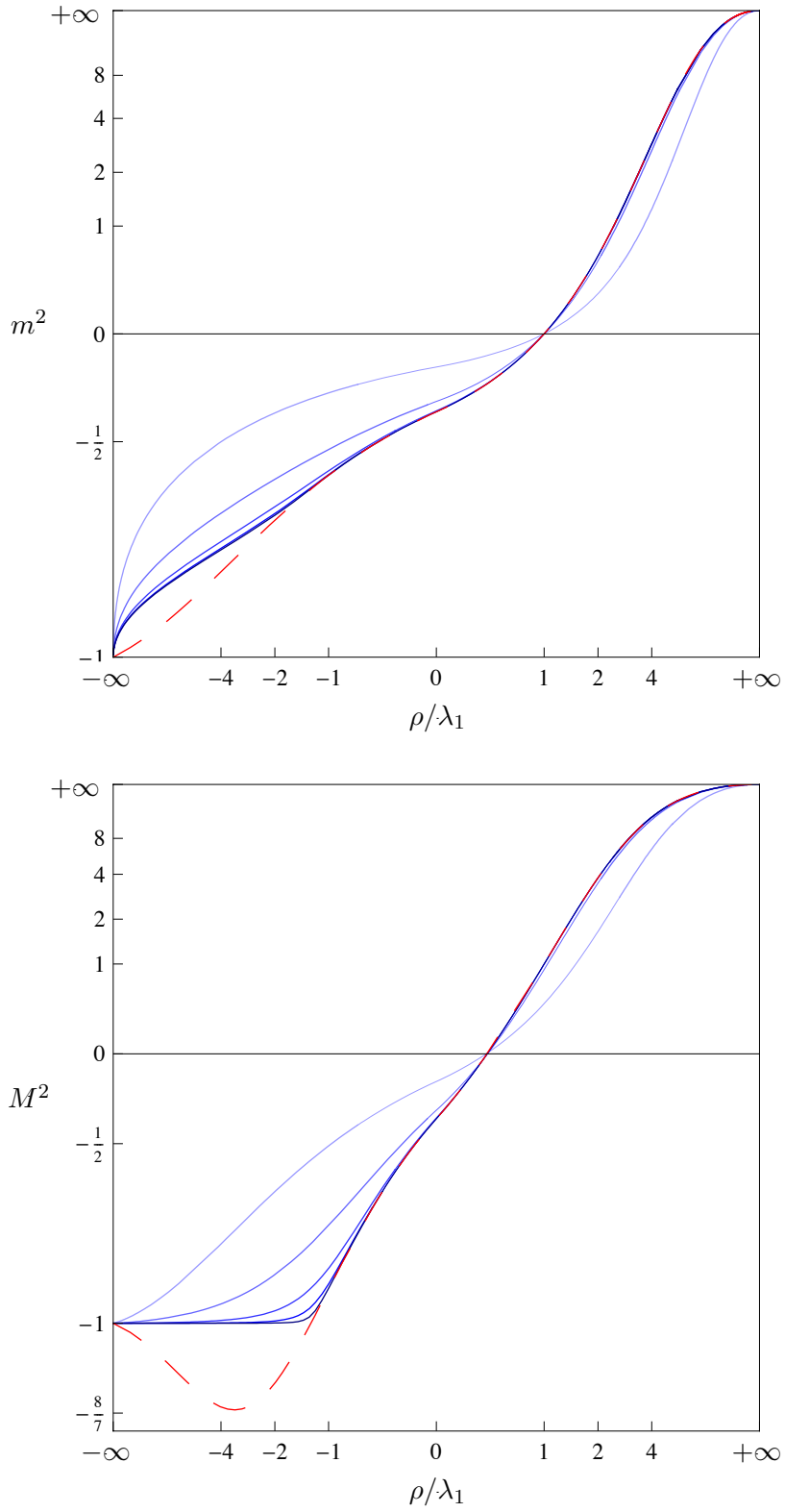

Figure 3.6: Plot of the mass amplitudes $m^2 = u'$ (up) and $M^2 = u' + 2\rho u''$ (down) for (from light blue to dark blue) $N = 1, 10, 100, 1000, 100000$. The field is normalized like ρ/λ_1 and we used the rescaling $\rho \to \frac{\rho}{1+|\rho|}$ and $u' \to \frac{u"}{2+u'}$. The dashed curve corresponds to the large N potential.

couplings have to be fixed (λ_1 and λ_2 for instance).

3.4 Synthesis

We computed series expansions of the 3-dimensional $O(N)$ symmetric critical potential from a non-perturbative flow equation for the effective potential, neglecting the field renormalisation. The expansions have been made about the vanishing field, the minimum of the potential and for large positive and negative values of the field with an arbitrary number of fields N. The dependence on boundary conditions of these expansions can be reduced to a set of one or two parameters maximum (for each expansions) that have to be carefully chosen in order to obtain genuine physical fixed point solution. In the case $N \to \infty$ a full solution can be achieved under the form of the closed expression (3.21) from which an exhaustive classification of the physical fixed point solutions can be given, parametrised by a parameter c related to the marginal coupling or the ϕ^6 operator. Using this solution all the dependence on parameters of the local expansions can be lifted and the singularity structure of the critical potential has been completely worked out. When $N < \infty$ a full solution seems to be out of reach. Therefore we rely on a numerical integration of the flow that leads to the fine tuning of the expansions parameters corresponding to their value at the WF fixed point. This fine tuning process leading the WF fixed point can also be interpreted as the condition to have a singularity-free potential on the real axis [64].

Expansions	A	B	C	D
Transverse	none	m^2	γ	ζ
Longitudinal	ρ_0, λ	m^2	γ	$\zeta, \bar{\zeta}$

Table 3.2: Summary of the different expansions and their respective parameters.

For $\rho \geq 0$ the potential at finite N shows a progressive approach to the large N exact result (see 3.6). This is reflected by the expansions (3.74), (3.67) and (3.80) that are qualitatively similar to the equivalent expansions at $N = \infty$. The expansion's coefficients at finite N are smooth functions of N (for $N \geq 2$) and therefore the large N limit can be achieved and we recover the coefficients of (3.32), (3.41) and (3.50) of the large N solution. This similarity allows for similar fixed point solutions when $N \leq \infty$. For instance if we consider the expansion about vanishing field (3.41) at large N the values of the mass parameter $m^2 = 0, -0.388\ldots, -1$ correspond respectively to the Gaussian, WF and convexity fixed

point solutions. The convexity fixed point is associated to the infrared completion of the potential [138] and a detailed analysis of this phenomenon is given in chapter 5. The WF value can be computed, in a first approximation, by solving $\lambda_n = 0$ for an increasing order. This is related to the maximisation of the convergence domain of the expansion which coincides with the vanishing of the highest coefficient through Cauchy's test. The very same method can be applied to the coefficients (3.74) with N finite and the same three fixed point solutions can be located. This argues in the sense that the large N limit is a sensible approximation scheme within the LPA and it provides a good qualitative picture of the critical potential for positive ρ.

For ρ negative this picture is modified thanks to the competition between the transverse and longitudinal modes. This drastic change is manifest at the level of the expansion about $\rho = -\infty$ at infinite N which can not be recover from the finite N coefficients (3.86). At the technical level this is due to the fact that the second order differential operator that appeared when longitudinal modes are present possess a zero mode operator $\sqrt{-\rho}$. This operator is a leading contribution when transverse modes dominate therefore the behaviour of the critical potential close to its convexity bound is sensibly different for $N = \infty$ and $N < \infty$. To be more precise when both longitudinal and transverse modes are present ($N > 1$) only the longitudinal mode contributes to the cancellation of the scaling of the effective potential (i.e the term $-2u'$ in (3.2)). Then this mechanism determined the universal leading contribution from the longitudinal mode to be equal to the inverse of the scaling dimension of u' as long as a longitudinal mode is present ($b = 1/2$). On the other side the leading contribution of the transverse modes is non universal and not fixed but only constrained to be positive ($a > 0$) due to the convexity bound. In the particular case of a single scalar field (Ising model) the only mass amplitude is the longitudinal one which allows to reorganize the expansion about $\rho = -\infty$ where this contribution is absent. Finally we outline the importance of the expansion for imaginary fields which revals the specific contributions, from both massive and massless modes, to the critical potential as a consequence of the nonlinear part of the flow. However this domain conserves some universal features as, for example, the inversion of the mass amplitudes for both N finite and infinite.

Chapter 4

Integration of renormalisation group flows

After focusing on the behaviour of the infrared potential at criticality (in 3 dimensions) we concentrate here on its scaling away from fixed point solutions with a special emphasis on the role of the regularisation scheme. Indeed, within the framework of the functional renormalisation group, the precise way the infrared momenta are integrated out depends on the choice of a cutoff function that obeys only certain specific conditions. In the following we argue that the integration of the RG flow can be performed while preserving the arbitrariness of the infrared regularisation. This idea first appeared in [31] and afterward in [139]. Then we give an example of application of this principle by solving, at the level of the LPA, the flow for the effective potential at the leading order of the $1/N$ approximation. A scale dependent potential is computed for arbitrary infrared regularisation and dimension. By imposing sensible boundary conditions at the level of the bare potential, we can study the occurrence of second order phase transition for $2 < d < 4$. We briefly analyse the consequence of a specific infrared cutoff choice on the convergence of local expansion of the critical potential about the potential minimum. Also a short account is given on the absence of such phenomena in 2 dimensions although the LPA is not reliable in that case at the quantitative level. Finally we study the possibility of first-order transition and tricritical behaviour. First and second order phase transitions are identified to surfaces within the parameters space of a ϕ^6 model. The critical index ν is evaluated at the intersection of this two surfaces (tricritical line) but also at the end point of it, allowing comparison with results form another method.

4.1 Flow integration and threshold functions

We start by discussing the implication of the momenta integration from the point of view of the flow equation for the effective action and then for the effective potential. Thus we support the commutativity of the momenta and RG scale integration by providing a concrete example with the calculation an $O(N)$ symmetric potential a large N. Running couplings are computed and convergence properties of a polynomial expansion around the minimum of the potential are briefly discussed.

4.1.1 Measure and integral operator

The process of solving the flow $\partial_t \Gamma_k$ for a given expansion of the effective action usually includes an integration on position (or momentum) space and field indices. It is summarized in the trace operator that reads

$$\mathrm{Tr} \equiv \sum_a \int d^d x \tag{4.1}$$

in positions space. The completion of the trace operator does not put any constraints on the fields content of the action. It only requires a diagonalisation in field and momentum space to reduce it to a simple summation. However at the technical level the completion of the operator (4.1) makes the choice of a specific regulator function compulsory. But this requirement is of a purely technical nature as the integrand on the right hand side of the flow equation

$$\left(\Gamma_k^{(2)}[\phi] + R_k\right)^{-1} \partial_t R_k \tag{4.2}$$

is finite for high and low momentum thanks to the presence of the regulator and its derivative as detailled in chapter 2. This general property of the flow is ultimately the consequence of the basic requirements on the function R_k to be a proper regulator which allows only a narrow range of momenta to contribute to the flow $\partial_t \Gamma_k$. These conditions on R_k also ensure the interpolation between a UV and an IR action (see details in chapter 2). Therefore we have a decoupling between the completion of (4.1) and the effective integration on the energy scale t and the fields. This important remark is the motivation for solving and studying the flow for an arbitrary regulator.

Although the previous statement is completely general we choose here to illustrate more precisely this idea with the example of a scalar $O(N)$ theory within the LPA. In that case we recall that the flow for the effective action reduces to the flow for an effective potential from which all informations can be extracted. For convenience we reproduce

here this flow that has been given in chapter 2

$$\partial_t u = (d-2)\rho u' - du + v_d(N-1)\,\ell(u') + v_d\,\ell(u' + 2\rho u''). \tag{4.3}$$

In this dimensionless setup we clearly identify a linear part related to the classical scaling of the potential and the field. The second part of the equation encodes the non-perturbative quantisation of the flow, where the operator (4.1) and the regulator are present through the threshold function

$$\ell(\omega) = -\int_0^\infty dy\, y^{d/2+1} \frac{r'(y)}{P^2+\omega}\,. \tag{4.4}$$

Similarly to the integrand of the trace operator, the integrand of the threshold function (4.4) is finite for the all range of momenta. We recall here the expression of the dimensionless inverse propagator

$$P^2 = y\,[\,1 + r(y)\,] \tag{4.5}$$

which is strictly positive for all momenta because of the presence of the infrared regulator. For high momenta, the dimensionless propagator (4.5) generically increases with y like $P^2 \sim y$ and thus the integrand of (4.4) tends to zero for $y \gg 1$. In the opposite regime, when $y \ll 1$, the term $y^{d/2+1}$ takes over and cancels the integrand of (4.4). We also remind that $P^2 > 0$ marks the infrared regularisation of the flow (4.3). Following this brief discussion, we introduce the integral operator

$$\mathcal{I}[f(y)] = \int_0^\infty d\mu\, f(y) \tag{4.6}$$

with a specific measure μ that is defined on the functions space of regulators as we shall detail in the following. From a formal point of view $\mathcal{I}$ is a functional acting on an arbitrary function $f(y)$. Such operator notation has been first introduced in [31] and subsequently in the appendix of [139]. It allows to reformulate (4.4) under the useful form

$$\ell(\omega) = \mathcal{I}\left[\frac{P^{d+2}}{P^2+\omega}\right] \tag{4.7}$$

and it is normalized such that $\mathcal{I}[1] = 1$. Taking into a account this normalisation and assuming a regulator function monotonous piecewise for $y \geq 0$, the integral measure simply reads

$$d\mu(y) = -\frac{2}{d}\,\frac{r'(y)\,dy}{[1+r(y)]^{\frac{d}{2}+1}}, \tag{4.8}$$

$$d\mu(r) = -\frac{2}{d}\,\frac{dr}{(1+r)^{\frac{d}{2}+1}} \tag{4.9}$$

in momentum and regulator space respectively. We note that because $r'(y) < 0$ the boundaries of integration in (4.6) have to be inverted when we used $d\mu(r)$. Therefore we are naturally led to the measure

$$\mu = (1+r)^{-d/2} \tag{4.10}$$

for the space of all possible (dimensionless) regulator. Also, the operator $\mathcal{I}$ enjoys specific simplification properties when particular cutoff functions $r(y)$ are used. In the case of an optimised cutoff [70, 71, 72] for example with $r(y) = (1/y - 1)\theta(1-y)$ we have $\mathcal{I}[f(P)] = f(1)$. Another simplification comes with the sharp cutoff $r(y) = (\beta/y)\theta(1-y)$ (with $\beta \to \infty$), where only $y = 1$ contributes due to the θ function entailing $\mathcal{I}[f(P)] = \mathcal{I}[f(\sqrt{1+r})]$.

The introduction of an integral operator that corresponds to the completion of the trace operator in the original flow equation allows us to reformulate the flow for the effective potential (4.3) like

$$\partial_t u = (d-2)\rho u' - du + (N-1)\,\mathcal{I}\left[\frac{P^{d+2}}{P^2+u'}\right] + \mathcal{I}\left[\frac{P^{d+2}}{P^2+u'+2\rho u''}\right], \tag{4.11}$$

where we performed, as usual, the rescaling $u \to u/(\frac{d\,v_d}{2})$ and $\rho \to \rho/(\frac{d\,v_d}{2})$. From the structural point of view the flow (4.11) is similar to the one we studied in Chapter 3 for an optimised cut-off at criticality. Indeed, it suffices to ignore the integral operator and set P to one in (4.11) to obtain exactly the same flow. For large amplitude we still have a suppression of the fluctuation effects encoded into the nonlinear part of the flow. However the analysis is more subtle in a phase with SSB where typically $u' < 0$ and $u' + 2\rho u'' < 0$ and possible instabilities can occur for low momentum. In that case the amplitudes u' or $u' + 2\rho u''$ approach $-C$ where C is the minimum of P^2 and is a natural *gap* [140] rooted in the infrared regularisation of the flow. The nature of this singularity is highly dependent on the regulator, as we can anticipated from (4.11), and this aspect will be examined in detail in Chapter 5.

4.1.2 Full solution

Despite the utility of (4.11), the idea of inverting momentum and scale/field integration can be fully exploited in the large N limit where a closed form solution to the flow is available. Repeating the process to obtain (3.17) when $N \to \infty$ we obtain from (4.11)

$$\partial_t u' = (d-2)\rho u'' - 2u' - u''\,\mathcal{I}\left[\frac{P^{d+2}}{(P^2+u')^2}\right]. \tag{4.12}$$

The technical simplification occurring in this limit, i.e the suppression of the highest derivative related to the radial mode, allows for the decomposition of (4.12) in a system

of a coupled ordinary differential equations along the characteristic curves of (4.12). In addition to the technical reformulation of (4.12), we consider also the integration on ρ and t only, following the analysis of the previous section, and thus we factor out the integral operator $\mathcal{I}$ from the differential equation (4.12). By this we mean that the equation (4.12) can be written under the form $\partial_t u' = \mathcal{I}[F(\rho, u', u'')]$ and that the solution of (4.12) can be constructed by solving first $\partial_t u' = F(\rho, u', u'')$ and then apply the integral operator $\mathcal{I}$ on its solution. Therefore we apply first the method of characteristic to the equation $\partial_t u' = F(\rho, u', u'')$ that leads to the system ordinary differential equations

$$\frac{du'}{dt} = -2u' , \tag{4.13}$$

$$\frac{d\rho}{du'} = \left(\frac{d-2}{2}\right)\frac{\rho}{u'} - \frac{1}{2u'}\,\frac{P^{d+2}}{(P^2+u')^2} . \tag{4.14}$$

The first equation is trivial and its solution is $C_1 = u'e^{2t}$. The second one is linear for the function $\rho(u')$ and its integral can be directly expressed in terms of hypergeometric function (see [141, 117, 118] for instance) whose integral representation is

$${}_2F_1(a,b,c,z) = \frac{\Gamma(c)}{\Gamma(b)\Gamma(c-b)}\int_0^\infty dt\; t^{b-1}\;\frac{(1-t)^{c-b-1}}{(1-tz)^a}. \tag{4.15}$$

We recall that the function (4.15) that can be regarded as a one-valued analytic function on the complex plane cut along the real axis from 1 to $+\infty$. After a simple substitution and careful choice of the parameters $\{a, b, c\}$ we are led to a solution of the form $C_2 = \rho \cdot |u'|^{1-d/2} - \mathcal{G}(u')$ with $(\nu = \frac{d}{2} + 1)$ (We can choose other representation)

$$\mathcal{G}(z) = \frac{1}{2\nu}\,\mathcal{I}\left[\left(\frac{P^2}{|z|}\right)^\nu {}_2F_1\left(2, \nu, \nu+1, -\frac{P^2}{z}\right)\right] - \frac{i\pi d}{4} . \tag{4.16}$$

The complex constant $-i$ ensures that $\mathcal{G}(z\,P^2)$ is a real-valued function for $-1 \le z \le 0$ and for $z \ge 0$ it is set to one when $d = 3$ and to zero for $d > 3$ (d integer). We applied also the operator $\mathcal{I}$ to the solution of the second characteristic to recover the dependence on momentum integration and consequently the regularisation. The function (4.16) can also be thought as the analytic continuation of the effective potential at large N for complex fields excluding the cut from $u' = -\min_{y\ge 0} P^2$ to $-\infty$. Then the singularity structure which is intimately linked to the existence of continuum limit (see chapter 3) is here totally accessible via (4.16) modulo its dependence on a specific regulator. Finally the most general solution to (4.12) can be constructed

$$\rho \cdot |u'|^{1-d/2} - \mathcal{G}(u') = F(u'e^{2t}) \tag{4.17}$$

where the precise form of the function $F(z)$ is fixed by boundary conditions at a microscopic scale $t = 0$. The solution (4.17) contains all informations about the scaling of the

effective potential from an arbitrary UV scale $k = \Lambda$ to the full effective potential, i.e including all quantum fluctuations, at $k = 0$. It is also valid for an arbitrary and continuous dimension although for $d = 2$ we have to introduce a non-vanishing anomalous dimension. It describes a potential indifferently in or out of a symmetry breaking phase as well as at the phase transition.

4.1.3 Running couplings

Once the form of the microscopic potential is fixed all running coupling constants can be computed out of (4.17). This owns to fact that the effective potential is the generating function of all the couplings hence knowing its flow amounts to know the flow of the entire parameter space. For example if we choose the microscopic potential to be $u'_\Lambda = \lambda_\Lambda(\rho - \kappa_\Lambda)$ then the running minimum of the potential is given by

$$\rho_0 = \kappa_\star + (\kappa_\Lambda - \kappa_{cr})\, e^{t(2-d)}. \tag{4.18}$$

We easily see that for $\kappa_\Lambda = \kappa_{cr}$ the classical minimum possess a critical value for which ρ_0 is getting unrenormalised or scale invariant. For $d > 2$ and $\kappa_\Lambda < \kappa_{cr}$ the dimensionless minimum diverges towards $-\infty$ indicating a vanishing real (dimensionful) minimum hence the system is driven in its symmetric phase. By opposition if $\kappa_\Lambda > \kappa_{cr}$ the system remains in a phase with spontaneous symmetry breaking. The critical value of the classical minimum can be naturally expressed for arbitrary regulator. We found

$$\kappa_{cr} = \frac{\mathcal{I}[P^{d-2}]}{d-2}. \tag{4.19}$$

Incidentally the fixed point value $\kappa_\star$ happens to be the same as κ_{cr}. The running quartic coupling $u''(\rho_0) \equiv \lambda$ can also be evaluated for $2 < d < 4$ from (4.17)

$$\lambda = \frac{\lambda_\star}{1 + (\lambda_\star/\lambda_\Lambda - 1)\, e^{t(4-d)}}. \tag{4.20}$$

For $d \geq 4$ the running of λ is qualitatively different and this will be detailed in the next section. This is directly related to the existence (or not) of continuous phase transition as a function of the dimensionality. For the time being we focus on feature of (4.17) while keeping an arbitrary dimension. From (4.20) a fixed point value for the quartic coupling is also clearly identified

$$\lambda_\star = \frac{d-2}{\mathcal{I}[P^{d-4}]}. \tag{4.21}$$

Alternatively the results (4.20) and (4.18) can be derived from the system of β-functions for the parameters ρ_0 and λ. In a phase with spontaneous symmetry breaking we have

the simple decoupled system

$$\beta_{\rho_0} = -(d-2)\rho_0 + \mathcal{I}[P^{d-2}], \tag{4.22}$$

$$\beta_{\lambda} = (d-4)\lambda + 2\lambda^2\,\mathcal{I}[P^{d-4}]. \tag{4.23}$$

4.1.4 Scaling solutions

Up to now we detailed the construction of a solution which explicitly depends on the scale and therefore describes the flow away from criticality. However, we know as well that scale invariant solutions can be worked out by other means than tuning the classical (or initial) parameters from (4.17) (see chapter 3). The search of fixed point solutions is also directly possible by looking for solutions of (4.12) with $\partial_t u' = 0$. The solution is simply given by the solution of the second characteristic of the flow equation that we recall here ($\nu = 1 + d/2$)

$$\rho = |u'|^{d/2-1}\,[\,c + \mathcal{G}(u')\,] \tag{4.24}$$

where $\mathcal{G}$ is given by (4.16). Only a specific choice of the constant c leads to a physical fixed point solution [64] and a systematic study of the continuum limit for the model can be carried either from an analytical (local or global) solution or, by solving numerically the scaling equation (for instance see [142] for $N = 1$). Here our intentions are more modest in the sense that we would like to outline simply the influence of the regulator on the convergence of local expansions of (4.24). Also we take $d = 3$ in (4.24) in order to establish a meaningful example with a known non-trivial scaling solution. In that case the solution can be represented by

$$\rho = c \cdot |u'|^{1/2} + \mathcal{I}\left[P\,{}_2F_1\left(2, -\frac{1}{2}, \frac{1}{2}, -\frac{u'}{P^2}\right)\right] \tag{4.25}$$

which is just the solution (3.21) with a shift in the constant c. With this representation we can directly see that the choice of a specific solution, i.e a particular value for c, and a fortiori a fixed point solution, is completely decoupled from the regularisation. This is a specificity of the large N model where the LPA becomes exact and therefore it is expected that physical quantities, like critical exponents, that depend on c are insensitive to the regularisation scheme. However it is fundamental to recognize that the approach towards a scaling solution is regulator dependent. Again from (4.25), if we choose a series representation (3.20) for the hypergeometric function about the minimum of the potential ($u' = 0$) then the coefficient of the order n is

$$a_n = (-1)^n \left(\frac{1+n}{1-2n}\right) \mathcal{I}\Big[P^{1-2n}\Big] \tag{4.26}$$

where we ignored the term proportional to c as it have no impact on the convergence expansion of (4.25) about $u' = 0$. In this representation the influence of the regulator on the convergence is clearly identified. As an example, ensuring a common normalisation of the regulator function (for instance $r(1/2) = 1$), the convergence radius for an optimised cutoff is 1 but only 1/2 for a sharp cutoff (see figure 4.1).

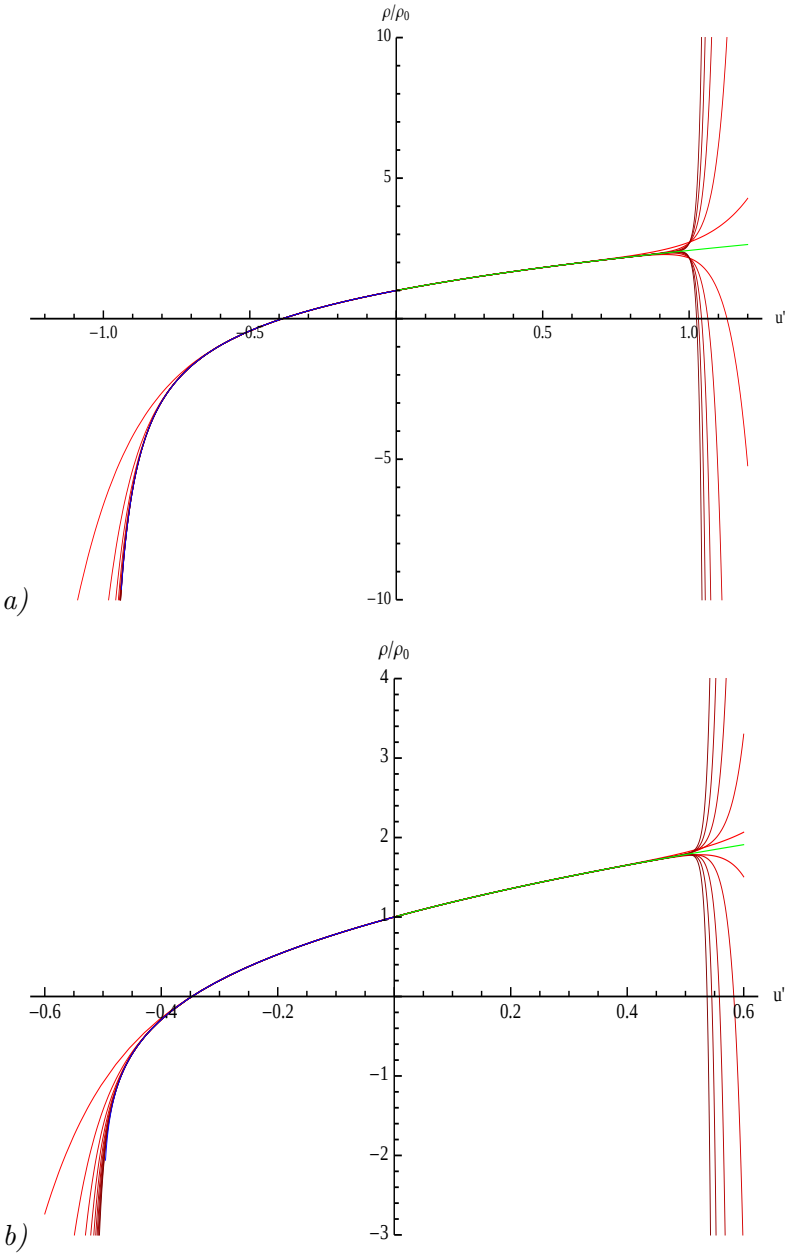

Figure 4.1: Expansions of $\rho(u')$ with the common normalisation with $r(1/2) = 1$ for a) a sharp cut-off and b) an optimised cut-off. The curves in red correspond to expansions at the order $n = \{9 \times 1, \ldots, 9 \times 10\}$. On both graphics we rescaled the field such that the potential minimum is located at $\rho_0 = 1$.

At a more general level the convergence of (4.26) is related to the momentum contribution

shaped by the regulator in the term $\mathcal{I}[P^{1-2n}]$. Provided a finite and peaked contribution from the measure μ of the integral operator, the dominant contribution is actually coming from the minimum of P^2 [70]. This dominant contribution from the momenta located in the vicinity of the minimum of P^2 is transparent from an evaluation for large values of n of the coefficient (4.26) which leads to

$$|a_n| \sim \mathcal{I}\left[\left(\frac{1}{P^2}\right)^n\right]. \tag{4.27}$$

Then, if we apply the Cauchy-Hadamard criteria, we clearly see that the maximisation of convergence radius calls for a maximisation of the minimum of P^2 summarised in the formula [70]

$$C_{opt} = \max_{RS}\left(\min_{y\geq 0} P^2(y)\right). \tag{4.28}$$

The symbol $\max_{RS}$ indicates here a maximisation with respect to the parameters of the cutoff function which determined its precise shape. The coefficient C_{opt} corresponds directly to the largest, or optimised, convergence radius for the expansion (4.26) and is a consequence of an optimal shape for the momentum integration.

The formula (4.24) offers also a direct interpretation for the behaviour at large positive u'. In that case the leading contribution is given by the regulator independent term proportional to the constant $c \neq 0$. The non-universal leading corrections can also be summed and show a qualitatively different expansion depending on the regulator chosen. The general structure of the expansion of the hypergeometric (non universal) part of (4.24) about $z \equiv 1/u' = 0$ is the following

$$\mathcal{G}(z) = z^\gamma\left(a_0 + a_1\, z + a_2\, z^2 + a_3\, z^3 + \dots\right) \tag{4.29}$$

where the exponent γ is, in the simplest cases, a rational number and it depends on the regularisation. Naturally the coefficients a_n depend also on the regulator but they have a lesser influence on the convergence of (4.29). The power γ can be computed easily for simple regulators and we found $\gamma = 1, 3/2, 2$ for respectively a sharp, a quadratic and an optimized regulator. This is in contrast with the analysis about $u' = 0$ where the regularisation influence was limited to the coefficients and a maximisation of the convergence radius was sufficient to ensure the fastest convergence for the whole series. Here we have at least one supplementary prior criteria which is the maximisation of the exponent γ enforcing the suppression of the corrections to the universal behaviour $c\cdot|u'|^{\nu-2}$ in (4.24). It will be interesting to know if in the case of a class of regulators with the same value for γ but different subleading coefficients a_n, a similar criterion about the convergence

of (4.29) can also be established similarly to the expansion about $u' = 0$. Nevertheless leading corrections to the universal behaviour of the potential are

$$u = \frac{16}{9\pi^2}\,\rho^3 + \mathcal{O}(\ln \rho) \tag{4.30}$$

where we indicated the logarithmic correction due to a sharp regulator which dominates the corrections from an optimised regulator proportional to $\mathcal{O}(1/\rho^2)$ or from a quadratic regulator of the form $\mathcal{O}(1/\rho)$. As a final comment we would like to outline that a detailed analysis of the convergence of (4.29) and its impact on the choice of a regulator would be a important complement to the analysis for $u' = 0$. We hope this will be the subject of further investigation.

4.2 Application to phase transitions

We turn now our attention towards the application of the analytical solution (4.17) to the study of continuous and discontinuous phase transitions at large N for arbitrary cutoff scheme. The absence of such phenomena in 2 dimensions is put in evidence. Finally we describe the evolution of a effective potential with two minimas where an approximated condition for a first-order transition is given. Following this we investigate the line of tricritical points that appears at the conjunction of the two type of transitions and compute the critical exponent ν on and and the end of the tricritical line.

4.2.1 Second-order phase transition

Having determined the full flow for the effective potential it is now legitimate to use our results to recover the known features of our model, namely the second-order phase transition occurring when $d = 3$. As noticed in the previous section, for a simple quadratic bare potential, the running of the minimum of the potential (4.18) possess a critical initial value $\kappa_\Lambda = \kappa_{cr}$ that cancels the scale dependence of the minimum. Choosing this specific value for the classical minimum, the general solution (4.17) is driven towards a scale independent, or fixed point, expression for the effective potential given in implicit form by

$$\rho = \mathcal{I}\left[\, P\, {}_2F_1\left(2, -\frac{1}{2}, \frac{1}{2}, -\frac{u'}{P^2}\right)\right]. \tag{4.31}$$

This process indeed singles out a unique value for the integration constant c in (4.25) corresponding to the known Wilson-Fisher fixed point, signature of a continuous phase transition. As for the effective potential, fixed point values for the minimum and the

quartic coupling can easily be calculated

$$\kappa_\star = \mathcal{I}[P], \tag{4.32}$$

$$\lambda_\star = \frac{1}{\mathcal{I}[P^{-1}]} \tag{4.33}$$

and higher couplings can be computed along similar lines (see previous discussions). These critical values appear naturally in the running of their respective couplings (4.18) and (4.20) with $d = 3$. The fixed point solutions have been studied in some details in the previous section therefore we concentrate on solutions that deviate slightly from it and on the near-critical behaviour of our model. As notice before the symmetric breaking mechanism is mainly driven by the potential minimum. Starting from the symmetry broken phase with $\delta\kappa \equiv \kappa_\Lambda - \kappa_{cr} > 0$ we stay with a non-vanishing minimum in the infrared limit $t \to -\infty$, hence no phase transition occurs. The situation is opposite when $\delta\kappa < 0$, the minimum vanishes as we integrate out gradually low momenta and the transition to a symmetric phase occurs precisely when

$$t = -\ln\left[\frac{|\delta\kappa|}{\kappa_\star}\right]. \tag{4.34}$$

We easily see from this simple expression that we can 'delay' the transition by choosing $|\delta\kappa| \ll 1$. Another consequence of this small deviation is that the renormalised trajectory within the parameters space of our model can be set arbitrarily close to the Wilson-Fisher fixed point before deviating from it accordingly to the relevant character of the perturbation.

In the symmetric regime the polynomial form of the effective potential in dimensionful units can be derived from the full solution (4.17) and when $k \to 0$ and $\Lambda \gg U'$ we have

$$U(\bar{\rho}) = \left(\frac{4}{3\pi}\right)^2 \left(|\delta\kappa|^2\Lambda^2\,\bar{\rho} + |\delta\kappa|\Lambda\,\bar{\rho}^2 + \frac{1}{3}\,\bar{\rho}^3\right). \tag{4.35}$$

We note that this expression does not show an explicit dependence on the regularisation scheme apart from $\kappa_\star$ in $\delta\kappa$. This suppression of the regulator dependence is rooted in the asymptotic behaviour of (4.31) with $u' = k^{-2}\,U' \to \infty$ and $\rho = k^{-1}\,\bar{\rho} \to \infty$ when $k \to 0$. But the scheme dependence through $\delta\kappa$ is illusory in the sense that the bare value for the potential minimum can be chosen arbitrarily so that the specific value of κ_{cr} does not have a fundamental impact on the effective potential and its scaling. On the quantitative level the expressions (4.35) and (4.34) allow to compute the different critical exponents in an

independent way

$$\beta \quad = \lim_{|\delta\kappa|\to 0} \frac{d[\ln\sqrt{\rho_0}]}{d[\ln|\delta\kappa|]} = \quad 1/2, \tag{4.36}$$

$$\nu \quad = \lim_{|\delta\kappa|\to 0} \frac{d[\ln\sqrt{U'(0)}]}{d[\ln|\delta\kappa|]} = \quad 1, \tag{4.37}$$

$$\zeta \quad = \lim_{|\delta\kappa|\to 0} \frac{d[\ln U''(0)]}{d[\ln|\delta\kappa|]} = \quad 1 \tag{4.38}$$

where the independence on the renormalisation scheme is here completely clear.

4.2.2 Absence of phase transition

In the 2 dimensional case the function (4.16) has a simple expression

$$\mathcal{G}(z) = -\frac{1}{2}\mathcal{I}\left[\frac{P^2}{P^2+z}\right] - \frac{1}{2}\mathcal{I}\left[P^2\,\log\left(\frac{|z|}{P^2+z}\right)\right] \tag{4.39}$$

which for a quadratic classical potential leads to

$$\rho = \left(\frac{u'e^{2t}}{\lambda_\Lambda} + \kappa_\Lambda\right) + \mathcal{G}(u') - \mathcal{G}(u'e^{2t}) \tag{4.40}$$

where no specific value of the classical minimum appears leading to a scaling solution. The running minimum is given by

$$\rho_0 = \kappa_\Lambda + t\cdot\mathcal{I}[P^2] \tag{4.41}$$

so that the potential minimum vanishes at the renormalisation group 'time'

$$t = -\frac{\kappa_\Lambda}{\mathcal{I}[P^2]}. \tag{4.42}$$

It is also easy to check from (4.40) that at the classical scale ($t = 0$) the minimum of the potential is zero as well. Therefore no phase transition occurs in that case where only a symmetric phase exists in accordance with the Mermin-Wagner theorem [143]. It is clear that the presence of a regulator term in (4.40) does not alter the flow of the potential in a significant way.

In the last part of this section we turn our attention to the four dimensional case where the general solution reads

$$\rho = \frac{u'}{\lambda_\Lambda} + \frac{\kappa_\Lambda}{e^{2t}} - u'\Big(\mathcal{G}(u'e^{2t}) - \mathcal{G}(u')\Big) \tag{4.43}$$

with the same initial conditions as previously (except that $\lambda_\Lambda = \bar{\lambda}_\Lambda$ and $\kappa_\Lambda = \bar{\rho}_{0\Lambda}/\Lambda^2$) and $\mathcal{G}(z)$ from (4.16). As in the case $d = 3$, we note a critical value for the classical minimum $\kappa_\Lambda = \kappa_{cr} \equiv \mathcal{I}[P^2]/2$. But, when $t \to -\infty$ with this critical value for the

classical minimum, only the trivial (gaussian) solution $u'_\star = 0$ survives in four dimensions. Therefore no critical phenomena occurs in this dimensionality although one can compute the running of the parameters

$$\kappa = \kappa_\star + (\kappa_\Lambda - \kappa_{cr})\, e^{-2t}, \tag{4.44}$$

$$\lambda = \frac{1}{1/\lambda_\Lambda - t} \tag{4.45}$$

with $(\kappa_\Lambda - \kappa_{cr}) \ll 1$. Following this, in dimensionful units the running of the quartic coupling behaves like

$$U'' = \frac{\bar{\lambda}_\Lambda}{1 - \frac{\bar{\lambda}_\Lambda}{2}\mathcal{I}\Big[\ln\Big(\frac{U'}{\Lambda^2}\frac{e^{3/2}}{P^2}\Big)\Big]} \longrightarrow 0 \tag{4.46}$$

as the mass scale set by $U' = k^2 u'/\Lambda^2$ is much smaller than the ultraviolet cutoff scale Λ. This result recovers the triviality of the scalar theory [15, 144, 145, 146, 147, 148] in four dimensions with a vanishing coupling constant for arbitrary regulator and independently on the phase we are sitting [50, 127]. The triviality problem is related to the fact that the running quartic coupling encounters a Landau pole for high momentum when the continuum limit $\Lambda \to \infty$ is taken [149]. Indeed when the UV scale Λ is much higher than the mass scale set by U', the UV coupling $\bar{\lambda}_\Lambda$ is forced to increase following the relation

$$\frac{1}{U''} - \frac{1}{\bar{\lambda}_\Lambda} = \ln\Lambda + \mathcal{I}[\ln P] - \ln\sqrt{U'} - \frac{3}{4} \tag{4.47}$$

while keeping U'' and U' fixed. The bare coupling diverges such that $\frac{1}{\bar{\lambda}_\Lambda} \to 0$ and the UV cutoff reaches a finite limit Λ_L. In this context the derivatives of the potential correspond to the renormalised parameters of the theory in the infrared and there are, in principle, measurable. Thus we set $m_R^2 = U'$ and $\lambda_R = U''$ and these are fixed while Λ increases. Consequently the cutoff Λ hits a limit value at

$$\Lambda_L = \mathcal{I}[1/P] \cdot m_R \cdot \exp\left(\frac{1}{\lambda_R} + \frac{3}{4}\right) \tag{4.48}$$

where the role of the regularisation scheme is explicit although it is concerned (a priori) with the regularisation of the lowest momenta.

4.2.3 Sextic coupling and tricriticality

Before discussing the occurrence of discontinuous transitions within the functional RG in three dimensions, we first introduce briefly the concept of the first-order transition and its possible coexistence with a second-order transition at a so-called tricritical point (or line). For clarity and simplicity we make this analysis from view-point of the phenomenological Laudau's theory of phase transitions [150] (for a more recent reference see also [57]).

Phenomenological discussion

In Laudau's approach to phase transitions it is assumed that the free energy F of a statistical system is an analytic function of an average (or mean) field ϕ and therefore it can be written like

$$F = a\,\phi^2 + b\,\phi^4 + c\,\phi^6 + \mathcal{O}(\phi^8) \tag{4.49}$$

where it is assumed that the coefficients a, b and c are smooth functions of the temperature T. The expansion (4.49) assumes a free energy symmetric under the $O(N)$ group and ϕ represents a vector with N components in complete analogy with the first chapter. From now on we neglect the contribution $\mathcal{O}(\phi^8)$ and consider a sextic potential at most.

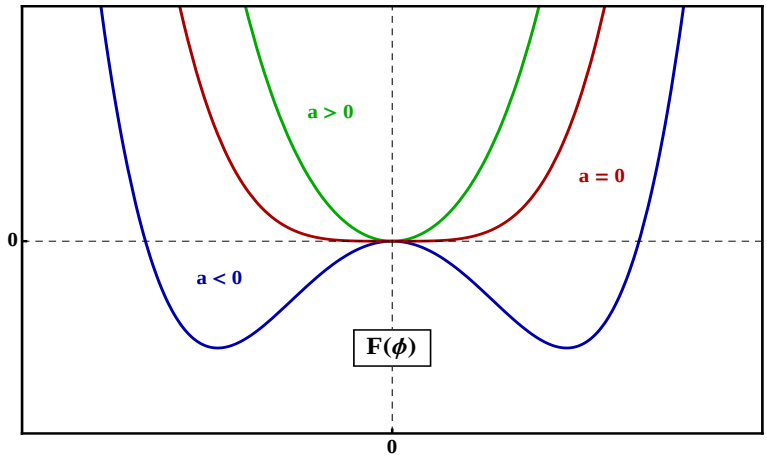

Figure 4.2: Evolution of the free energy (4.49) for a vanishing sextic coupling during a second order phase transition.

The advantage of introducing such functional $F(\phi)$, in the context of phase transitions, is that its minimum, noted ϕ_0, is an order parameter whose value is zero (non-zero) when the system is symmetric (unsymmetric). For instance, if we first consider the simpler case with $c = 0$ (no sextic coupling) and solve the equation $0 = \frac{dF}{d\phi}$, we found that all the possible values of the minimum are given by the doublet

$$\phi_0 = \pm\sqrt{-\frac{a}{2b}}\,. \tag{4.50}$$

In that case both minima have the same amplitude and because we are considering a free energy $F(\phi)$ bounded from below we have the constraint $b > 0$. Then for $a > 0$ the roots (4.50) are complex but the physical minimum is located at $\phi = 0$. With these remarks in mind it is now easy to identify the two phases shown by a ϕ^4 system. For $a < 0$ we are in

a non-symmetric phase, characterized by the doublet of real non-vanishing minima (4.50) (lowest blue curve on figure 4.2). Then, as a is approaching zero continuously (through a variation of the temperature for example), the two minima (4.50) merge at $\phi_0 = 0$ and the system is ending up in a symmetric phase. In this case it is clear that the phase transition is occurring for $a = 0$ exactly (highest red curve on figure 4.2) and, because the minima evolved in a continuous manner, the transition is of second order. As mentioned before for $a > 0$ the minimum stays at the origin and the system remains in its symmetric phase (highest green curve on figure4.2). Naturally the transition occurs for any strictly positive b and the black line on figure 4.4 represents logically a possible second order phase transition.

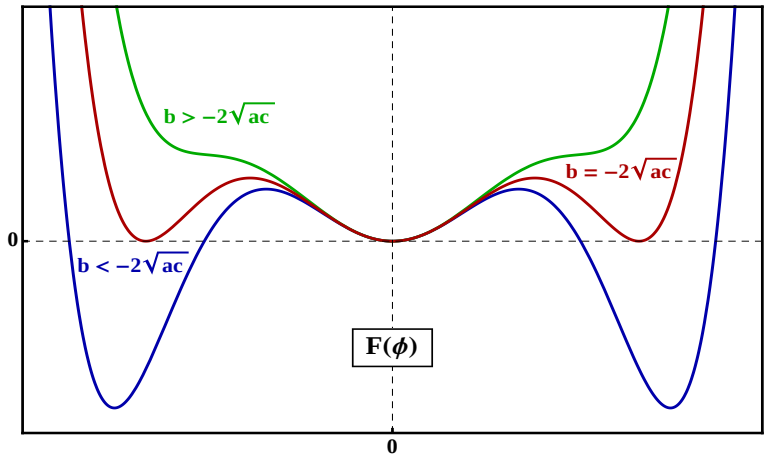

Figure 4.3: Evolution of the free energy (4.49) during a first order phase transition.

For a non-vanishing sextic coupling ($c \neq 0$) the situation is slightly more involved as, mechanically, we have to consider a possibly larger number of minima. However we can clearly see from the equation $0 = \frac{dF}{d\phi}$ that $\phi = 0$ will always be an extremum. If $a < 0$, the origin is a maximum then we have a pair of symmetric minima with a similar shape for F with $c = 0$ and therefore, a similar analysis. Consequently we focus here on the case $a > 0$ and $c > 0$ such that our free energy is bounded from below and possesses three minima at $\phi = 0, \pm\phi_0$ with

$$\phi_0 \;=\; \sqrt{\frac{1}{3c}\Big(-b + \sqrt{b^2 - 3ac}\Big)}\,. \tag{4.51}$$

From now on we are in a position to identify a different type of transition from previously. Indeed if the two minima $\pm\phi_0$ are lower than the one located at zero we can discard it and consider only a global minimum at the non-vanishing value $-\phi_0$ or $+\phi_0$ (lowest blue curve

on figure 4.3). This situation is similar to the case $a < 0$ in the previous ϕ^4 model and it corresponds to the unsymmetric phase of the ϕ^6 model. By opposition, if the minimum at the origin is the lowest then the global minimum of the system is also locate at zero field and the system in its symmetric phase (highest green curve on figure 4.3).

The two phases we just described are separated by the case where the minima at zero and at $\pm\phi_0$ show the same depth (middle red curve on figure 4.3). In that specific situation the minimum show a 3-fold degenerescence and the specific value of the parameters of F for which this is happening can be determined through the equation $0 = F(|\phi_0|)$. This leads to the simple relation

$$b = -2\sqrt{ac} \tag{4.52}$$

that summarizes the condition for the transition between the two phases and it is represented by a dashed red line on figure 4.4. A crucial remark is that, during the transition from one phase to another, the value of the minimum evolves discontinuously. Indeed the global minimum have to jump from $|\phi_0|$ to zero (or conversely) in order to complete the transition. This discontinuous evolution is the signature of a first order transition characterized by the existence of latent heat.

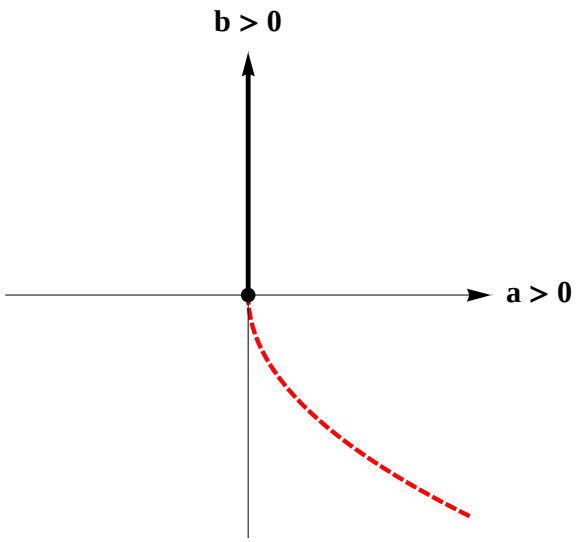

Figure 4.4: Phase diagram for the ϕ^6 model of the free energy F within phenomenological Landau's approach.

In the context of our study, a particularly interesting situation is when the lines representing first and second order phase transitions meet at $a = b = 0$ on figure 4.4. This point is designated as 'tricritical point' [151] and shows specific critical properties (see

[152] or a general review of tricritical phenomena). We note in passing that, close to the tricritical point, the second order behaviour can be dominated by the tricritical behaviour, specifically in the region $a < 0$ and $b > 0$.This 'crossover' can arise when the conditions of tricriticality and of second-order transition are mildly satisfied leading to the crossover line $b \sim \sqrt{-ac}$. To conclude this brief qualitative discussion we mentioned that a tricritical point has been observed experimentally, for instance, in He^3-He^4 systems [153] and is characterised, at the theoretical level, by mean-field values for the critical exponents [154] (see also [155] for a description of the phase diagram).

Functional RG analysis

Following our previous qualitative discussion from the viewpoint of mean field approximation, we pursue here this analysis using the functional renormalisation group. The objective now is to extract qualitative and quantitative informations from our set-up about the coexistence of first and second-order transitions at large N in 3 dimensions. For this purpose we use the analytical solution (4.17) as a starting point for which we introduce specific and appropriate boundary conditions. Therefore a classical potential with (at least) two minima, i.e containing an operator ϕ^6, is used. The competitive renormalisation of the minima can give rise to a discontinuous evolution of the order parameter, signature of a first-order phase transition. Thus, in dimensionless units, we impose a bare potential of the form

$$u'(t=0) = \lambda_\Lambda \left(\rho - \kappa_\Lambda\right) + \frac{\tau_\Lambda}{2}\left(\rho - \kappa_\Lambda\right)^2 \tag{4.53}$$

where the dimensionless sextic coupling τ_Λ entails two minima for the potential. We recall, for convenience, that the full solution for the running of the potential is given by

$$\rho = |u'|^{1/2}\left[\mathcal{H}(u'e^{2t}) + \mathcal{G}(u') - \mathcal{G}(u'e^{2t})\right] \tag{4.54}$$

where the function is explicitly given by the expression (4.16) with $d = 3$. The function $\mathcal{H}(z)$ results from the inversion of (4.53)

$$\mathcal{H}(z) = \kappa_\Lambda + \frac{1}{\tau_\Lambda}\left(-\lambda_\Lambda \pm \sqrt{\lambda_\Lambda^2 + 2\tau_\Lambda z}\right). \tag{4.55}$$

The symbol $\pm$ is the sign of the degenerescence of the minimum. The potential about its minimum away from the origin is preferably described with a positive sign ($\pm = +$) whereas the negative case describes the potential with its minimum located the origin ($\pm = -$). We follow here mainly the analysis carried in [128]. When $\kappa_\Lambda < 3\lambda_\Lambda/\tau_\Lambda$ the potential possess only one minimum and the situation is similar to a quartic case. A

continuous transition occurs from a broken to a symmetric phase, both phases separated by a fixed point solution (see previous analysis). A new situation arises when $\kappa_\Lambda > 3\lambda_\Lambda/\tau_\Lambda$ and two minima coexist, one at the origin and the other at $\Lambda\kappa_\Lambda$. With the minimum about the origin being the deepest, the second minimum is getting deeper due to renormalisation effects. The curvature at the origin is also decreasing along the flow and at some point the second minimum (away from zero) becomes the absolute minimum of the effective potential (for a detailed analysis see [128]). If we consider the running minimum as a function of the classical one, a discontinuity is observed indicating a first-order transition. Unfortunately it is not possible to determine precisely the range of parameters for which this transition occurs. For this we need to know the relative depths of the two minima and this is seemingly not achievable in the large N approximation. Nevertheless the solution (4.54) can still be exploited as we focus on regions away from the top of the barrier. Using $u'e^{2t} = U'/\Lambda^2$ and $u' = U'/k^2$ it is possible to extract a condition for a vanishing of the curvature about origin from (4.54) when $k \to 0$ and it is given by the relation

$$\kappa_\Lambda = \mathcal{I}[P] + \frac{2\lambda_\Lambda}{\tau_\Lambda}. \tag{4.56}$$

As mentioned in [128] this condition is not sufficient for a first-order transition (degeneresence of the vacuum) and only a weakly first-order transition is reached for $\lambda_\Lambda \to 0$. Nonetheless two critical surfaces can be identified within the parameters space, one corresponding to a second-order transition ($\kappa_\Lambda = \mathcal{I}[P]$) and the other to a first-order transition ($\kappa_\Lambda = \mathcal{I}[P] + 2\lambda_\Lambda/\tau_\Lambda$). Therefore a tricritical behaviour is expected for the conditions $\lambda_\Lambda = 0$ and $\kappa_\Lambda = \mathcal{I}[P]$. For $U'/\Lambda^2 \ll 1$, we obtained

$$\frac{\bar{\rho}}{\Lambda} + |\delta\kappa| = \frac{3\pi}{4}\sqrt{\frac{U'}{\Lambda^2}} + \left(\frac{1}{\lambda_\Lambda} - 2\,\mathcal{I}[P^{-1}]\right)\frac{U'}{\Lambda^2} + \mathcal{O}\left(\left(\frac{U'}{\Lambda^2}\right)^2\right) \tag{4.57}$$

where the term proportional to U'/Λ^2 is suppressed in the range $|\delta\kappa| \ll \lambda_\Lambda$. In that regime we are close to a second-order transition and we recover the symmetric potential (4.35). Also we find the same critical exponent $\nu = 1$, characteristic of the large N limit. On the contrary in the opposite regime $|\delta\kappa| \gg \lambda_\Lambda$, the universal term $\sqrt{U'/\Lambda^2}$ and the regulator dependent term $\mathcal{I}[P^{-1}]$ are subleading and the potential near the origin is of the form

$$U(\bar{\rho}) = \lambda_\Lambda\left(|\delta\kappa|\Lambda^2\,\bar{\rho} + \frac{\Lambda}{2}\,\bar{\rho}^2\right) \tag{4.58}$$

and have the same type of regulator dependence than the potential (4.35) that we discussed already. In that case the critical exponent has mean-field value $\nu = 1/2$. There the tricritical line is associated to mean-field exponents as it is exposed in [132]. However, the

end of the tricritical line is characterized by non-standard value for ν and it seems difficult to obtain it from (4.54) probably because of the approximations we made.

This end point is associated with the so-called BMB phenomenon [130] and in order to study its specific critical indices more deeply we take as a new starting point the scaling version of (4.12) and its solution (4.25). The solution (4.25) for large positive u' have a universal leading behaviour

$$\rho = \left(c + \frac{3\pi}{4}\right)\sqrt{u'} + \dots \tag{4.59}$$

where the dots represent non-universal corrections. The coefficient c is, a priori, free of choice and for instance the unique Wilson-Fisher fixed point corresponds to $c = 0$. We know also from Chapter 3 that the expansion about the minimum of the potential shows the existence of a marginal operator that can be chosen as a parameter of the expansion. For the expansion (3.32) the coefficient are then given by

$$\begin{aligned} &\rho_0 = 1\,, \quad \lambda_2 = 0, \quad \lambda_3 = \tau, \quad \lambda_4 = -6\tau^2, \\ &\lambda_5 = -60\tau^3\,, \quad \lambda_6 = 30(1 - 28\tau)\tau^3\,, \dots \end{aligned} \tag{4.60}$$

The vanishing of λ_2 is the necessary condition to recover the tricritical behaviour as we discussed earlier. The marginal coupling τ is naturally directly linked to the constant c and by simply inserting (3.32) into (4.59) we found

$$\tau = \frac{2}{c^2}. \tag{4.61}$$

There we can relate the tuning of the marginal coupling τ to the tuning of c and then, we can recover the tricritical line that was find previously. Indeed for the range

$$\frac{3\pi}{4} < |c| < \infty \tag{4.62}$$

the solution (4.25) describes a line of fixed point solutions between the gaussian solution $u' = 0$, corresponding to the upper bound, and the end point of the tricritical line corresponding to the lower bound. This specific end point value is also visible from (4.59) as it cancels the universal contribution and leads to a possible, regulator dependent, singular potential at $\rho = 0$. This is at this point that we recall that a perturbation $\delta u'$ around a scaling solution of (4.12) is given, for arbitrary regularisation, by the exact expression

$$\delta u' = C\, e^{\theta t}\, u''\, (u')^{\frac{1}{2}(\theta+1)} \tag{4.63}$$

where u' and u'' are derivatives of the scaling potential. Using this relation and local expressions for u', it is possible to compute the spectrum of possible eigenvalues θ as it

was done in chapter 3. The critical index ν corresponds to the negative inverse of first possible eigenvalue (see (3.4)). Using the expression (4.59) it is clear that for the range (4.62), i.e when we are sitting on the tricritical line, and requiring that the perturbation is analytical at the origin we find the mean-field result

$$\nu = \frac{1}{2} \tag{4.64}$$

in accordance with our previous approach. When we are at the end of the tricritical point we have $c = -3\pi/4$ and the non-universal corrections become dominant (see previous sections). The derivative of the scaling potential in that case is singular and the nature of the singularity depends on the regulator, to wit

$$u' \propto \frac{1}{\rho^{\alpha}}. \tag{4.65}$$

For instance we found $\alpha = \frac{1}{2}, \frac{2}{3}, 1$ for respectively an optimised, a quadratic and a sharp regulator. Putting (4.65) into (4.63) we found that

$$\delta u' \propto \frac{e^{\theta t}}{\rho^{\frac{\alpha}{2}(\theta+3)+1}}. \tag{4.66}$$

Providing that the perturbation $\delta u'$ have pole at the origin that remains analytical we end up with the constraint

$$\frac{\alpha}{2}(\theta + 3) = 0 \tag{4.67}$$

at least for the first possible eigenvalue $\theta = \omega_0$. It is striking that despite the non-universal character of the corrections (4.65), it leads to the same universal critical exponent

$$\nu = \frac{1}{3} \tag{4.68}$$

in accordance with the result from [132]. This result illustrates in a evident way the specificity of the 'BMB' fixed point solution. We note also that the logarithmic singularity at the origin found in [132] for the critical potential is actually a spurious consequence of the sharp regularisation that we can recover simply by setting $\alpha = 1$ in (4.65).

4.3 Synthesis

In chapter 3 we studied in detail analytical solutions of the critical flow equation in three dimensions for a given, optimised, regulator function. In this chapter we extended this study to arbitrary Wilsonian regulator and provide an exact analytical expression for the effective potential while neglecting the radial mode. Then we gave a detailed analysis of universal aspects of phase transitions from a scale-dependent potential, completing the

study from a scale-independent standpoint given chapter 3. In the following we summarise the results of this chapter.

First we argued that the process of integration of the flow equation is separated from the choice of a specific infrared regularisation scheme. Indeed, thanks to the structure of the flow, the usual general requirements on the regulator function are sufficient to guarantee the finiteness of the flow for all range of momenta, hence allowing to separate the integration on fields and renormalisation scale. This property can be read off from the threshold function within the flow equation for an $O(N)$ symmetric scalar potential. Via a simple reformulation of this nonlinear part of the flow in terms of integral operator, we can interchange in practice the order of integration between momenta and fields/renormalisation scale. We illustrated this procedure by the calculation of the exact solution of the flow for large N values with arbitrary regulator and dimensions.

In a second part we used this solution to investigate possible phase transitions depending on the dimensionality of the system. For $d < 4$ a second-order phase transition is clearly identified with the related Wilson-Fisher fixed point solution and fixed point parameters are computed for arbitrary cutoff. Then we focused on first-order transition phenomena with the analysis of the competitive renormalisation of the two minima in the presence of a sextic coupling. In this context, we emphasized the possibility of tricriticality at the coincidence of continuous and discontinuous transitions. We computed the value of the critical exponent ν on this tricritical line and found a non-standard value at its ends. We hope this will be part of a systematic and more general study of the different phases of a scalar ϕ^6 model with a detailed discussion of the BMB phenomenon.

Chapter 5

Convexity as a fixed point

The property of convexity of the effective potential is a well-known consequence of the effective action Γ being a Legendre transform of the Schwinger functional $\ln Z$, and was first noted in [101, 18]. In geometrical terms this quality ensures that the curvature of the potential at the origin, and the potential itself, are bounded from below. Although this situation seems to be of no problem in a symmetric phase, difficulties arise when one uses perturbative approximations to evaluate the effective potential in the broken phase. There, the quantum corrections are expected to erase concave contributions and lead to a flat potential within its inner part. Unfortunately, within such an approach, the potential seems to become complex for some finite value of the field [19, 20, 21] and therefore a continuous, real and convex potential seems to be a challenge for such approximation methods. Thus, in such context, the functional RG appears as an appropriate tool to investigate this genuine non-perturbative phenomenon that is the convexity of the effective potential. We note that the approach to convexity has already been investigated using such a method, but with somewhat different implementations in [44, 45, 25] and [156]. Here we evaluate the infrared potential in its broken phase via a fully analytical approach based on the flow equation for an $O(N)$ symmetric effective potential at the leading order of the derivative expansion (LPA). After a comprehensive analysis of the lowest momentum integration, an approximated analytical solution for the deep infrared regime is constructed for a large class of regulators. This solution is then used to uncover and study in detail the deep infrared completion of the potential, its approach to convexity and the role of the regularisation. Following this, we interpret from a new perspective the flattening of the non-convex part of the potential as the consequence of the presence of an infrared stable fixed point that prevails in the deep infrared (IR) scaling of the effective potential.

5.1 Infrared RG flow

The scaling of the effective potential, as we are getting closer to the full potential, relies essentially on the specific regularisation scheme within any approximations of the effective action. This scheme dependence of the RG flow (at the level of the LPA)

$$\partial_t u' = (d-2)\rho u'' - 2u' + v_d\,(N-1)\,u''\,\ell'(u') + v_d\,(u'' + 2\rho u''')\,\ell'(u' + 2\rho u'') \tag{5.1}$$

lies into the threshold function

$$\ell'(\omega) = -\frac{1}{2}\int_0^\infty dy y^{d/2}\,\frac{\partial_t r(y)}{(P^2+\omega)^2} \tag{5.2}$$

which encodes the precise momentum integration. Consequently, after a brief discussion on instabilities related to the integration of the flow in the deep infrared, we detail in this section the momentum dependence of (5.2) for very low momenta and single out the key features of this function in order to facilitate the flow integration. This will lead us to a simple classification of the regularisation schemes with respect to their stability properties as the full potential is approached.

5.1.1 Flow integration and instabilities

As we noted in the previous section, the completion of convexity is related to the integration (or summation) of the lowest momenta contribution (long-distance physics) hence, the role of the infrared regularisation is crucial. In a phase with spontaneous symmetry breaking (SSB) the non-convexity of the potential is monitored by the infrared renormalisation scale k as we are getting closer to a convex potential. Typically the flattening of the inner part of the potential occurs like [45, 25]

$$U_k' \geq -\alpha\, k^2 \tag{5.3}$$

as $k \to 0$ where the constant α depends on the chosen regulator. Subleading field and momentum dependent corrections to (5.2) can be computed as well but we can already note the influence of the renormalisation scheme within SSB phase, i.e in dimensionless units $u' < 0$, as we are integrating the smallest energies. From the point of view of the flow equation (5.1) for the effective potential this means that in the regime where $u' < 0$ and $u' + 2\rho u'' < 0$, the dominant contribution is coming from the nonlinear part of the flow encoded in the regulator dependent threshold function $\ell(\omega)$. This specificity makes the integration of the flow when $k \to 0$ a delicate matters as we are getting closer to a possible singularity whose position and nature depend on the regulator. This aspect is of

practical relevance for numerical integration where the existence of this singularity leads to possible instabilities as we are getting infinitesimally close to the pole for some range of k [25].

Following these remarks a closer look on the behaviour of threshold functions for negative amplitudes ($\omega < 0$) is needed and on its relation to very low momentum integration. As we pointed out before the momentum contribution in the threshold function is mainly inherited from the full flow equation for the effective action, with a differentiated contribution from its numerator and denominator. In (5.2), only a narrow range, peaked around $y \sim k^2$, contributes to the numerator thanks to the derivative term. The main contribution is coming from the denominator whose minimum, with respect to the momentum y, gives logically a maximum contribution to the integrand of $\ell'(\omega)$. This is tempered by the fact that the contribution from $y^{d/2}$ (for very small y) can offset the divergence of the effective propagator $(P^2 + \omega)^{-1}$ but we will discuss this later and we focus first on the influence of the propagator. The value of propagator at its minimum is denoted, as previously, by

$$C = \min_{y \geq 0} P^2(y). \tag{5.4}$$

and forms a *gap* whose origin comes from the infrared regularisation of the theory [140]. This strictly positive gap C is the leading momentum contribution to the effective propagator and it corresponds to the position of the singularity present in the flow equation that we discussed earlier. As we integrate progressively lower momenta, the negative amplitude is approaching the value $-C$ pushing the flow in a strongly nonlinear regime. This approach corresponds to the convexity completion of the potential as we tend to the full effective potential. For $\omega = u'$ then $u' \to -C$ so that $\alpha = C$ in (5.2). Following that discussion it is clear that the pole existence in the flow, consequence of the IR regularisation, is at the origin of a convex potential when $k \to 0$ and that the details of an approach to convexity are contained in the corrections to (5.2).

5.1.2 Parametrized approach

Although the main contribution (5.4) helps to understand the origin of the IR completion of the effective potential, a more sophisticated Ansatz seems mandatory to investigate more deeply this issue. Therefore, in order to refine the momentum contribution of the propagator, we Taylor expand it around its minimum y_0 which leads us to two different cases. The first case A is when the minimum of P^2 is non-zero, leading to the expansion

$$P^2 \;=\; C + \;\alpha_{2n}\,(y - y_0)^{2n} \tag{5.5}$$

where α_{2n} is the first non-vanishing Taylor's coefficient about y_0. Because y_0 is a absolute minimum of P^2 the polynomial contribution (5.5) is only in even power of the momentum. In the case B, where the minimum is at vanishing momentum, we have an even simpler Ansatz

$$P^2 = C + \alpha_n y^n. \tag{5.6}$$

It is important to note that, for both cases, a large n means that a large number of coefficients vanish leading to an increasingly flat propagator about its minimum. In addition to the approximations (5.5) and (5.6) we have to evaluate the other terms in the integrand of $\ell'(\omega)$ in the vicinity of y_0. We note that we kept a non-vanishing anomalous dimension in the evaluation of $\partial_t r(y)$ to simplify the limit $d \to 2$ if necessary. The derivative term in (5.2) around the minimum of P^2 takes respectively the form

$$\partial_t r(y_0) = \frac{C}{y_0} + \frac{\eta}{2}\left(1 - \frac{C}{y_0}\right) \tag{5.7}$$

in the case A with $y_0 \neq 0$ and

$$\partial_t r(0) = \frac{C}{y}\left(1 - \frac{\eta}{2}\right). \tag{5.8}$$

in the case B when $y_0 = 0$. We note in passing that for the case B the contribution from the scaling of the regulator, proportional to $1/y$, lowers the contribution in positive power $y^{d/2}$ coming from the measure. Once the integrand of $\ell'(\omega)$ have been properly approximated the integration can be performed for arbitrary regulator and we found the generic behaviour

$$\ell'(\omega) = \frac{\delta}{(C+\omega)^\gamma} \tag{5.9}$$

where the proportionality coefficient δ and the nature of the singularity γ are naturally regulator dependent. The expression (5.9) is the leading contribution for an expansion in momentum of the threshold function around the minimum of effective propagator within the regime $0 < C + \omega \ll C$. We clearly identify the constant C as the position of the singularity on the negative real axis ($C > 0$) and it can be constrained to be as negative as possible following the criterion of optimisation detailed in [70]. However it can not be shifted arbitrarily away along the negative axis and usually it reaches a finite value according the optimisation criterion. This criterion, although useful for other practical purposes, does not influence the approach to convexity. The coefficient δ is given by

$$\delta = \left(1 - \frac{\eta}{4}\right) \frac{y_0^{2n}/2}{(\alpha_{2n})^{\frac{1}{2n}}} \frac{(2n-1)\pi}{n^2 \sin(\frac{\pi}{2n})}, \tag{5.10}$$

in the case A and in the case B we found

$$\delta = \left(1 - \frac{\eta}{2}\right) \frac{C/2}{(\alpha_n)^{\frac{d}{2n}}} \frac{(2n-d)\pi}{n^2 \sin(\frac{d\pi}{2n})}. \tag{5.11}$$

The coefficient δ is not an important parameter as it can be rescaled into u and ρ according to the invariance of flow noted in chapter 2. On the contrary, the nature of the singularity γ is the most important parameter and it differs substantially in cases A and B. In the first case of a non-vanishing minimum of the propagator the exponent reads

$$\gamma = 2 - \frac{1}{2n} \tag{5.12}$$

where the index n is a positive integer which varies for different classes of regulators. From this simple expression we can directly relate the flatness of the propagator arounds its minimum to the strength of the singularity, hence to the detailed approach of $1+u' \to 0$. The flatter is P^2 around y_0 the stronger is the pole of $\ell'(\omega)$ and an increasing number of Taylor's coefficients in (5.5) vanish. Also in the case A the exponent γ is consequently bounded to

$$\frac{3}{2} \leq \gamma \leq 2 \tag{5.13}$$

which translates, as we will see later, in remarkable properties for the convexity completion of the effective potential. In this context it should be noted that the sharp cutoff is a notable exception as it belongs to case A but is not analytical at its minimum. It corresponds formally to the limit case $\gamma = 1$ (or $n = 1/2$). The regulators that belong to case B are characterised by the singularity nature

$$\gamma = 2 - \frac{d}{2n} \tag{5.14}$$

where the index n is now offset by the presence of the dimension. This immediately imply that for higher dimensions the pole of the flow is weakened and the convexity approach is strongly influenced by the dimension for the class B regulator. This is in total contrast with class A, where this approach is completely independent of the dimensionality. Naturally when n is large the dependence on d drops out and ultimately we recover the upper bound $\gamma = 2$ common to classes A and B. Another fundamental difference is that class B regulators possess only the upper bound

$$\gamma \leq 2 \tag{5.15}$$

which let the possibility of an absence of singularity in the flow with dramatic consequences on the infrared completion of the potential. This situation will be detailed in the next section. We can also recover a sharp cutoff type of regularisation providing $n = d/2$. The presence of the dimension (5.14) can be directly traced down to a propagator's minimum at vanishing momenta. Indeed for low momenta the term $(P^2 + \omega)^2$, within $\ell'(\omega)$, develops

a singularity about $y = 0$ when $C + \omega \to 0^+$. Then the contribution from the inverse propagator P^2 and the mass amplitude ω in the infrared is proportional to y^{-2n}. This contribution is balanced by the one coming form the threshold function measure $dyy^{d/2-1}$. The product of these contributions leads to an infrared divergence $\ell'(\omega) \propto y^{d/2-2n}$ in which regulator and dimensional measure effects add up. This only occurs because type B regulators enhance zero-momentum contribution. By comparison, type A regulators lead to $\ell'(\omega) \propto (y - y_0)^{-2n}$ only. Finally we note that for $n < d/2$ the momentum measure dominates the propagator leading to $\gamma < 1$ with a possible non singular flow in ω.

From a technical point of view the approximations (5.5) and (5.6) have the advantage of reducing the functional dependence of $\ell'(\omega)$ on $r(y)$ to a dependence on the parameters $\{C, \gamma, \delta\}$ where only γ is truly essential when $C + \omega$ is small but strictly positive. Also, to complete our comments, we remark that even if the pole is stronger by a power of $(d-1)/(2n)$ for case A with respect to the case B, $\gamma = 2$ is the common upper bound leading to the strongest singularity given by

$$\ell(\omega) = \frac{\delta}{C+\omega} \quad \Rightarrow \quad \ell'(\omega) = -\frac{\delta}{(C+\omega)^2}. \tag{5.16}$$

This corresponds to the same singularity structure that for an optimised regulator [71]. Another example of a specific flow is given by the case $\gamma = 1$ which leads to a logarithmic singularity in the flow with

$$\ell(\omega) = \delta \ln(C+\omega) \quad \Rightarrow \quad \ell'(\omega) = \frac{\delta}{C+\omega}. \tag{5.17}$$

This example corresponds to the sharp cutoff but also to the exponential regulator $r(y) = 1/(e^y - 1)$ in 4 dimensions (case B). We recall that, owing to $n \geq 1$ ($\gamma \geq 3/2$), type A regulators always entail a stronger pole than a logarithm and the sharp cutoff is considered as a limit case. Finally we point out that formally $(C+\omega)^\gamma$ is analytic only for $n \in \{1/4, 1/2, \infty\}$ (case A) and $n \in \{d/4, d/2, \infty\}$ (case B).

5.2 Approximated flow

After the necessary parametrisation of the threshold function that encapsulates the details of the momentum integration, we are now in measure to build an approximated solution reliable in the deep infrared regime, i.e when $C+\omega$ is small. Such a solution is constructed in the following sections and we use it to study in a comprehensive way the convexity completion of the potential. The regularisation scheme dependence is analysed and all universality classes are included ($N \geq 1$).

Case	A	B
y_0	> 0	0
γ	$2 - \frac{1}{2n}$	$2 - \frac{d}{2n}$
P^2	$C + \alpha_{2n}(y - y_0)^{2n}$	$C + \alpha_n y^n$

Table 5.1: Classification of the regulator due the position of the minimum of P^2. We show the Taylor approximation of the inverse propagator and the pole index associated to it.

5.2.1 Infrared and large N limits

The aim of the previous discussion was to detail and analyse in some depth the crucial behaviour of threshold function in the vicinity of their potential pole. This was done with the ambition of studying the flow of the effective potential in the deep infrared where these singularities play an essential role. The second step is to construct a solution to the flow, with threshold functions conveniently parametrised, that is correct within the regime of interest i.e the deep infrared. The flow for the effective potential in our case can be written

$$\partial_t u = (d-2)\rho u' - 3u + \left(1 - \frac{1}{N}\right)\frac{1/(\gamma-1)}{(1+u')^{\gamma-1}} + \frac{1}{N}\frac{1/(\gamma-1)}{(1+u'+2\rho u'')^{\gamma-1}} \tag{5.18}$$

where we made the substitutions $u \to N\,\delta\,C^{1-\gamma}\,u$ and $\rho \to N\,\delta\,C^{-\gamma}\,\rho$. These substitutions are induced by the symmetries of the differential equation and lead to a more readable flow where we retained only essential features according to our analysis and parametrisation of $\ell'(\omega)$. Moreover it has the advantage of making the large N approximation totally transparent as the higher derivative term (containing u''), corresponding to the radial mode, is suppressed as $N \to \infty$ only leaving the Goldstone contribution $\propto (1 - 1/N)$ survive. Again, in accordance with what have been said previously the position of the singularity in amplitude about $-C$ is irrelevant for our concerns and only the nature of the singularity γ is meaningful. Despite these minor changes, solving (5.18) remains a formidable task and it is quite natural to look for an approximation scheme that allows an analytical treatment of the convexity approach. As a preliminary remark we note that this is essentially the presence of the second derivative u'' which makes (5.18) intractable and without it we would be in position to solve analytically the flow in complete analogy with the large N approximation scheme.

Following this, we adopt here a strategy of successive approximations to solve (5.18) within the deep infrared when $t \to -\infty$. We consider first a condition on the highest

derivative of the general form

$$G(\rho, u, u', u'') \ll 1 \tag{5.19}$$

which allows to rewrite the original flow (5.18) at the leading order $n = 1$ of our approximation like

$$\partial_t u = F_n(\rho, u, u'). \tag{5.20}$$

Then, once a solution to (5.20) is found, we can use it to check a posteriori if the condition (5.19) is verified. If (5.19) is true in some regime, the solution u_n to (5.19) can be considered as a correct approximated solution to (5.18) within this regime of interest. Also we can used the solution u_n of (5.20) to express G in terms of u and u' only and to formulate an higher order equation (5.20) with $n = 2$. If the solution u_2 of this equation still fulfills (5.19) then it is again a correct approximated solution to (5.18). This process can naturally be iterated from an order n to $n+1$ as long as the condition (5.19) is fulfilled. The condition (5.19) ensures that the approximated solution u_n converges towards the exact u of (5.18) when $n \to \infty$. This approach have been used in the context of $U(1)$-Higgs theory in [139].

Applying this strategy to the flow equation asks for the crucial formulation of a condition (5.19) that will lead to a correct approximation of the full flow. Such a condition can be formulated by rewriting the radial nonlinear part of the flow like

$$\frac{1}{N}\frac{1}{(1+u'+2\rho u'')^{\gamma-1}} = \frac{1}{N}\frac{1}{(1+u')^{\gamma-1}}\left(1-\frac{2\rho u''}{1+u'+2\rho u''}\right)^{\gamma-1}. \tag{5.21}$$

Under this form we see in a evident way that the unique condition

$$\frac{2\rho u''}{1+u'+2\rho u''} \ll 1 \tag{5.22}$$

leads to a flow similar to (5.20). This last condition only implies constraints on the higher derivatives of the potential u' and u'' but not on u. This is in accordance with the fact that convexity bounds apply on mass amplitudes therefore only to derivatives of the potential ($-1 \leq \omega$). Reinserting (5.21) with (5.22) into (5.18) gives the approximated flow for u'

$$\partial_t u' = (d-2)\rho u'' - 2u' - \frac{u''}{(1+u')^{\gamma}} \tag{5.23}$$

where the irrelevant constant $(\gamma - 1)$ has disappeared thanks to the differentiation. The equation (5.23) forms the leading order of the approximation to (5.18) and is in all respect similar to the flow equation in the large N approximation except for the singularity nature γ. This change is normal as we take into account large classes of regulator in our calculation. The fact that we recover the large N flow is not surprising as well because the neglected term in (5.21) is proportional to $1/N$. The reason behind this is that only the

radial mode contributes to the second derivative of the potential therefore its suppression leads to a flow containing only Goldstone modes. Following this, our approximation (5.22) can be understood as a projection of (5.18) on the large N flow, including finite N corrections iteratively. The technical advantage of the equation (5.23) is that it can be solved in a closed analytical form, provided $d \neq 2$ and $\gamma \neq 1$, by the method of characteristics. Through this method we can transform (5.23) into a system of two ordinary differential equations (the characteristic equations) given by

$$\frac{du'}{dt} = -2u' , \tag{5.24}$$

$$\frac{d\rho}{du'} = \left(\frac{d-2}{2}\right)\frac{\rho}{u'} - \frac{1}{2u'}\frac{1}{(1+u')^{\gamma}} . \tag{5.25}$$

The first equation is simple to integrate and its solution is

$$C_1 = u' e^{2t}. \tag{5.26}$$

By opposition, the solution of the second characteristic equation has a more involved structure and contains most of the non-trivial flow information. This solution can be cast into the form

$$C_2 = \rho \cdot |u'|^{1-d/2} - \mathcal{G}(u') \tag{5.27}$$

where the absolute value can be removed for positive u'. The function $\mathcal{G}(x)$ results from the complete integration of the second characteristic and have the integral representation

$$\mathcal{G}(x) = -\frac{1}{2}\int_{x_0}^{x} dy\, \frac{y^{-d/2}}{(1-y)^{\gamma}} . \tag{5.28}$$

The function $\mathcal{G}(x)$ can be also expressed in terms of hypergeometric function [141, 157] with the use of its integral representation that we recall here for convenience

$${}_2F_1(a,b,c,z) = \frac{\Gamma(c)}{\Gamma(b)\Gamma(c-b)}\int_0^{\infty} dt\; t^{b-1}\,\frac{(1-t)^{c-b-1}}{(1-tz)^{a}} \tag{5.29}$$

and that can be regarded as a one-valued analytic function on the complex plane cut along the real axis from 1 to $+\infty$. With the substitution $1/y = tz$ and choosing $\{a,b,c\} = \{\gamma, (d/2)-1+\gamma, (d/2)+\gamma\}$, we finally ends up with the closed expression

$$\mathcal{G}(x) = \frac{(-1)^{\gamma}}{2\nu}\,\frac{1}{|x|^{\nu}}\,{}_2F_1\left(\gamma,\nu,1+\nu,-\frac{1}{x}\right) - \frac{i\,\pi\,\Gamma(\nu)}{2\,\Gamma(d/2)\,\Gamma(\gamma)} \tag{5.30}$$

where $\nu = \frac{d}{2} - 1 + \gamma$ and the complex constant ensures that the function remains real for $-1 < x < 0$. Using (5.27) and (5.26) we can finally represent the general solution of (5.23) by the relation

$$\rho \cdot |u'|^{1-d/2} - \mathcal{G}(u') = F(u' e^{2t}) \tag{5.31}$$

where the function F is fixed by boundary conditions [1]. Once these boundary conditions are specified the relation (5.31) contains all the informations about the potential u' and its scaling. We choose the bare potential at a scale $t = 0$ (or $k = \Lambda$) to be $u'(t = 0) = \lambda_\Lambda(\rho - \kappa_\Lambda)$. The initial scale Λ is chosen such that $1 + u' \ll 1$ where the approximation of the threshold function (5.9) is valid. With this condition one can easily identified a running minimum for the potential given by

$$\rho_0 = \kappa_\star + \delta\kappa_\Lambda \, e^{t(2-d)} \tag{5.33}$$

with $\delta\kappa_\Lambda = \kappa_\Lambda - \kappa_{cr}$ and $\kappa_\star = \kappa_{cr} \equiv 1/(d-2)$. For $\delta\kappa_\Lambda > 0$ the dimensionless minimum diverges towards $+\infty$ maintaining the model into the broken phase ($\rho_0 \neq 0$). The function $F(x)$, with a simple quartic classical potential, reads

$$F(x) = \left(\frac{x}{\lambda_\Lambda} + \kappa_\Lambda\right) \cdot |x|^{1-d/2} - \mathcal{G}(x)\,. \tag{5.34}$$

In the infrared limit $t \to -\infty$ the right hand side of (5.31) diverges as $u'e^{2t} \equiv x \to 0$. The function $\mathcal{G}$ diverges with the same power as the first term of $F(x)$ according to

$$\mathcal{G}(x) = \frac{1}{d-2}\,|x|^{1-d/2} \;+\; \mathcal{O}(|x|^{2-d/2}) \tag{5.35}$$

when x approaches 0. From this we can read off the critical value of the running minimum $\kappa_{cr} = 1/(d-2)$. Then the diverging term $\delta\kappa_\Lambda \, e^{t(d-2)}$, which corresponds to the running minimum, forces the left hand side of (5.31) to diverge as well. In that case, the only possible non-trivial scaling solution for the potential is induced by the known singularity of the hypergeometric function $\mathcal{G}$ about -1. This singularity is a branch point from -1 along the negative axis and this structure leads to the solution

$$u' = -1 \tag{5.36}$$

which is interpreted as the convexity completion of the effective potential within a broken phase. This infrared fixed point solution is induced by the scaling of the minimum following the relation

$$\rho_0 - \rho = \frac{1}{2}\,\frac{1}{\gamma - 1}\,\frac{1}{(1+u')^{\gamma-1}} \tag{5.37}$$

where the power scaling of the potential towards (5.36) comes from the leading order of the Laurent expansion of $\mathcal{G}$ around $x = -1$ for $\gamma > 1$ and $d > 2$. The asymptotic

[1] It is worth mentioning that in the case where d is odd, the expression (5.30) simplifies to

$$\mathcal{G}(x) = \frac{|x|^{1-d/2}}{d-2}\;{}_2F_1\left(\gamma, 1-\frac{d}{2}, 2-\frac{d}{2}, -x\right) \tag{5.32}$$

which is real-valued for $-1 < x < 0$.

relation (5.37) details the deep infrared completion of the potential for the inner part of the potential $\rho < \rho_0$. It shows in a simple manner how the scaling of the minimum enforces the flattening of the potential within a phase with spontaneous symmetry breaking. Also it can be normalized such that $u'(\rho_0) = 0$ by simply subtracting the constant $(1/2)/(\gamma-1)$ to the right hand side of (5.37). The influence of the regularisation is controlled by the index γ which reinforces the pole entailing a smoother approach to (5.36) as we getting closer to the upper limit $\gamma = 2$ (see Figure 5.1).

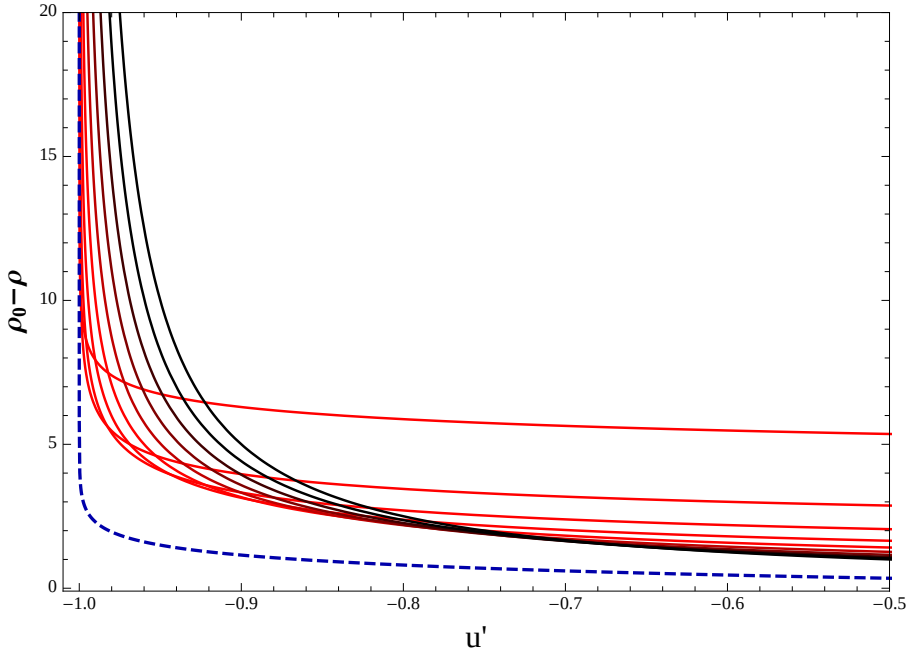

Figure 5.1: Infrared scaling of the dimensionless potential u' towards convexity for the regulator index $1 < \gamma \leq 2$ (the darker are the red curves the higher is γ). The sharp cutoff approach (formally $\gamma = 1$) is represented by the dashed blue curve.

On the opposite side, a weaker value for γ entails an abrupt variation in the vicinity of (5.36). The limit case $\gamma = 1$ will be examined in detail later. The dimension does not affect the scaling of the potential itself directly but rather increases the minimum scaling which in turn forces the completion of u'. Finally we note that (5.37) has subleading logarithmic corrections for $\gamma = 2$ whereas for $1 < \gamma < 2$ these corrections remain power-like although non-analytic.

The asymptotic relation when $t \to \infty$ allows us to verify a posteriori the condition (5.22). From (5.37) we compute easily that $u'' = 2(1+u')^\gamma$ hence

$$\frac{2\rho u''}{1+u'+2\rho u''} = \frac{4\rho(1+u')^{\gamma-1}}{1+4\rho(1+u')^{\gamma-1}} \quad \longrightarrow \quad 0 \tag{5.38}$$

when $1 + u' \to 0$ provided $\gamma > 1$. This legitimates the neglect of the radial mode con-

tribution for $N > 1$ in the deep infrared. Also, as the correction to the approximated flow (5.23) appears to be arbitrarly small, there is no need for higher order corrections to (5.37). The smallness of (5.38) ensures that the approach to convexity is completely dominated by the leading order term (5.37). This supports as well the super-universal character of the fixed point solution (5.36) as the dependence on N drops out of the flow at the leading order of our approximation (5.23) which does not suffer from the arbitrarily small corrections (5.38). Scaling for higher order operators can also be computed out of (5.37). We found

$$u^{(n+1)} = \left(\frac{\alpha}{2}\right)^{\alpha} \frac{\Gamma(n+\alpha)}{\Gamma(\alpha)} \frac{1}{(\rho_0 - \rho)^{\alpha+n}} \tag{5.39}$$

with $n \geq 1$ and $\alpha = 1/(\gamma - 1)$. Form this expression it is clear that as long as $\delta\kappa_\Lambda > 0$ then $u^{(n+1)} \propto e^{t(2-d)(\alpha+n)} \to 0$ which is subleading with respect to the scaling of u' towards (5.36) as $n \geq 1$. The dependence of the scaling of higher operators is similar to the one of the potential derivative and a maximally smooth approach towards convexity is again obtained for $\gamma \to 2$.

As we can see from the running potential (5.33) the large N model possesses two phases whose separation corresponds to the critical value for the classical minimum $\kappa_{cr} = \frac{1}{d-2}$ for $d > 2$. The infrared flow is mainly driven by the minimum running and in the broken phase, i.e when $\delta\kappa_\Lambda > 0$, its divergence enforces the potential convexity and this situation is discussed in many details in subsequent sections. But we have also to analyse the situation where $\delta\kappa_\Lambda \leq 0$, where well-known infrared fixed points are dominating the flow instead of the solution (5.36). When a critical value is chosen for the classical minimum such that $\delta\kappa_\Lambda = 0$ the minimum is unrenormalised and for $2 < d < 4$ the solution (5.31) converges towards the Wilson-Fisher fixed point solution

$$\rho = |u'|^{d/2-1}\, \mathcal{G}(u') \tag{5.40}$$

where the absolute value can be removed for $u' > 0$. This solution is a generalisation of the one presented in chapter 3 for an optimised cutoff ($\gamma = 2$) in three dimensions. For $d > 4$ the critical potential simply evolves towards the Gaussian solution $u' = 0$ for all field values. Clearly in both situation $u' \geq -1$, which imply a convex potential so that the convexity solution does not modify the known phases on the $O(N)$ models. Finally, even more simpler is the case $\delta\kappa_\Lambda < 0$ where the dimensionless minimum is driven towards $-\infty$ which means that the system ends up in the symmetric phase with a dimensionful minimum at the origin. In all evidence such a phase corresponds to a convex potential and the minimum running knowingly imposes $u' \geq 0$ for all fields.

5.2.2 Sharp Cutoff

The case $\gamma = 1$ has been excluded of our calculation until now because it corresponds to a particular pole structure for the flow $\partial_t u$. Indeed we already noted that this choice of index leads in fact to a logarithmic nonlinear part and we have to adapt slightly our previous strategy of solution in the regime $t \to -\infty$. Following the same philosophy than precedently, we can write the flow for a sharp cutoff directly like (using the same normalisation as before)

$$\partial_t u = (d-2)\rho u' - 3u + \log\left(\frac{1}{1+u'}\right) + \frac{1}{N}\log\left(1 - \frac{2\rho u''}{1+u'+2\rho u''}\right) \tag{5.41}$$

using the multiplicative property of the logarithmic function. Here the decoupling between massive and massless mode is even more evident as N drops off by a simple rewriting of the flow. Within this formulation we apply the same scheme by imposing a priori the condition (5.22) that leads to

$$\partial_t u' = (d-2)\rho u'' - 2u' - \frac{u''}{1+u'}. \tag{5.42}$$

The general solution of this flow is of the same form as (5.31) but the function $\mathcal{G}$ slightly differs

$$\mathcal{G}(x) = -\frac{1}{d}\frac{1}{|x|^{d/2}}\,{}_2F_1\left(1\,,\,\frac{d}{2}\,,\,1+\frac{d}{2}\,,\,-\frac{1}{x}\right) - \frac{i\,\pi}{2}\,. \tag{5.43}$$

This expression is real value for $-1 < x < 0$ because of the presence of the complex constant. We can clearly anticipate that the singularity structure around $x = -1$ will be different thanks to the first index of the hypergeometric representation (5.43). If we impose again a quartic bare potential we obtain the same function F as (5.34) with the same limit (5.35) when $t \to -\infty$. This means that we have exactly the same running minimum (5.33) as before. Consequently for $\delta\kappa_\Lambda > 0$, the minimum's running enforces again the scaling of u' towards -1 leading to the fixed point solution (5.36). However this time the approach of the pole, characterized by the first index of (5.43), is logarithmic at the leading order of the Laurent expansion. In this case the asymptotic expression about the solution (5.36) is simply

$$\rho_0 - \rho \;=\; \frac{1}{2}\log\left(\frac{1}{1+u'}\right). \tag{5.44}$$

The scaling relation (5.44) shows again the completion of convexity for the inner part of the potential induced by the running of the minimum. We note in passing that (5.44) can be obtained from (5.37) (with the correct interpolation at $u'(\rho_0) = 0$) using the definition of the logarithm as a limit when $\gamma - 1 \equiv \epsilon \to 0$. This transition towards a convex potential

is steeper in the vicinity of (5.36) thanks to the logarithm in (5.44) (see Figure 5.1). The minimum scaling increases with the dimension $d > 2$ in a complete similar way to the case $\gamma > 1$. Higher derivatives scaling from (5.44) are given by

$$u^{(n+1)} = 2^n \, e^{2(\rho-\rho_0)} \tag{5.45}$$

where we recall that $\rho_0 \propto e^{t(2-d)} \to +\infty$ when $t \to -\infty$. Comparatively to the algebraic scaling (5.39) we have here a exponential completion of $u^{(n+1)} = 0$ for $n \geq 1$. The relation (5.45) illustrates the steep transition to convexity specific to the sharp cutoff where a deviation on ρ_0 is immediately exponentiated leading an increased sensibility to numerical errors. Moreover, using again (5.44), we obtain $u'' = 2(1 + u')$ thus the neglected term in (5.42) reads

$$\frac{2\rho u''}{1 + u' + 2\rho u''} = \frac{4\rho}{1 + 4\rho} \quad \longrightarrow \quad 0 \tag{5.46}$$

only for $\rho \to 0$. This reduce the domain of validity of our solution in the vicinity of the origin and then fail to describe the flattening of the entire inner part of the potential on the contrary to the case $\gamma > 1$. This check disqualify the sharp cutoff for a reliable study of the deep infrared scaling of the effective potential unless in the immediate vicinity of $\rho = 0$.

To close the discussion we would like to outlined that despite the fact the anomalous dimension is expected to be negligible in the deep infrared critical regime (and has been set to zero up to now), it is simple to reintroduce it. This remark, that concerns all classes of regulators, is important in two dimensions where the anomalous dimension governs the approach to convexity [25] and we need to make the replacements $(d-2)\rho u'' \to (d-2+\eta)\rho u''$ and $2u' \to \eta u'$ in (5.42) such that for $d \to 2$ the structure of the flow and our results remain valid. The large N solution (5.31) (with (5.30)) can be also directly amended by $d \to \eta + 2$ to cover the case $d = 2$ and all results derived from it are modified in consequence. It is assumed in that case that the anomalous dimension remains a strictly positive for all values of k (see [25] for details).

5.2.3 Ising model

When a single field is present in the flow equation (5.18), the approach to convexity can not be the result of the dominance the massless mode anymore. In that specific case the only mass amplitude is given by

$$w = u' + 2\rho u'' \tag{5.47}$$

and is solely responsible of the infrared completion of the potential when $w \to 0$. In passing we note that the function is nothing else but the second derivative of the potential in field unit $w \equiv V''(\varphi)$. Therefore it is more appropriate to formulate the flow (5.18) in terms of the radial mass amplitude w in order to study the infrared scaling of the potential. Furthermore we can write the flow for w bearing in mind that we would like to keep the same strategy of iterative solution as for $N > 1$. This reasoning for $N = 1$ leads to the flow

$$\partial_t w = (d-2)\rho w' - 2w - \frac{w'}{(1+w)^\gamma}\left(1 + 2\rho\left(\frac{w''}{w'} - \frac{\gamma\, w'}{1+w}\right)\right). \tag{5.48}$$

The similarities of structure with the large N case are striking and conduct to the natural condition

$$2\rho\left(\frac{w''}{w'} - \frac{\gamma\, w'}{1+w}\right) \ll 1 \tag{5.49}$$

which leads us indeed to the same flow as in the large N approximation where the massless amplitude u' is just replace by the massive one w. Beyond the approximations (5.49) and (5.22), it is clear that the possibility of the completion of convexity at large N validates the minimal structure of the flow necessary for a convex potential and approximation around it. This can be seen as an effect of the super-universal character of the convexity approach, where the distinction on N no longer matters as $t \to -\infty$. To investigate more in depth this aspect we proceed to the next step of our calculation by imposing (5.49) to (5.48) and obtain as expected

$$\partial_t w = (d-2)\rho w' - 2w - \frac{w'}{(1+w)^\gamma}\,. \tag{5.50}$$

We note that this time we include the sharp cutoff case because the rewriting of the flow in terms of w is made at the level of the flow for u' where there is no drastic change in the structure of the equation for $\gamma = 1$ (no logarithmic term). The equation is identical to (5.23) with $u' = w$ therefore its solution is given by (5.31) with the appropriate amplitude. Using again a quartic expression $w(t=0) = \lambda_\Lambda(\rho - \kappa_\Lambda)$ as a boundary condition we obtain the same running as (5.33) where we replace the minimum ρ_0 by the field configuration χ for which we have $w(\chi) = 0$ all along the flow. The specific value χ corresponds to the real (dimensionless) field $\varphi_0 = \sqrt{2\chi}$ for which $V''(\varphi_0) = 0$. When $\delta\kappa_\Lambda > 0$ the running of χ leads to the fixed point solution $w = -1$ with the same approach as before, to wit

$$\chi - \rho = \frac{1}{2}\,\frac{1}{\gamma - 1}\,\frac{1}{(1+w)^{\gamma-1}}\,. \tag{5.51}$$

If we normalise this expression such that $w(\chi) = 0$ then the limit $\gamma - 1 \to 0$ can be safely achieved to obtain the sharp cutoff scaling (5.44). The scaling behaviour is identical to

what we observed for $N > 1$, except that the role of the minimum is now played by the field configuration χ, for which the mass (in unit of φ) vanishes, forces w to scale towards -1. Nevertheless the minimum of the potential ρ_0 for which $u'(\rho_0) = 0$ is simply related to χ. This field can be expressed as the ratio (for $u''(\chi) \neq 0$)

$$\chi = -\frac{u'(\chi)}{2u''(\chi)} \tag{5.52}$$

and assuming u' is analytic about some field configuration ξ we have, at the leading order in ρ, the relation $u'(\rho) = u'(\xi) + u''(\xi)\,(\rho - \xi)$. Then identifying $\rho \to \rho_0$ and $\xi \to \chi$ we obtain

$$\chi = \frac{\rho_0}{3} \tag{5.53}$$

that indicates that the running of χ is indeed induced by that of the potential minimum ρ_0. The asymptotic relation (5.51) is used again to confirm a posteriori the approximation (5.49). From (5.51) we get $w' = 2(1+w)^\gamma$ and $w'' = 4\gamma(1+w)^{2\gamma-1}$ in the vicinity of $w = -1$ which imply

$$\frac{w''}{w'} = 2\gamma(1+w)^{\gamma-1}\,, \tag{5.54}$$

$$\frac{\gamma\, w'}{1+w} = 2\gamma(1+w)^{\gamma-1}\,. \tag{5.55}$$

therefore the corrections to (5.50) cancel. This indicates that the behaviour (5.51) fully describes the approach to convexity in the regime $t \to -\infty$. The cancellation of (5.49) can be viewed as the consequence of the absence of competition between the radial and the Goldstone modes. Originally the corrections for the flow $\partial_t u'$ could be interpreted as the effect of the radial mode when $N < \infty$ but when $N = 1$ this interpretation is less pertinent. Indeed it appears, in this particular case only, that the neglect of higher derivatives of $w(\rho) = V''(\varphi)$ is an even more accurate approximation. But it is not in contradiction with previous results as $1 + u' \to 0$ is still true. Merely the approximated flow in terms of amplitude $w = u' + 2\rho u''$ take into account simply the effect of u'' that were neglected in first place. In consequence the convexity completion is reproduced more accurately and still induced by the potential minimum scaling.

5.3 Approach to convexity

In the following we focus on the consequences of the asymptotic behaviour (5.37) for the flattening of the dimensionful potential within its non-convex part. We recall that we found a solution for the renormalisation group flow of the effective potential that describes

correctly the infrared completion of convexity when all fluctuations are integrated out. The approach to a convex potential is found to be model-independent and sensible to a specific infrared regularisation scheme. Provided a sufficient regularisation such that a pole structure in the dimensionless potential flow is maintained, the dimensionful potential curvature in the broken phase is given by

$$U'(\bar{\rho}) = -\,k^2 \,+\, k^{2+\alpha(d-2)} \left[k^{d-2} \,+\, \frac{2}{\alpha}\,(\bar{\rho}_0 - \bar{\rho}) \right]^{-\alpha} . \tag{5.56}$$

We note that the potential has been normalized to $U'(\bar{\rho}_0) = 0$. The regulator dependence is taken into account via the coefficient

$$\alpha \,=\, \frac{1}{\gamma - 1} \tag{5.57}$$

with $1 \leq \alpha \leq \infty$. When $\alpha = 1$ we recover an optimised smooth type of regularisation whose typical form of regulator has been put forward in [71]. The situation $\alpha \to \infty$ corresponds to a sharp regularisation of the lower modes that still guarantee a convex infrared potential despite its stiff approach to convexity. In the continuation of our analysis the formula (5.56) describes the approach to convexity for the inner part of the potential within the domain of validity

$$1 + \frac{2}{\alpha}\, k^{2-d}\,(\bar{\rho}_0 - \bar{\rho}) \,\gg\, 1\,. \tag{5.58}$$

This condition is in practice always verified as $\bar{\rho}_0 - \bar{\rho} \neq 0$ and $k \to 0$ with $d > 2$. The potential (5.56) is the leading term of an expansion in $(\bar{\rho}_0 - \bar{\rho})$ whose subleading orders are logarithmic and can be computed from higher orders of the expansion (5.35). This corrections become dominant when $\alpha \to \infty$ as we will see later. The potential (5.56) can be integrated, we found

$$U(\bar{\rho}) = k^2\,(\bar{\rho}_0 - \bar{\rho}) + \Omega\, k^d \left[\left(1 + \frac{2}{\alpha}\, \frac{\bar{\rho}_0 - \bar{\rho}}{k^{d-2}} \right)^{1-\alpha} - 1 \right] \tag{5.59}$$

with $\Omega = \frac{1}{2}\frac{\alpha}{1-\alpha}$ and we normalized the potential such that it vanishes at its minimum. Under the form (5.59) the behaviour for small value of k is easier to analyse. As we integrate lower modes we clearly see the flattening of the inner part of the potential as

$$\lim_{k \to 0} U(\bar{\rho}) = 0 \tag{5.60}$$

for $\bar{\rho} < \bar{\rho}_0$. We recognize at the leading order the regulator independent contribution proportional to $(\bar{\rho}_0 - \bar{\rho})$ and already obtained at the one-loop approximation of the effective potential in [44]. The subleading corrections to this universal behaviour are in inverse power of the field but remain non-singular within $0 < \bar{\rho} < \bar{\rho}_0$. This power is regulator

dependent and becomes potent when k approaches zero. If we set $U(\bar{\rho}) = k^2\,(\bar{\rho}_0 - \bar{\rho}) + V(\bar{\rho})$, the regulator dependent corrections are in the deep infrared

$$V(\bar{\rho}) \;=\; \tilde{\Omega}\; k^{d+\alpha(d-2)}\,(\bar{\rho}_0 - \bar{\rho})^{1-\alpha} \tag{5.61}$$

where $\tilde{\Omega} = \Omega\,(2/\alpha)^{1-\alpha}$. The power $k^{d+\alpha(d-2)}$, as a function of k, is gradually flatter when $\alpha \to 1$ favoring a smoother transition to a completely flat potential. In an opposite manner, the maximisation of α (or minimisation of γ) accelerates the approach to convexity with an enhanced suppression of $V(\bar{\rho})$ when $k \to 0$. For a fixed regularisation (fixed α), the dimension d have a similar role to α, with a sleeker behaviour in k for $d \to 2$ and faster suppression of $V(\bar{\rho})$ for $k \to 0$ when d increases.

In the logic of our analysis optimised and sharp regularisations appear as limit case and any regulator that ensures a convex potential should interpolates between this two extreme schemes, i.e satisfies $1 < \gamma < 2$. Although these specific cases seem to be singular in the expression (5.59) the potential can be obtained by limiting processes. Using the definition of the logarithm as a limit the potential (5.59) reads in the limit $\alpha \to 1$ (or $\gamma \to 2$)

$$U(\bar{\rho}) = k^2\,(\bar{\rho}_0 - \bar{\rho}) - \frac{k^d}{2}\,\ln\left(1 + \frac{2(\bar{\rho}_0 - \bar{\rho})}{k^{d-2}}\right). \tag{5.62}$$

The logarithmic function ensures that non-universal contributions to the convexity approach are proportional to $\propto k^d \ln k$ and it is field independent. The presence of the logarithm softens the suppression of the subleading contribution by an additional cancellation when $k \sim 1$. At the opposite when k approaches 0 the logarithm amplifies the generic behaviour $\propto k^d$. All other contribution in powers of k are subleading to (5.62) when $k^{d-2} \to 0$. This improved stability is particularly appreciable in a numerical implementation of the flow [25]. In the sharp case when $\alpha \to \infty$ we used the definition of the exponential function as a limit and get

$$U(\bar{\rho}) = k^2\,(\bar{\rho}_0 - \bar{\rho}) - \frac{k^d}{2}\left[e^{-2(\bar{\rho}_0 - \bar{\rho})k^{2-d}} - 1\right]. \tag{5.63}$$

Here the presence of the exponential modifies drastically the completion of convexity by a quick suppression of $V(\bar{\rho})$ as $k \to 0$. Considering $\bar{\rho} \sim \bar{\rho}_0/2$ for instance, then the suppression is proportional to $\propto k^d\, e^{-k^{2-d}}$ which is in total contrast with the smooth approach offered by an optimized regulator and favors the sensibility to numerical error. Hence the choice of a specific regulator results in a qualitatively and quantitatively different approach to a convex potential. Again, the strongest divergence in the threshold function leads to the "best" approach to $U' \geq 0$ for $\rho \leq \rho_0$ and this is achieved for $\gamma = 2$ (see figure 5.2).

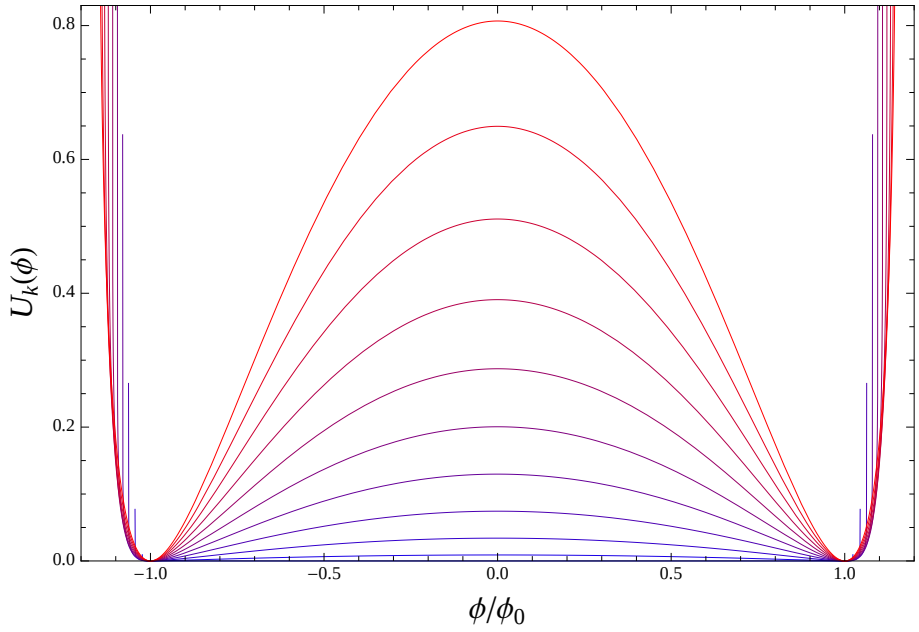

Figure 5.2: Approach to convexity for the effective potential $U_k(\phi)$ with an optimised cut off from (5.62) in three dimensions for $k = n/10 + 10^{-10}$ for $n = \{0, 1, 2, \ldots, 9, 10\}$.

5.4 Non-convexity

We point out in this section that specific cutoff functions can cause a non-convex potential as all the momentum range is integrated. It is shown that insufficiencies of a given regularisation scheme in a given dimension leads to an RG flow that stops at a finite infrared scale therefore to a non-flat potential. After a general analysis, a specific example is given using a power-like regulator that leads to a Callan-Symanzik type of RG flow in four dimensions.

5.4.1 Unstable flow

We saw that the approach to convexity is closely related to the singularity structure of the renormalisation flow of the effective potential. The index γ of the singularity is the crucial parameter on which convexity completion mainly depends. This permits to classify regulators into two main classes A and B whose characteristic indices differ significantly. In the case A the singularity is induced by the flatness of the effective propagator around a non-vanishing minimums that guarantees $\gamma \geq 3/2$. This quality of the class A regulator automatically ensures that a convex potential is reached when all modes are integrated out and the details of the infrared completion depend on the precise value of γ. This qualify class A regulators as highly reliable for the integration of the lower modes with a

stable behaviour in the vicinity of (5.36). In contrast with this case, class B regulators allow for an index dependent on the dimension that breaks the lower bound that we had for class A regulator. Ultimately this is an effect of the addition of the contributions from the integration measure of $\ell'(\omega)$ and from the minimum of the effective propagator located at vanishing momentum. In this case the limit case $\gamma = 1$ corresponds to a cancellation of the contribution with $d = 2n$ and to a completion of convexity similar to the sharp cutoff following (5.44). If the contribution from the propagator wins over the measure then we are in the situation $\gamma < 1$ where the convexity completion is put in question. This ambiguity can easily be spotted from the flow (5.18) which does not show any singularity for $\gamma < 1$.

Fortunately enough for a stricly positive index γ the solution (5.31) with (5.30) are still completely valid and so is the expansion of $\mathcal{G}(x)$ around -1. With a quartic bare potential when $t \to -\infty$ the right hand side of (5.31) behaves exactly the same and $F(x)$ diverges like $\propto |x|^{1-d/2}$ when $x \to 0$. As we are in a broken phase $u' < 0$ and the left hand side of (5.31) is forced again towards (5.36) but in this case the flow stops at a finite value of t that corresponds exactly to $u' = -1$. In the vicinity of $u' = -1$ the relation (5.37) is correct but the singularity is absent simply because $\gamma < 1$. It reads more simply in the form

$$1 + u' = \Big((1 - 2(1-\gamma)(\rho_0 - \rho)\Big)^{\frac{1}{1-\gamma}}. \tag{5.64}$$

Consequently the right hand side of (5.64) vanishes as we integrates out lower and lower modes and the renormalisation flow ends at the finite scale $k > 0$. A direct consequence is that the effective potential retains a negative curvature in its inner part, hence remains non-convex because of the specific momentum regularisation.

For the case $\gamma = 0$ the approximation (5.9) fails due to the contribution of high momenta y which have to be properly regularised. If we imposed a supplementary UV cutoff Λ we recover a convergent representation for $\ell'(\omega)$. Then when $1 + \omega \ll 1$ we can ignore legitimately this UV regularisation because of the infrared focus of our calculation. Finally we found that $\ell'(\omega) = \delta\, \ln(1+\omega)$ and if we take the additional assumption $2\rho u'''/(3u'') \ll 1$ at the level of the flow $\partial_t u'$ instead of $\partial_t u$ we ends up with the approximated infrared flow

$$\partial_t u' = (d-2)\rho u'' - 2u' + u''\, \ln(1+u') \tag{5.65}$$

where the coefficient δ has been rescaled into u and ρ as usual. The equation (5.65) can be integrated analytically by usual methods. We still obtained a solution of the general

form (5.31) but the function $\mathcal{G}$ is given now by

$$\begin{aligned}\mathcal{G}(x) &= \frac{2}{d(d-2)}\frac{(-1)^{d/2}}{(1+x)^{d/2}}\,{}_2F_1\left(\frac{d}{2},\frac{d}{2},1+\frac{d}{2};\frac{1}{1+x}\right)\\ &\quad+\frac{|x|^{1-d/2}}{d-2}\left(\frac{2}{d-2}+\ln(1+x)\right)-\frac{i\,\pi}{d-2}\,.\end{aligned}\tag{5.66}$$

The function $\mathcal{G}$ is real-valued for $-1<x<0$ and diverges when $x\to 0$ but vanishes when $x\to -1$. Following the same reasoning as for $0<\gamma<1$, $t\to-\infty$ forces u' to scale towards -1 and the eft hand side of (5.31) vanishes. So the renormalisation scale ends up again at a finite value entailing a non-convex potential. This calculation and analysis are very similar for $\gamma<0$ and we still obtain a non-convex potential for the same reason.

5.4.2 Specific example

To illustrate in a crude way the problem of some regularisation scheme for the completion of convexity we take the example of a simple inverse regulator $r(y)=1/y$. It corresponds to a Callan-Symanzik type of flow that can also be obtained using an exponential cutoff like $r(y)=y(e^y-1)^{-1}$ in 4 dimensions. This is a class B regulator with a Taylor index $n=1$ so that in 3 dimensions the singularity index is given by $\gamma=1/2$. Within a quartic bare potential, the solution to the flow in the deep infrared corresponds to the simple relation

$$\rho_0-\rho=1-\sqrt{1+u'}\tag{5.67}$$

with a scaling minimum $\rho_0=\delta\kappa_\Lambda e^{-t}$. We precise that we focus only the case $\delta\kappa_\Lambda>0$ as for $\delta\kappa_\Lambda<0$ we ends up with $\rho_0=0$ at some scale and so in a symmetric hence convex phase. Here subleading order vanishes exponentially when $t\to\infty$. Through the simple relation (5.67) we clearly see that as the minimum increases the right hand side of (5.67) is enforced to increase as well. Because the solution is restricted to $-1<u'<0$, the only possible evolution of the potential is $u'\to-1$. The potential can not cross the branch point about $u'=-1$ hence the renormalisation scale stops. If we neglect the presence of the field in (5.67) then we have a precise value for the end scale $k_{end}=\delta\kappa_\Lambda$. In 4 dimensions the situation is changed as $\gamma=0$ and we have a flow of the logarithmic form (5.65). When $t\to-\infty$ the solution boils down again to a very simple scaling relation

$$u'=\frac{1}{t}\,(\rho_0-\rho)\tag{5.68}$$

with $\rho_0=\kappa\,e^{-2t}$. As $t<0$ the flow stops again at a finite scale because the solution to the flow contains a logarithmic term like $\ln(1+u')$ (see (5.66)) which forbids the branch

point $u' = -1$ to be crossed. Hence we still remain with a non-convex potential thanks to the regularisation.

As a concluding remark we would like to emphasize that the value $\gamma = 1$ marks frontier in the space of all possible regulators. Indeed for $\gamma \geq 1$ we always reach a convex potential when all fluctuations are taken into account. The limit case $\gamma = 1$ corresponds to a sharp separation between high and low modes and is characterised by a very stiff approach to convexity that leads to stability problems in a numerical integration of the flow. At the level of the flow this crucial property for the regulator can be easily linked to the infrared completion of the potential following the scheme

$$\ell'(\omega) \propto \frac{1}{(1+\omega)^{\gamma}} \quad \Rightarrow \quad \rho_0 - \rho \propto \frac{1}{(1+\omega)^{\gamma-1}} \,. \tag{5.69}$$

Even the slightest deviation $\epsilon = 1 - \gamma \ll 1$ from the critical value of the singularity index leads to a non-convex potential as it suppresses the singularity of the flow in the infrared (see the pole structure in (5.30)).

5.5 Convexity fixed point

Previously, the conditions for the obtention of a convex infrared effective potential have been clearly stated and studied. Thus we discuss in this section the scaling of the potential in terms of fixed point and compute its associated critical indices. Those can be calculated from the asymptotic behaviour of the potential when $k \to 0$. The role of the potential minimum is recognized and analyse thoroughly and the super-universal character of the approach to convexity is justified.

5.5.1 Scaling towards convexity

Up to now, the scaling of the potential in the deep infrared region, i.e when momenta are almost all integrated, have been worked out through different analytical approaches. First we noted that the scaling solutions of $\partial_t u' = 0$ at large N shows a particular configuration when the constant of integration c in (3.21) tends to $\pm\infty$. This solution was then identified through a local expansion about the minimum of the potential with finite and infinite components. Finally, a dominant analysis of the flow equation for the effective potential at finite N, together with an exact solution of the flow at large N, lead to the conclusion that the convexity of the effective potential is achieved through the solution

$$u' = -1 \tag{5.70}$$

where the subleading corrections to this behaviour appear in the asymptotic relation (5.37). Indeed the solution (5.70) have a simple interpretation in terms of infrared fixed point which dominates the completion of the potential for very low energies and within the non-convex part of the potential. Following this interpretation it is quite natural to compute the set of eigenvalues that drive the infrared scaling of any operator in the vicinity of (5.70). For this we use the important relation (5.37) that encapsulates the essential scaling informations of the potential in accordance with our previous analysis. By differentiating it with respect to the logarithmic RG scale t, we obtain the eigenvalue equation

$$\partial_t u' = \left(\frac{d-2}{\gamma-1}\right)(1+u') \tag{5.71}$$

where the scaling of the mass term is related to the eigenvalue $\left(\frac{d-2}{\gamma-1}\right) > 0$. Thus it is an irrelevant operator and small perturbation around (5.70) will be suppressed. For instance, if we introduce $\epsilon = 1 + u'$ then the flow is driven exponentially towards (5.70) such that $\epsilon(t) \sim \exp\left[\left(\frac{d-2}{\gamma-1}\right)t\right]$ as $t \to -\infty$. From (5.71) we still observe the enhancement of the scaling when the dimensionality increases. The effect of the regularisation is also manifest with an acceleration of the scaling towards (5.70) when $\gamma \to 2$. The case $\gamma = 1$ is related to a sharp regularisation of the lower modes leading to a non algebraic approach of (5.70) and it will be discussed later. Also we remark in passing that as we are getting closer to $d = 2$, the flow is 'slower' towards convexity. We outline that the dependence on the dimension of the eigenvalue related in (5.71) is directly inherited from the scaling of the minimum of the potential given by

$$\partial_t \rho_0 = (d-2)\,\rho_0\,. \tag{5.72}$$

This scaling is already known to be at the origin of the scaling of u' from (5.37) amended by the regularisation dependence of the infrared scaling. The relation (5.72) is easily justifiable from the running minimum (5.33) at large N. Again it reflects the prominent role play by the non-perturbative running of the minimum. The scaling exponents of higher order operators can also be simply computed from (5.37) by systematically differentiating the asymptotic relation with respect to the squared field ρ as the effective potential is the generating function of all the couplings. We obtained the relation

$$\partial_t u^{(n)} = (d-2)\left(n - \frac{\gamma-2}{\gamma-1}\right)u^{(n)} \tag{5.73}$$

for $n > 1$. There we still identify the contribution from the minimum but the higher operators scale towards their gaussian values at vanishing coupling. Their irrelevant scaling towards $u^{(n)} = 0$ is also enhanced as n increases and as $\gamma \to 1$ as well (the case $\gamma = 1$ will

be treated later). Alternatively the eigenvalues of higher couplings in (5.73) can be read off from the n-derivative of the dimensionless potential (5.39). If we switch to dimensionful units in (5.39) we obtain

$$u^{(n)} \propto \frac{k^{(d-2)(n-\frac{\gamma-2}{\gamma-1})}}{(\bar{\rho}_0-\bar{\rho})^{(n-\frac{\gamma-2}{\gamma-1})}} \tag{5.74}$$

where it is clear that from a simple scale derivative of the n-derivative potential $u^{(n)} \equiv k^{(d-2)n-d}\, U^{(n)}$ we get the eigenvalues appearing in (5.73). Here the presence of a non-trivial running vacuum modifies strongly the infrared completion of the potential hence its approach to convexity. The self-consistence of the scaling (5.71) can also be checked by reinserting it into the flow (5.23). Using (5.37), we observe that the scaling of $1+u' \to 0$ results from the cancellation between the $-2u'$, coming from the canonical scaling of the mass term, and the nonlinear fluctuation term $\frac{u''}{(1+u')^\gamma}$ that encodes the non-perturbative quantisation of the flow. The term related to the canonical scaling of the field $(d-2)\rho u''$ is proportional to $(1+u')^\gamma$ and then, subleading to the scaling of $\partial_t u'$ because of $\gamma > 1$. Finally we would like to detail here the running of renormalised mass term with respect to its bare value. In this example the (microscopic) scale Λ at which the potential is defined arbitrarly is assumed to be close to $k = 0$ where the solution (5.31) is correct and the scaling relation (5.37) verified. Thus considering the relation (5.37) at both scales $k = \Lambda$ and $k \ll \Lambda$, we have in dimensionless units

$$\frac{k^2+U'_k}{\Lambda^2+U'_\Lambda} = \left(\frac{k}{\Lambda}\right)^{2+\frac{d-2}{\gamma-1}} \tag{5.75}$$

as k approaches 0. In this relation we assumed that $\kappa_\Lambda \gg \kappa_{cr}$ in (5.33) and that $\kappa_\Lambda, \rho_0 \gg \rho$. In the relation (5.75) we recover the features of the infrared scaling of the potential with the effect of the dimensionality and of the regularisation. In addition of these effects we identified as well the contribution from the scaling of the mass term $[U'] = -2$. Thus, (5.75) gives the details of the scaling of towards a convex potential in the broken phase. We observe the progressive appearance of infrared divergences associated with the presence of massless modes, i.e an effective potential with a zero curvature at the origin and a non-vanishing minimum.

Before switching to the detailed interpretation the fixed point solution (5.70) it is legitimate to ask whether this solution is apparent from a local expansion of the critical potential as studied in chapter 3. Indeed it is expected that, as a proper fixed point solution, the convexity fixed point should be accessible for some value of the integration constant appearing in the scaling solution of (5.23) (with $\partial_t u' = 0$). Following our previous

result that $u' = -1$ corresponds to the convexity bound we expand the scaling solution $\rho = |u'|^{d/2-1}[\mathcal{G}(u') + c]$, where $\mathcal{G}$ is given by (5.30) and c is the integration constant, around $u' = -1$. The leading term of the Laurent expansion around he singularity yields to (subleading terms are ignored)

$$c - \rho = \frac{1}{2}\frac{1}{\gamma - 1}\frac{1}{(1+u')^{\gamma-1}} \tag{5.76}$$

where in the light of the analysis of (5.37) the constant c, related to the exactly marginal coupling discussed in chapter 3, plays the role of the potential minimum. Then, tuning the marginal coupling such that c diverges allows to compensate the divergence of the l.h.s of (5.76) and to relax the constraint on ρ such that all values of the field are allowed and, at the same time, $u' = -1$. Thus by an extreme tuning of c (i.e of the marginal coupling) we obtain a well-defined fixed point solution corresponding to a flat potential $U' = 0$ only from a local approximation of the effective potential.

5.5.2 Interpretation

A simple analysis of the convexity fixed point (5.70) can be given by comparing its eigenvalues spectrum to the spectrum obtained about the Gaussian fixed point solution $u' = 0$, that we computed in chapter 3. In that case the linearisation of the flow equation about this trivial solution leads to the Gaussian spectrum (n is a positive integer)

$$\omega_{G,n} = (d-2)n - d \tag{5.77}$$

that is solution to the eigenvalues equation $\partial_t \delta u^{(n)} = \omega_n \, \delta u^{(n)}$. We precise that the spectrum (5.77) corresponds to a polynomial basis for the eigenperturbation $\delta u^{(n)}$ around the Gaussian fixed point solution $u^{(n)} = 0$. Also, the canonical scaling of the field operators for an $O(N)$ symmetric potential can be read off from $[U^{(n)}] = (d-2)n - d$. As usual the first eigenvalue ($n = 1$) is related to the relevant scaling of the mass operator ϕ^2. The rest of the spectrum is stable according to the dimensionality. For $n > \frac{d}{d-2}$ we have an infinite number of stable directions towards $u^{(n)} = 0$ whereas for $n < \frac{d}{d-2}$ we have a finite number of unstable directions, and for $n = \frac{d}{d-2}$ we have a marginal contribution. By comparison, we have at the convexity fixed point the following spectrum

$$\omega_{C,n} = (d-2)\left(n - \frac{\gamma - 2}{\gamma - 1}\right) \tag{5.78}$$

where the eigenbasis is now the monomials of the field ρ^n themselves. The comparison between the two spectrum $\omega_{G,n}$ and $\omega_{C,n}$ is easy and facilitates the understanding of the infrared scaling the potential within the broken phase. As we outlined previously the

gaussian eigenvalues are simple to interpret and the contribution $(d-2)n$ is inherited from the canonical dimension of the squared field $\rho = \phi^2/2$, whereas $-d$ is due to the integration measure from the action. In the spectrum (5.78), i.e at the convexity fixed point, the measure contribution is replaced by a contribution from the scaling of the minimum ρ_0 equal to $-(d-2)\left(\frac{\gamma-2}{\gamma-1}\right)$ which includes regularisation effects. This contribution is also identifiable in (5.74) where its origin from the scaling of the non-trivial minimum is transparent. Thus the sole presence of the running minimum, provided $1 < \gamma \leq 2$, allows to stabilize all the operators in the vicinity of (5.70) for which we had $\omega_{G,n} < 0$ for $n \leq \frac{d}{d-2}$ in the Gaussian case. In that context the running minimum overshadows the contribution from the measure and stabilises the infrared scaling of the potential, inducing the completion of convexity. In physical terms the minimum sets an additional mass scale that is responsible for the change to an irrelevant scaling the previously relevant directions. In return, the dependence of (5.78) on γ induces a sensitivity on the regularisation scheme that can possibly, as we saw, destroy convexity when type B cutoff are employed (see previous analysis). Keeping $1 < \gamma \leq 2$, the attractiveness of (5.70) increases as the convexity index γ is getting closer to one, leading to a sharper (or faster) transition to a convex potential. By contrast, we see that a smoother transition to convexity can be achieved by minimising (but not cancelling) the contribution from the running minimum that amounts to maximise γ. This property was already emphasized in the detailed analysis of (5.37) and we will not discuss it further here. Also the present discussion echoes with the analysis of the momenta contribution from the threshold function that leads to the parametrisation (5.9), where the measure contribution was circumvented in the case of type A regulators. Finally we note that when $d \to 2$ the effect of the minimum is amplified and entails the stabilisation of an increasing number of opertors as $\frac{d}{d-2} \to \infty$. Also, for very large order operator ($n \to \infty$) we have the relation $\omega_C - \omega_G \propto 1/n$ that implies the coincidence of the Gaussian and convexity fixed points.

5.5.3 Sharp regularisation

In this section we focus on the analysis of the eigenvalues spectrum corresponding to a sharp regularisation scheme. Indeed the case $\gamma = 1$ have been excluded from the discussion as it provides a distinctive scaling towards convexity. In the vicinity of (5.70) the mass term responds to the scaling via the eigenvalues equation

$$\partial_t u' = (d-2)\,(1+u')\,\log\left(\frac{1}{1+u'}\right) \tag{5.79}$$

derived from (5.44). The logarithmic approach towards $(1+u') \to 0$ is characteristic of the sharp cutoff regulator and can be seen directly from the flow (5.41). The scaling (5.79) can again be checked by inserting it into (5.42) and use the fundamental relation (5.44). We still have the exact cancellation between the fluctuation term and the mass term when $u' \to -1$. The eigenvalue for higher order derivative of the potential are also computable, and using (5.45) and (5.79) that leads to

$$\partial_t u^{(n)} = (d-2)\,\log\left(\frac{1}{1+u'}\right) u^{(n)} \tag{5.80}$$

for n positive integer. In the interpretation of (5.80), which seems to be diverging at first sight, we have to consider that $u^{(n)}$ tends to zero thanks to (5.45) that entails $u^{(n)} = 2^{n-1}(1+u') \to 0$ such that this offsets the divergence of the logarithmic term in (5.80). Thus we reach the convexity fixed point for all the higher couplings as $\partial_t u^{(n)} \to 0$ when $1+u' \to 0$. From the relations (5.79) and (5.80) we can directly remark the poor stability entailed by sharp the regularisation of the lowest momenta. As we are in sitting in the broken phase $(1+u' < 0)$, the approach to the fixed point $\partial_t u' = 0$, and therefore the transition to a convex potential, is more abrupt than for the case $\gamma > 1$. Typically for $1+u' = \epsilon \ll 1$ we compare the sharp (logarithmic) approach $\partial_t u' \propto \epsilon \log(1/\epsilon)$ to the smoother (algebraic) approach $\partial_t u' \propto \epsilon$ for $\gamma > 1$ when $\epsilon \to 0$. In the continuity of this analysis we note that the small deviation ϵ from the convexity fixed point is attracted towards convexity such that $\epsilon(t) \sim \exp\left[-e^{t(2-d)}\right]$ when $t \to -\infty$ which, again, is in contrast with the situation $\gamma > 1$. This leads us to the conclusion that the sharp cutoff regulator constitutes a limit case for the full completion of the potential when $k \to 0$. It forms a lower bound in the space of possible regulators with reduced stability properties in the immediate vicinity of a convex potential. Regulators with a convexity index lower than that of the sharp regulator entail automatically a non-convex potential in the infrared limit.

5.6 Enhanced convexity

As a final step of our study of the convexity approach within the functional renormalisation group, we would like to extend here the discussion of the deep infrared potential behaviour using an alternative RG formulation that provided flow equations with similar structure. Indeed, as we pointed out in previous chapters, several version of Wilson's renormalisation group ideas exist and we choose here the form proposed in [158] for scalar field theories and called proper-time renormalisation group (PTRG). In [75] a flow equation for the effective

potential is given that possess (almost) the same structure as the flow (5.1) although the space of regulator is larger. Therefore it is extremely tempting to extend our analysis of the deep infrared scaling of the potential to the flow proposed in [75]. Our approximation technique for the solution of the flow (5.1) can be applied and we found an unusual completion of the potential for an exceptional choice of regulator. However we outlined that approximation are not equivalent, order by order, in both RG formulations, hence approximated flows and results from both approaches are not in one to one correspondence [75]. Nevertheless we believe that this concise study of the convexity approach using the PTRG formulation will complete our previous results and that it will motivate further investigation of the critical infrared potential.

5.6.1 Flow and approximation

The flow given in [75] using the approach proposed in [158] is very similar in structure to the flow we studied previously provided a specific choice of regulator function with the correct asymptotic behaviour (see [75] for details). We choose here, for convenience, to use this flow equation directly without going into the details of its derivation. At the leading order of the derivative expansion the flow equation for the effective potential from PTRG approach is given in arbitrary dimension by the differential equation

$$\partial_t u = (d-2)\rho u' - 3u + (N-1)\,\frac{\alpha}{(1+u')^{m-d/2}} + \frac{\alpha}{(1+u'+2\rho u'')^{m-d/2}} \tag{5.81}$$

where $\alpha = \frac{\Gamma(m-d/2)}{2^d \pi^{d/2}\Gamma(m)}$. The parameter $m \geq d/2$ controls the shape of the regulator and for the range $d/2 < m \leq 1 + d/2$ we recover the flow (5.18) that described the infrared flow in the vicinity of the pole of the threshold function. The case $m = d/2$ corresponds to the sharp regulator case (with $\gamma = 1$). In (5.81) we know already that the constant α is irrelevant for our purpose and that it can be rescaled into ρ and u. Thus our previous analysis of the infrared scaling of the potential and its convexity completion is here completely valid within $d/2 \leq m \leq 1 + d/2$. Furthermore, due to a larger choice of regulator, we can extend its validity to $m \geq 1 + d/2$. Indeed there is not essential change in (5.18) for $\gamma > 2$ and our fixed point analysis of the infrared potential scaling, as long as $\gamma < \infty$, still correct. This shows that the PTRG allows for regularisation schemes that enhance the effect of the lowest modes integration and therefore provide an even slicker transition to a convex potential. This enhanced contribution, as m increases, of the non-convex region was already noted in [75]. An interesting case, that has been not studied yet, is the limit $m \to \infty$ that corresponds to an exponential form for the nonlinear part of the flow related to the fluctuation effects. This specific case can be seen as the equivalent

(heuristically) to $\gamma \to \infty$ although approximated flows can not be directly compared. However if we replace $u \to u/m$ in (5.81) (or $u \to u/(\gamma-1)$ in (5.18)) then normalise the potential and the field to absorb any constant, we can safely take the limit $m \to \infty$ ($\gamma \to \infty$) to obtain

$$\partial_t u = (d-2)\rho u' - 3u + (N-1)\, e^{-u'} + e^{-(u'+2\rho u'')}\,. \tag{5.82}$$

The flow (5.82) is our main object of investigation here and we intend to construct an approximated solution along similar lines to the case $\gamma < \infty$ that we discussed earlier. The flow (5.82) can be rewritten into a more transparent form

$$\partial_t u = (d-2)\rho u' - 3u + \left[1 - \frac{1}{N}\left(1 - e^{-2\rho u''}\right)\right] e^{-u'} \tag{5.83}$$

where the constant N has been absorbed into u and ρ as usual. In this formulation it is clear that, following the same dominant balance analysis as for $\gamma < \infty$, a condition for a simpler equation, equivalent to the large N limit of the model, can be easily formulated. This condition reads

$$1 - e^{-2\rho u''} \ll 1 \tag{5.84}$$

and have to be fulfilled by the solution of the subsequent evolution for u. This evolution equation is technically tractable and is interpreted physically as the result of the dominance of the Goldstone modes over the radial mode in our specific regime of interest (5.84), which remains to be fulfilled. For this we have to solve (5.83) in the limit $N \to \infty$ and this is detailed in the next section as well as the approach to convexity for this specific flow. In passing we note that the large N limit in the case $m = \infty$ is also studied in [159].

5.6.2 Infrared scaling potential

Implementing the condition (5.84) leads to the exponential flow for the derivative of the potential

$$\partial_t u' = (d-2)\rho u'' - 2u' - \frac{u''}{e^{u'}}\,. \tag{5.85}$$

This equation is solvable analytically through standard techniques and the full solution is given by the relation

$$\rho \cdot (-u')^{1-d/2} - \mathcal{G}(u') = F(u' e^{2t}) \tag{5.86}$$

for $u' < 0$ (broken phase). As usual the function F is fixed by specific boundary conditions and we choose a quartic classical potential of the form $u'(t=0) = \lambda_\Lambda(\rho - \kappa_\Lambda)$. Using this, we can construct explicitly the right hand side of (5.86) and we obtain ($z < 0$)

$$F(z) = \left(\frac{z}{\lambda_\Lambda} + \kappa_\Lambda\right) |z|^{1-d/2} - \mathcal{G}(z)\,. \tag{5.87}$$

The function $\mathcal{G}$ results from the integration of the flow (5.85) and can be formulated in terms of incomplete Gamma function [117, 118, 157] for $d > 2$. In this formulation the dimension can be varied continuously and this solution provides an unified view on the possible phase of the large N limit model for the exceptional choice $m \to \infty$. We find

$$\mathcal{G}(z) = -\frac{i^d}{2}\,\Gamma\Big(1-\frac{d}{2}\,,\,z\Big) - \frac{i\pi}{2\,\Gamma(d/2)}\,. \tag{5.88}$$

The complex constant ensures that the function is real-valued on the negative axis $z < 0$. A fundamental remark is that in (5.88) the pole is removed towards $-\infty$ on the contrary to the case $\gamma < \infty$ where is was located at some finite value on the negative axis. This change can be spotted already in the exponential flow (5.85) that possess an essential singularity about $u' = -\infty$. On $]-\infty, 0[$ the function $\mathcal{G}(z)$ is analytical and diverges progressively as $z \to -\infty$. We identified a running minimum for the potential given by $\rho_0 = \kappa_\star + (\kappa_\Lambda - \kappa_{cr})e^{t(2-d)}$ with $\kappa_{cr} = \kappa_\star = \frac{1}{d-2}$. Along the same reasoning that we had in the previous section, for non-critical value of this minimum, we found that the potential scales towards $-\infty$ due to the divergence of the minimum. In the limit $t \to -\infty$ the solution (5.86) leads to the infrared scaling of the potential following the asymptotic relation

$$\rho_0 - \rho = -\frac{e^{-u'}}{2u'} \tag{5.89}$$

where the potential diverges towards its fixed point value $u' = -\infty$. The asymptotic relation (5.89) can be solved explicitly for u' and in the deep infrared the effective potential scaling is given by

$$u' = W\left(\frac{1}{2(\rho-\rho_0)}\right). \tag{5.90}$$

where $W(z)$ is the Lambert function [117, 160]. This function possess a minor branch for negative argument ($z < -1/e$) such that, on this branch, $W(z) \to -\infty$ as z approaches zero. This is this branch which is responsible for the scaling of the potential in (5.90) as ρ_0 diverges. From the relation (5.89) (or (5.90)) we have $u'' \sim -2u'e^{u'} \to 0$ when u' tends to $-\infty$ so the condition (5.84) is fulfilled and subleading corrections to (5.89) are exponentially suppressed. This confirm, a posteriori, the approximation (5.84) and therefore the validity of the relation (5.89) when $t \to -\infty$. Using (5.89) we can summarized the evolution of the mass term towards $-\infty$ through a simple relation that characterised the response of the potential to the scaling operator given by

$$\partial_t u' = (d-2)\,u'\,e^{u'} \tag{5.91}$$

and that is comparable to the previous relation we obtained for $\gamma < \infty$. This relation is in accordance with the cancellation of the right hand side of (5.85) with the exact compensation between the fluctuation term and the mass term. The exponential suppression in (5.91) is characteristic of the regulator and provides a smooth transition to a convex potential in total opposition with the approach offered by a sharp regularisation such as (5.79). Using the Lambert function the expression (5.91) becomes $u' = W\Big(\frac{\partial_t u'}{d-2}\Big)$ where we recover the fixed point approach $u' \to -\infty$ as $\partial_t u' \to 0$ along the minor branch of $W(z)$. A similar relation, although simpler, to (5.91) can be derived for the higher derivatives of the potential

$$\partial_t u^{(n)} = (d-2)\, n\, u^{(n)} \tag{5.92}$$

which reveals the same eigenvalues that for the optimised cutoff with $\gamma = 2$. This is in favor of the optimised cutoff which provided already for $\gamma = 2$ a strong stabilisation of higher orders operators in the infrared. Only the mass term possess a particular, enhanced, scaling towards $u' = -\infty$. Choosing $\epsilon = -1/u'$ in (5.91) we have $\partial_t \epsilon \propto \epsilon\, e^{-1/\epsilon}$ with a sensibly smoother approach of $\epsilon = 0$ than the sharp ($\gamma = 1$) or even the optimised ($\gamma = 2$) regularisation scheme. Any deviation ϵ from the fixed point is attracted following $\epsilon(t) \sim \Big[\mathrm{Ei}^{-1}\Big((2-d)t\Big)\Big]^{-1}$ where $\mathrm{Ei}^{-1}(z)$ is the inverse of the exponential integral [117, 118]. Finally we can switch back to dimensionful units to detail the infrared completion of the potential and compare it to the approaches (5.59), (5.62) and (5.63). The first derivative of the potential reads

$$\begin{aligned} U'(\bar\rho) &= -k^2\, \ln(\,2\,k^{2-d}\,) - k^2\, \ln(\bar\rho_0 - \bar\rho) \\ &\quad -k^2\, \ln\Big[\ln\Big(\,2\,(\bar\rho_0 - \bar\rho)\,k^{2-d}\Big)\Big] + \mathcal{O}\Big(\frac{\ln\eta}{\eta}\Big) \end{aligned} \tag{5.93}$$

with $\eta = \ln(2(\bar\rho_0 - \bar\rho))$ and within $\bar\rho_0 > \bar\rho$. The expression (5.93) shows a non-generic approach to convexity [25] at the leading order thanks to the peculiar behaviour of $u' = W\Big(\frac{1}{2(\rho-\rho_0)}\Big)$ on its minor branch as $u' \to -\infty$. The exceptional regularisation entails a strong contribution of the lowest modes that makes the approach (5.93) dependent on the dimension. Also when $d \to 2$ we recover the generic behaviour $U' \propto -k^2$. We note that the singularity about the minimum in (5.93) is simply due to the fact that we did not normalise the asymptotic relation (5.89) so that $u'(\rho_0) = 0$. Finally the expression (5.93) can be integrated to obtain an explicit expansion for the potential showing the flattening of $U(\bar\rho)$ for $\bar\rho < \bar\rho_0$

$$U(\bar\rho) = k^2\, \ln(\,2\,k^{2-d}\,)\,(\bar\rho_0 - \bar\rho) + k^2\,(\bar\rho_0 - \bar\rho)\Big(\ln(\bar\rho_0 - \bar\rho) - 1\Big) + \mathcal{O}\Big(e^\eta\, \ln\eta^{1/2}\Big)\,. \tag{5.94}$$

Clearly we obtain (5.60) when $k \to 0$. In contrast to the optimised case, it seems that the potential (5.94) is less flat for $0 < \bar{\rho} < \bar{\rho}_0$ than (5.62). However in the case (5.94) the progression towards a flat potential is 'delayed' thanks to the logarithm which entails a smoother or slower transition to convexity. Also the higher is the dimension the slower is the transition towards the complete flatness of the inner part. This remark closes our discussion of the extreme case $m = \infty$ (or $\gamma = \infty$) and it is fair to conclude that we covered in a comprehensive way the convexity phenomenon using non-perturbative RG methods for an exhaustive range of infrared Wilsonian regulators.

5.7 Synthesis

We analysed the deep infrared scaling of the effective potential at the level of the local potential approximation. We found that the completion of the potential within the broken phase is driven by the non-perturbative running of the potential minimum which enforces the flatness of the non-convex part of the potential. The approach to convexity is itself governed by a new attractive non-trivial infrared fixed point that is related to the existence of a pole in the flow equation structure. The observation of this singularity, and the infrared physics related to it, is complicated within a numerical approach since the flow becomes highly nonlinear in the deep infrared regime and we have the possibility of instabilities. Here we used analytical methods to compute the non-convex potential as almost all momenta are integrated and the control, as well as the interpretation, of these instabilities are related to the stabilisation of the RG flow in the vicinity of the convexity fixed point. We studied as well the dependence of the convexity completion on the renormalisation scheme and distinguished two main classes of regulators based on their convexity index γ. For $\gamma > 1$ we reach a convex potential as $k \to 0$ with an enhancement of the process for an increasing γ whereas for $\gamma < 1$ the flow stops and convexity stays out of reach. The case $\gamma = 1$ forms a boundary within the space of all regulators and corresponds formally to a sharp separation between high and low momenta. Nevertheless, due to the predominance of the massless modes in the infrared regime of theory, the fixed point related to convexity have a super-universal character. It is also present for a single radial mode whose study is facilitated using the correct mass amplitude in the vicinity of the flow singularity. We outline that we extended this super-universal convexity fixed point analysis to proper-time renormalisation group flows that allowed us to cover a broader range of regulators. An extreme choice of regulator, within this setup, leads to a non-standard completion of the convexity thanks to a strong enhancement of the contribution from the non-convex region

of the potential.

Chapter 6

Summary

In this thesis, we have studied the infrared behaviour of $O(N)$-symmetric scalar quantum field theories in low dimensions, using modern renormalisation group techniques. The main achievements of this work can be summarised as follows.

Firstly, we have provided new analytical schemes to address and analyse critical scalar theories. At infinite N, this has provided us with a complete and exact solution of the theory. In addition, we have shown the applicability of new series expansions at small, large and imaginary field. This allowed us to study the analytical structure of the potential at criticality and to locate singularities in the complex plane with great precision. Interestingly, the radii of convergence overlap and allow for a complete reconstruction of the full effective potential, leaving no free parameters. An exhaustive search for fixed point solution has been performed using the full analytical expression of the scaling potential. Furthermore, we have also been able to show that our results are independent of the underlying regularisation. This provides us with an important starting point for analytical studies beyond the limit of infinite N. From a structural point of view, we added a technique to integrate non-perturbative RG flows by noting that the RG scale integration can be interchanged with the momentum integration. This observation leads to exact analytical solutions for arbitrary regularisation scheme. In a last part we also discussed the renormalisation of a sextic potential with several minima that opens the way to the study of tricriticality and the BMB phenomenon.

At finite N, we have applied our new expansion techniques to leading order in the derivative expansion in three euclidean dimensions. In this case, due to the presence of the radial mode, our analytical solutions are bound to series expansions in field monomials. Here, and unlike the case of infinite N, the exact expansions still depend on remaining free parameters, which are fixed using numerical methods. As a result, we find high-accuracy

values for critical exponents for the Ising-like universality class, and a reliable picture for the second-order phase transition including the approach to convexity. In particular we outlined the specific contributions of the massless and massive amplitudes for large complex value of field i.e in the vicinity of the convexity bound shown by the flow.

In phases with spontaneous symmetry breaking, we have also analysed the approach to convexity of the effective potential, both at finite and infinite N. Here, we have been able, for the first time, to show that the approach to convexity is governed by a new, infrared attractive, fixed point. This is an important new result and resolves a long-standing puzzle. In addition, we have computed the scaling exponents towards convexity, and shown that these are independent of N and, therefore, super-universal. The results are also independent of the Wilsonian momentum cutoff, as long as the momentum regularisation is suitable for strongly-correlated low-momentum fluctuations.

To conclude this summary we would like to outline some possible continuation of the present work. Beyond the detailed study of tricriticality that we already mentioned, it would be very important to develop further analytical methods to solve the flow equation for finite N, at and away from criticality with a non-vanishing anomalous dimension. The objective would be to obtain an intimate understanding of the analytical structure of the critical potential and of the convergence towards it with the ambition of establishing enhanced approximation scheme. Also the nonlinear sigma model would be an attractive subject to study taking into account that it is is related to the linear theory by sending the quartic coupling to infinity [161]. In this context we will be interested on how the properties of the linear theory survive (or not) in the nonlinear case.

Bibliography

[1] P. W. Higgs, "Broken symmetries, massless particles and gauge fields," *Phys.Lett.*, vol. 12, pp. 132–133, 1964. 1

[2] P. W. Higgs, "Broken Symmetries and the Masses of Gauge Bosons," *Phys.Rev.Lett.*, vol. 13, pp. 508–509, 1964. 1

[3] F. Englert and R. Brout, "Broken Symmetry and the Mass of Gauge Vector Mesons," *Phys.Rev.Lett.*, vol. 13, pp. 321–323, 1964. 1

[4] G. Guralnik, C. Hagen, and T. Kibble, "Global Conservation Laws and Massless Particles," *Phys.Rev.Lett.*, vol. 13, pp. 585–587, 1964. 1

[5] T. Kibble, "Symmetry breaking in nonAbelian gauge theories," *Phys.Rev.*, vol. 155, pp. 1554–1561, 1967. 1

[6] Y. Nambu, "Axial vector current conservation in weak interactions," *Phys.Rev.Lett.*, vol. 4, pp. 380–382, 1960. 1

[7] Y. Nambu and G. Jona-Lasinio, "Dynamical Model of Elementary Particles Based on an Analogy with Superconductivity. 1.," *Phys.Rev.*, vol. 122, pp. 345–358, 1961. 1

[8] Y. Nambu and G. Jona-Lasinio, "Dynamical Model of Elementary Particles Based on an Analogy with Superconductivity. 2.," *Phys.Rev.*, vol. 124, pp. 246–254, 1961. 1

[9] J. Bardeen, L. Cooper, and J. Schrieffer, "Theory of superconductivity," *Phys.Rev.*, vol. 108, pp. 1175–1204, 1957. 1

[10] G. Aad *et al.*, "Observation of a new particle in the search for the Standard Model Higgs boson with the ATLAS detector at the LHC," *Phys.Lett.*, vol. B716, pp. 1–29, 2012, 1207.7214. 1

[11] S. Chatrchyan *et al.*, "Observation of a new boson at a mass of 125 GeV with the CMS experiment at the LHC," *Phys.Lett.*, vol. B716, pp. 30–61, 2012, 1207.7235. 1

[12] A. Pelissetto and E. Vicari, "Critical phenomena and renormalization group theory," *Phys.Rept.*, vol. 368, pp. 549–727, 2002, cond-mat/0012164. 3, 53

[13] K. G. Wilson, "Renormalization group and critical phenomena. 1. Renormalization group and the Kadanoff scaling picture," *Phys.Rev.*, vol. B4, pp. 3174–3183, 1971. 3, 8

[14] K. G. Wilson, "Renormalization group and critical phenomena. 2. Phase space cell analysis of critical behavior," *Phys.Rev.*, vol. B4, pp. 3184–3205, 1971. 3, 8

[15] K. Wilson and J. B. Kogut, "The Renormalization group and the epsilon expansion," *Phys.Rept.*, vol. 12, pp. 75–200, 1974. 3, 9, 10, 72

[16] L. Kadanoff, "Scaling laws for Ising models near T(c)," *Physics*, vol. 2, pp. 263–272, 1966. 3, 8

[17] K. G. Wilson and M. E. Fisher, "Critical exponents in 3.99 dimensions," *Phys.Rev.Lett.*, vol. 28, pp. 240–243, 1972. 3, 15

[18] J. Iliopoulos, C. Itzykson, and A. Martin, "Functional Methods and Perturbation Theory," *Rev.Mod.Phys.*, vol. 47, p. 165, 1975. 3, 23, 81

[19] S. R. Coleman and E. J. Weinberg, "Radiative Corrections as the Origin of Spontaneous Symmetry Breaking," *Phys.Rev.*, vol. D7, pp. 1888–1910, 1973. 3, 81

[20] S. R. Coleman, "Secret Symmetry: An Introduction to Spontaneous Symmetry Breakdown and Gauge Fields," *Subnucl.Ser.*, vol. 11, p. 139, 1975. 3, 81

[21] E. J. Weinberg and A.-q. Wu, " Understanding Complex Perturbative Effective Potentials ," *Phys.Rev.*, vol. D36, p. 2474, 1987. 3, 24, 81

[22] J. Polchinski, "Renormalization and Effective Lagrangians," *Nucl.Phys.*, vol. B231, pp. 269–295, 1984. 4, 9, 10

[23] C. Wetterich, "Exact evolution equation for the effective potential," *Phys.Lett.*, vol. B301, pp. 90–94, 1993. 4, 6, 10, 13, 28

[24] N. Tetradis and C. Wetterich, "Critical exponents from effective average action," *Nucl.Phys.*, vol. B422, pp. 541–592, 1994, hep-ph/9308214. 4, 15, 18, 23, 28, 32

[25] J. Berges, N. Tetradis, and C. Wetterich, "Nonperturbative renormalization flow in quantum field theory and statistical physics," *Phys.Rept.*, vol. 363, pp. 223–386, 2002, hep-ph/0005122. 4, 6, 11, 12, 14, 16, 21, 81, 82, 83, 94, 98, 111

[26] D. F. Litim, "Derivative expansion and renormalization group flows," *JHEP*, vol. 0111, p. 059, 2001, hep-th/0111159. 4, 15

[27] D. F. Litim and D. Zappala, "Ising exponents from the functional renormalisation group," *Phys.Rev.*, vol. D83, p. 085009, 2011, 1009.1948. 4, 15

[28] J. Berges, N. Tetradis, and C. Wetterich, "Critical equation of state from the average action," *Phys.Rev.Lett.*, vol. 77, pp. 873–876, 1996, hep-th/9507159. 4

[29] J. Berges and C. Wetterich, "Equation of state and coarse grained free energy for matrix models," *Nucl.Phys.*, vol. B487, pp. 675–720, 1997, hep-th/9609019. 4

[30] J. Berges, N. Tetradis, and C. Wetterich, "Coarse graining and first order phase transitions," *Phys.Lett.*, vol. B393, pp. 387–394, 1997, hep-ph/9610354. 4

[31] D. F. Litim, "Scheme independence at first order phase transitions and the renormalization group," *Phys.Lett.*, vol. B393, pp. 103–109, 1997, hep-th/9609040. 4, 60, 62

[32] D. F. Litim, "Wilsonian flow equation and thermal field theory," 1998, hep-ph/9811272. 4

[33] B. Bergerhoff, F. Freire, D. F. Litim, S. Lola, and C. Wetterich, "Phase diagram of superconductors from nonperturbative flow equations," *Phys. Rev. B*, vol. 53, pp. 5734–5757, Mar 1996. 4

[34] H. Gies, "Running coupling in yang-mills theory: A flow equation study," *Phys. Rev. D*, vol. 66, p. 025006, Jul 2002. 4

[35] J. M. Pawlowski, D. F. Litim, S. Nedelko, and L. von Smekal, "Infrared behavior and fixed points in landau-gauge qcd," *Phys. Rev. Lett.*, vol. 93, p. 152002, Oct 2004. 4

[36] D. F. Litim, M. C. Mastaler, F. Synatschke-Czerwonka, and A. Wipf, "Critical behavior of supersymmetric O(N) models in the large-N limit," *Phys.Rev.*, vol. D84, p. 125009, 2011, 1107.3011. 4

[37] M. Heilmann, D. F. Litim, F. Synatschke-Czerwonka, and A. Wipf, "Phases of supersymmetric O(N) theories," 2012, 1208.5389. 4

[38] M. Reuter, "Nonperturbative evolution equation for quantum gravity," *Phys.Rev.*, vol. D57, pp. 971–985, 1998, hep-th/9605030. 4

[39] M. Niedermaier and M. Reuter, "The Asymptotic Safety Scenario in Quantum Gravity," *Living Rev.Rel.*, vol. 9, p. 5, 2006. 4

[40] R. Percacci, "Asymptotic Safety," 2007, 0709.3851. 4

[41] D. F. Litim, "Fixed Points of Quantum Gravity and the Renormalisation Group," 2008, 0810.3675. 4

[42] A. Codello, R. Percacci, and C. Rahmede, "Investigating the Ultraviolet Properties of Gravity with a Wilsonian Renormalization Group Equation," *Annals Phys.*, vol. 324, pp. 414–469, 2009, 0805.2909. 4

[43] M. Reuter and F. Saueressig, "Quantum Einstein Gravity," *New J.Phys.*, vol. 14, p. 055022, 2012, 1202.2274. 4

[44] A. Ringwald and C. Wetterich, "Average action for the N component phi**4 theory," *Nucl.Phys.*, vol. B334, p. 506, 1990. 4, 11, 24, 81, 97

[45] N. Tetradis and C. Wetterich, "Scale dependence of the average potential around the maximum in phi**4 theories," *Nucl.Phys.*, vol. B383, pp. 197–217, 1992. 4, 11, 24, 25, 81, 82

[46] C. Bagnuls and C. Bervillier, "Exact renormalization group equations. An Introductory review," *Phys.Rept.*, vol. 348, p. 91, 2001, hep-th/0002034. 6, 28

[47] H. Gies, "Introduction to the functional RG and applications to gauge theories," 2006, hep-ph/0611146. 6, 14

[48] B. Delamotte, "An Introduction to the nonperturbative renormalization group," 2007, cond-mat/0702365. 6

[49] O. J. Rosten, "Fundamentals of the Exact Renormalization Group," *Phys.Rept.*, vol. 511, pp. 177–272, 2012, 1003.1366. 6

[50] J. Zinn-Justin, *Quantum Field Theory and Critical Phenomena*. Oxford University Press, fourth ed., 2002. 6, 17, 32, 36, 72

[51] C. Itzykson and J.-B. Zuber, *Quantum Field Theory*. McGraw-Hill, 1980. 6

[52] M. E. Peskin and D. V. Schroeder, *An Introduction to Quantum Field Theory*. Westview Press, 1995. 6

[53] A. N. Vasiliev, *Functional Methods in Quantum Field Theory and Statistical Physics*. Gordon and Breach, 1998. 6

[54] D. Amit and M. Martin-Mayor, *Field theory, the renormalization group, and critical phenomena*. WorldScientific, third ed., 2005. 6, 32

[55] S. Coleman, *Aspects of Symmetry*. Cambridge University Press, 1985. 6

[56] M. Le Bellac, *Quantum and Statistical Field Theory*. Oxford University Press, 1992. 6

[57] N. Goldenfeld, *Lectures On Phase Transitions And The Renormalization Group*. Westview Press, 1992. 6, 72

[58] F. J. Wegner and A. Houghton, "Renormalization group equation for critical phenomena," *Phys.Rev.*, vol. A8, pp. 401–412, 1973. 9, 32

[59] T. R. Morris, "The Exact renormalization group and approximate solutions," *Int.J.Mod.Phys.*, vol. A9, pp. 2411–2450, 1994, hep-ph/9308265. 10

[60] C. Wetterich, "The Average action for scalar fields near phase transitions," *Z.Phys.*, vol. C57, pp. 451–470, 1993. 10, 17, 23

[61] C. Wetterich, "Improvement of the average action," *Z.Phys.*, vol. C60, pp. 461–470, 1993. 10, 17

[62] C. Wetterich, "Exact renormalization group equations for the average action and systematic expansions," *Int.J.Mod.Phys.*, vol. A9, pp. 3571–3602, 1994. 10

[63] T. R. Morris, "Derivative expansion of the exact renormalization group," *Phys.Lett.*, vol. B329, pp. 241–248, 1994, hep-ph/9403340. 10, 15

[64] T. R. Morris, "On truncations of the exact renormalization group," *Phys.Lett.*, vol. B334, pp. 355–362, 1994, hep-th/9405190. 10, 17, 22, 28, 58, 66

[65] U. Ellwanger, "Flow equations for N point functions and bound states," *Z.Phys.*, vol. C62, pp. 503–510, 1994, hep-ph/9308260. 10

[66] U. Ellwanger, "Collective fields and flow equations," *Z.Phys.*, vol. C58, pp. 619–627, 1993. 10

[67] M. Bonini, M. D'Attanasio, and G. Marchesini, "Perturbative renormalization and infrared finiteness in the Wilson renormalization group: The Massless scalar case," *Nucl.Phys.*, vol. B409, pp. 441–464, 1993, hep-th/9301114. 10

[68] C. Wetterich, "Average action and the renormalization group equations," *Nucl.Phys.*, vol. B352, pp. 529–584, 1991. 10, 17

[69] C. Wetterich, "Effective average action in statistical physics and quantum field theory," *Int.J.Mod.Phys.*, vol. A16, pp. 1951–1982, 2001, hep-ph/0101178. 11

[70] D. F. Litim, "Optimization of the exact renormalization group," *Phys.Lett.*, vol. B486, pp. 92–99, 2000, hep-th/0005245. 12, 18, 28, 30, 63, 68, 84

[71] D. F. Litim, "Optimized renormalization group flows," *Phys.Rev.*, vol. D64, p. 105007, 2001, hep-th/0103195. 12, 18, 28, 63, 86, 97

[72] D. F. Litim, "Critical exponents from optimized renormalization group flows," *Nucl.Phys.*, vol. B631, pp. 128–158, 2002, hep-th/0203006. 12, 19, 28, 29, 43, 50, 63

[73] D. F. Litim and J. M. Pawlowski, "Completeness and consistency of renormalisation group flows," *Phys.Rev.*, vol. D66, p. 025030, 2002, hep-th/0202188. 14

[74] A. Zee, *Quantum Field Theory in a Nutshell*. Princeton University Press, 2013. 14

[75] D. F. Litim and J. M. Pawlowski, "Perturbation theory and renormalization group equations," *Phys.Rev.*, vol. D65, p. 081701, 2002, hep-th/0111191. 14, 107, 108

[76] E. Brezin, J. Le Guillou, and J. Zinn-Justin, "Wilson's theory of critical phenomena and callan-symanzik equations in 4-epsilon dimensions," *Phys.Rev.*, vol. D8, pp. 434–440, 1973. 15

[77] D. Kazakov, O. Tarasov, and A. Vladimirov, " Calculation Of Critical Exponents By Quantum Field Theory Methods," *Sov.Phys.JETP*, vol. 50, p. 521, 1979. 15

[78] E. Brezin and J. Zinn-Justin, "Renormalization of the nonlinear sigma model in 2 + epsilon dimensions. Application to the Heisenberg ferromagnets," *Phys.Rev.Lett.*, vol. 36, pp. 691–694, 1976. 15

[79] E. Brezin, J. Zinn-Justin, and J. Le Guillou, "Renormalization of the Nonlinear Sigma Model in (Two + Epsilon) Dimension," *Phys.Rev.*, vol. D14, p. 2615, 1976. 15

[80] G. Parisi, "The Theory of Nonrenormalizable Interactions. 1. The Large N Expansion," *Nucl.Phys.*, vol. B100, p. 368, 1975. 15

[81] T. Morris, "Properties of derivative expansion approximations to the renormalization group," *Int.J.Mod.Phys.*, vol. B12, pp. 1343–1354, 1998, hep-th/9610012. 15

[82] T. R. Morris and M. D. Turner, "Derivative expansion of the renormalization group in O(N) scalar field theory," *Nucl.Phys.*, vol. B509, pp. 637–661, 1998, hep-th/9704202. 15

[83] T. R. Morris and J. F. Tighe, "Convergence of derivative expansions of the renormalization group," *JHEP*, vol. 9908, p. 007, 1999, hep-th/9906166. 15, 18

[84] L. Canet, B. Delamotte, D. Mouhanna, and J. Vidal, "Optimization of the derivative expansion in the nonperturbative renormalization group," *Phys.Rev.*, vol. D67, p. 065004, 2003, hep-th/0211055. 15

[85] A. Bonanno and D. Zappala, "Towards an accurate determination of the critical exponents with the renormalization group flow equations," *Phys.Lett.*, vol. B504, pp. 181–187, 2001, hep-th/0010095. 15

[86] M. Moshe and J. Zinn-Justin, "Quantum field theory in the large N limit: A Review," *Phys.Rept.*, vol. 385, pp. 69–228, 2003, hep-th/0306133. 17

[87] G. R. Golner, "Nonperturbative Renormalization Group Calculations For Continuum Spin Systems," *Phys.Rev.*, vol. B33, pp. 7863–7866, 1986. 17, 28

[88] M. D'Attanasio and T. R. Morris, "Large N and the renormalization group," *Phys.Lett.*, vol. B409, pp. 363–370, 1997, hep-th/9704094. 17, 32

[89] K.-I. Aoki, K.-i. Morikawa, W. Souma, J.-i. Sumi, and H. Terao, "The Effectiveness of the local potential approximation in the Wegner-Houghton renormalization group," *Prog.Theor.Phys.*, vol. 95, pp. 409–420, 1996, hep-ph/9612458. 17, 28

[90] K.-I. Aoki, K. Morikawa, W. Souma, J.-I. Sumi, and H. Terao, "Rapidly converging truncation scheme of the exact renormalization group," *Prog.Theor.Phys.*, vol. 99, pp. 451–466, 1998, hep-th/9803056. 17, 28, 30

[91] A. Margaritis, G. Odor, and A. Patkos, "Series expansion solution of the Wegner-Houghton renormalisation group equation," *Z.Phys.*, vol. C39, p. 109, 1988. 17, 28

[92] P. E. Haagensen, Y. Kubyshin, J. I. Latorre, and E. Moreno, "Gradient flows from an approximation to the exact renormalization group," *Phys.Lett.*, vol. B323, pp. 330–338, 1994, hep-th/9310032. 17

[93] F. Dyson, "The S matrix in quantum electrodynamics," *Phys.Rev.*, vol. 75, pp. 1736–1755, 1949. 17

[94] J. S. Schwinger, "On the Green's functions of quantized fields. 1.," *Proc.Nat.Acad.Sci.*, vol. 37, pp. 452–455, 1951. 17

[95] P. M. Stevenson, "Optimized Perturbation Theory," *Phys.Rev.*, vol. D23, p. 2916, 1981. Extended version of DOE-ER/00881-153. 18

[96] S.-B. Liao, J. Polonyi, and M. Strickland, "Optimization of renormalization group flow," *Nucl.Phys.*, vol. B567, pp. 493–514, 2000, hep-th/9905206. 18

[97] T. Papenbrock and C. Wetterich, "Two loop results from one loop computations and nonperturbative solutions of exact evolution equations," *Z.Phys.*, vol. C65, pp. 519–535, 1995, hep-th/9403164. 18

[98] R. Jackiw, "Functional evaluation of the effective potential," *Phys.Rev.*, vol. D9, p. 1686, 1974. 19

[99] S. R. Coleman, R. Jackiw, and H. D. Politzer, "Spontaneous Symmetry Breaking in the O(N) Model for Large N*," *Phys.Rev.*, vol. D10, p. 2491, 1974. 19

[100] A. Hasenfratz and P. Hasenfratz, "Renormalization Group Study of Scalar Field Theories," *Nucl.Phys.*, vol. B270, pp. 687–701, 1986. 22

[101] K. Symanzik, "Renormalizable models with simple symmetry breaking. 1. Symmetry breaking by a source term," *Commun.Math.Phys.*, vol. 16, pp. 48–80, 1970. 23, 81

[102] R. W. Haymaker and J. Perez-Mercader, "Convexity of the effective potential," *Phys.Rev.*, vol. D27, p. 1948, 1983. 23

[103] L. O'Raifeartaigh and G. Parravicini, "Effective Fields and Discontinuities in the Effective Potential," *Nucl.Phys.*, vol. B111, p. 501, 1976. 24

[104] Y. Fujimoto, L. O'Raifeartaigh, and G. Parravicini, "Effective Potential For Non-convex Potentials," *Nucl.Phys.*, vol. B212, p. 268, 1983. 24

[105] D. J. Callaway and D. J. Maloof, "Effective potential of lattice phi**4 theory," *Phys.Rev.*, vol. D27, p. 406, 1983. 24

[106] C. M. Bender and F. Cooper, "Failure of the naive loop expansion for the effective potential in phi**4 field theory when there is broken symmetry," *Nucl.Phys.*, vol. B224, p. 403, 1983. 24

[107] F. Cooper and B. Freedman, "Renormalizing the effective potential for spontaneously broken g phi**4 field theory," *Nucl.Phys.*, vol. B239, p. 459, 1984. 24

[108] M. Hindmarsh and D. Johnston, "Convexity of the effective potential," *J.Phys.A*, vol. A19, p. 141, 1986. 24

[109] R. Fukuda and E. Kyriakopoulos, "Derivation of the Effective Potential," *Nucl.Phys.*, vol. B85, p. 354, 1975. 24

[110] L. O'Raifeartaigh, A. Wipf, and H. Yoneyama, "The Constraint Effective Potential," *Nucl.Phys.*, vol. B271, p. 653, 1986. 24

[111] V. Branchina, P. Castorina, and D. Zappala, "Convexity property of the variational approximations to the effective potential," *Phys.Rev.*, vol. D41, pp. 1948–1952, 1990. 24

[112] J. Alexandre, V. Branchina, and J. Polonyi, "Instability induced renormalization," *Phys.Lett.*, vol. B445, pp. 351–356, 1999, cond-mat/9803007. 24

[113] J. Glimm and A. Jaffe, *Quantum Physics, A Functional Integral Point of View.* Westview Press, second ed., 1987. 25

[114] C. Bervillier, A. Juttner, and D. F. Litim, "High-accuracy scaling exponents in the local potential approximation," *Nucl.Phys.*, vol. B783, pp. 213–226, 2007, hep-th/0701172. 28, 55, 56

[115] M. G. Alford, "Critical exponents without the epsilon expansion," *Phys.Lett.*, vol. B336, pp. 237–242, 1994, hep-ph/9403324. 28

[116] J. Comellas and A. Travesset, "O(N) models within the local potential approximation," *Nucl.Phys.*, vol. B498, pp. 539–564, 1997, hep-th/9701028. 29

[117] F. W. J. Olver, D. W. Lozier, and R. F. Boisvert, *NIST Handbook of Mathematical Functions*. C.U.P, 2010. 29, 33, 64, 110, 111

[118] M. Abramowitz and I. A. Stegun, *Handbook of Mathematical Functions with Formulas, Graphs, and Mathematical Tables*. New York: Dover Publications, 1964. 29, 33, 64, 110, 111

[119] J. Nicoll, T. Chang, and H. Stanley, "Nonlinear Solutions of Renormalization-Group Equations," *Phys.Rev.Lett.*, vol. 32, pp. 1446–1449, 1974. 30

[120] J. Nicoll, T. Chang, and H. Stanley, "Global Features of Nonlinear Renormalization Group Equations," *Phys.Rev.*, vol. B12, pp. 458–478, 1975. 30, 43

[121] M. E. Fisher, S.-k. Ma, and B. Nickel, "Critical Exponents for Long-Range Interactions," *Phys.Rev.Lett.*, vol. 29, pp. 917–920, 1972. 32

[122] S.-k. Ma, "Critical Exponents for Charged and Neutral Bose Gases above lamda Points," *Phys.Rev.Lett.*, vol. 29, pp. 1311–1314, 1972. 32

[123] R. Abe, "Expansion of a critical exponent in inverse powers of spin dimensionality," *Progress of Theoretical Physics*, vol. 48, no. 4, pp. 1414–1415, 1972. 32

[124] E. Brézin and D. J. Wallace, "Critical behavior of a classical heisenberg ferromagnet with many degrees of freedom," *Phys. Rev. B*, vol. 7, pp. 1967–1974, Mar 1973. 32

[125] H. Stanley, "Spherical model as the limit of infinite spin dimensionality," *Phys.Rev.*, vol. 176, pp. 718–722, 1968. 32

[126] T. H. Berlin and M. Kac, "The spherical model of a ferromagnet," *Phys. Rev.*, vol. 86, pp. 821–835, Jun 1952. 32

[127] N. Tetradis and D. Litim, "Analytical solutions of exact renormalization group equations," *Nucl.Phys.*, vol. B464, pp. 492–511, 1996, hep-th/9512073. Revised version of HEP-TH 9501042. 32, 37, 72

[128] D. Litim and N. Tetradis, "Approximate solutions of exact renormalization group equations," 1995, hep-th/9501042. 32, 76, 77

[129] H. Bateman and A. Erdelyi, *Higher Transcendental Functions, Volume I*. Mc Graw-Hill, 1953. 33

[130] W. A. Bardeen, M. Moshe, and M. Bander, "Spontaneous Breaking of Scale Invariance and the Ultraviolet Fixed Point in O(n) Symmetric (phi^6 in Three-Dimensions) Theory," *Phys.Rev.Lett.*, vol. 52, p. 1188, 1984. 34, 38, 78

[131] W. A. Bardeen and M. Moshe, "Phase Structure of the O(N) Vector Model," *Phys.Rev.*, vol. D28, p. 1372, 1983. 34, 38

[132] F. David, D. A. Kessler, and H. Neuberger, "The Bardeen-moshe-bander Fixed Point And The Ultraviolet Triviality Of Phi**6 In Three-dimensions.," *Phys.Rev.Lett.*, vol. 53, p. 2071, 1984. 34, 38, 77, 79

[133] F. David, D. A. Kessler, and H. Neuberger, "A study of (phi**2)**3 in three-dimensions at N = infinity," *Nucl.Phys.*, vol. B257, pp. 695–728, 1985. 37, 38

[134] G. N. Mercer and A. J. Roberts, "A centre manifold description of contaminant dispersion in channels with varying flow properties," *SIAM J. Appl. Math.*, vol. 50, pp. 1547–1565, 1990. 39, 129

[135] D. F. Litim, "Universality and the renormalisation group," *JHEP*, vol. 0507, p. 005, 2005, hep-th/0503096. 43

[136] E. Ising, "Contribution to the Theory of Ferromagnetism," *Z.Phys.*, vol. 31, pp. 253–258, 1925. 53

[137] A. Juettner, D. Litim, and E. Marchais, "A numerical study of fixed points in 3d $\mathcal{O}(N)$-symmetric scalar field theories," *in preparation.* 55, 56

[138] D. Litim and E. Marchais, "Convexity as a fixed point," *in preparation.* 59

[139] F. Freire and D. F. Litim, "Charge crossover at the U(1) Higgs phase transition," *Phys.Rev.*, vol. D64, p. 045014, 2001, hep-ph/0002153. 60, 62, 88

[140] D. F. Litim, "Mind the gap," *Int.J.Mod.Phys.*, vol. A16, pp. 2081–2088, 2001, hep-th/0104221. 63, 83

[141] H. Bateman and A. Erdélyi, *Higher transcendental functions.* Calif. Inst. Technol. Bateman Manuscr. Project, New York, NY: McGraw-Hill, 1955. 64, 89

[142] A. Codello, "Scaling Solutions in Continuous Dimension," *J.Phys.*, vol. A45, p. 465006, 2012, 1204.3877. 66

[143] N. Mermin and H. Wagner, "Absence of ferromagnetism or antiferromagnetism in one-dimensional or two-dimensional isotropic Heisenberg models," *Phys.Rev.Lett.*, vol. 17, pp. 1133–1136, 1966. 71

[144] M. Luscher and P. Weisz, "Scaling Laws and Triviality Bounds in the Lattice phi**4 Theory. 2. One Component Model in the Phase with Spontaneous Symmetry Breaking," *Nucl.Phys.*, vol. B295, p. 65, 1988. 72

[145] A. Hasenfratz, K. Jansen, C. B. Lang, T. Neuhaus, and H. Yoneyama, "The Triviality Bound of the Four Component phi**4 Model," *Phys.Lett.*, vol. B199, p. 531, 1987. 72

[146] U. M. Heller, H. Neuberger, and P. M. Vranas, "Large N analysis of the Higgs mass triviality bound," *Nucl.Phys.*, vol. B399, pp. 271–348, 1993, hep-lat/9207024. 72

[147] D. J. Callaway, "Triviality Pursuit: Can Elementary Scalar Particles Exist?," *Phys.Rept.*, vol. 167, p. 241, 1988. 72

[148] O. J. Rosten, "Triviality from the Exact Renormalization Group," *JHEP*, vol. 0907, p. 019, 2009, 0808.0082. 72

[149] L. D. Landau, *Niels Bohr and the Development of Physics*. McGraw-Hill, 1955. 72

[150] L. D. Landau, E. M. Lifshitz, and L. P. Pitaevskii, *Statistical Physics*. Pergamon, 1980. 72

[151] R. B. Griffiths, "Thermodynamics Near the Two-Fluid Critical Mixing Point in He-3 - He-4," *Phys.Rev.Lett.*, vol. 24, pp. 715–717, 1970. 75

[152] I. D. Lawrie and S. Sarbach, "Theory of tricritical points," in *Phase Transitions and Critical Phenomena vol 9*, pp. 2–155, Academic Press, 1984. 76

[153] G. Ahlers and D. S. Greywall, "Second-sound velocity and superfluid density near the tricritical point in he^3-he^4 mixtures," *Phys. Rev. Lett.*, vol. 29, pp. 849–852, Sep 1972. 76

[154] E. K. Riedel and F. J. Wegner, "Tricritical exponents and scaling fields," *Phys. Rev. Lett.*, vol. 29, pp. 349–352, Aug 1972. 76

[155] M. Blume, V. J. Emery, and R. B. Griffiths, "Ising model for the λ transition and phase separation in he^3-he^4 mixtures," *Phys. Rev. A*, vol. 4, pp. 1071–1077, Sep 1971. 76

[156] D. F. Litim, J. M. Pawlowski, and L. Vergara, "Convexity of the effective action from functional flows," 2006, hep-th/0602140. 81

[157] I. S. Gradshteyn and I. M. Ryzhik, *Table of integrals, series, and products*. Elsevier/Academic Press, Amsterdam, seventh ed., 2007. 89, 110

[158] S.-B. Liao, "On connection between momentum cutoff and the proper time regularizations," *Phys.Rev.*, vol. D53, pp. 2020–2036, 1996, hep-th/9501124. 107, 108

[159] M. Mazza and D. Zappala, "Proper time regulator and renormalization group flow," *Phys.Rev.*, vol. D64, p. 105013, 2001, hep-th/0106230. 109

[160] R. M. Corless, G. H. Gonnet, D. E. G. Hare, D. J. Jeffrey, and D. E. Knuth, "On the lambert w function," in *ADVANCES IN COMPUTATIONAL MATHEMATICS*, pp. 329–359, 1996. 110

[161] A. Codello and R. Percacci, "Fixed Points of Nonlinear Sigma Models in $d \geq 2$," *Phys.Lett.*, vol. B672, pp. 280–283, 2009, 0810.0715. 115

Appendix A

Convergence

We have to estimate the radii of convergence of series of the form

$$f(x) = \sum_m \lambda_m x^m \,. \tag{A.1}$$

Provided the signs of the expansion coefficients follow a simple pattern such as having all the same, or alternating signs $(+-)$, standard tests of convergence including the ratio test or the root test are applicable. Here, we encounter series which often show a more complex sign pattern such as $(++--)$ where the standard tests fail, or at best provide a rough estimate for the radius of convergence.

Therefore, we use the method by Mercer and Roberts [134] devised for series which display a more complex pattern. The technique is motivated from the expansion of functions on the real axis which display a pair of complex conjugate poles in the complex plane such as

$$f(x) = \left(1 - \frac{x}{re^{i\theta}}\right)^\nu + \left(1 - \frac{x}{re^{-i\theta}}\right)^\nu \tag{A.2}$$

for non-integer ν, which has the expansion (A.1) with

$$\lambda_n = 2\,(-1)^n\, C_\nu^n\, \frac{\cos(n\,\theta)}{r^n} \tag{A.3}$$

for $|x| < r$. For large n, the sign of the coefficients is determined by the phase. For example, a singularity close to the imaginary axis with phase close to $\theta \approx \pi/2$ would imply the sign pattern $(++--)$. Returning now to a generic series (A.1), and under the assumption that the large-n behaviour can be modeled by (A.3), we can write every 4-tuple of coefficients in the form

$$\lambda_m \;=\; \frac{A_n}{(R_n)^m}\, \cos(m\,\theta_n + \xi_n)\,. \tag{A.4}$$

The four parameters A_n, R_n, θ_n and ξ_n can then be determined, leading to

$$R_n^2 = \frac{\lambda_{n-1}^2 - \lambda_{n-2}\lambda_n}{\lambda_n^2 - \lambda_{n-1}\lambda_{n+1}} \tag{A.5}$$

$$\cos\theta_n = \frac{1}{2}\left[\frac{\lambda_{n-1}}{\lambda_n\, R_n} + \frac{\lambda_{n+1}\, R_n}{\lambda_n}\right] \tag{A.6}$$

For large n, the asymptotic behaviour is deduced inserting the model coefficients (A.3) into (A.5) and (A.6), leading to

$$\frac{R}{R_n} = \left[1 - \frac{\nu+1}{n}\right]\left[1 + \frac{\nu+1}{2n^2}\,\frac{\sin(2n-1)\theta}{\sin\theta}\right] \tag{A.7}$$

up to a factor $[1 + \mathcal{O}(n^{-3})]$. For the angles, one finds

$$\frac{\cos\theta_n}{\cos\theta} = 1 + \frac{\nu+1}{n^2}\left[1 - \frac{\cos(2n-1)\theta}{\cos\theta}\right] \tag{A.8}$$

up to corresctions of order $1/n^3$. These expressions can be used to determine the radius R, angle θ, and nature ν of the convergence-limitating singularity. The technique fails provided that (A.5) becomes negative, or the absolute value of (A.6) larger than one.